

Alma Mater Studiorum – Università di Bologna

DOTTORATO DI RICERCA IN
Biologia Cellulare e Molecolare

Ciclo XXX

Settore Concorsuale: 05/I1

Settore Scientifico Disciplinare: BIO/18 GENETICA

Investigation of genetic risk variants for nicotine dependence
and cluster headache

Presentata da: Cinzia Cameli

Coordinatore Dottorato

Prof. Giovanni Capranico

Supervisore

Prof.ssa Elena Maestrini

Co-supervisore

Dott.ssa Elena Bacchelli

Esame finale anno 2018

TABLE OF CONTENTS

ABSTRACT	4
INTRODUCTION	6
CHAPTER 1 Nicotine dependence	6
1.1 Biological mechanisms	6
1.2 Nicotinic acetylcholine receptors.....	8
1.2.1 Protein structure	8
1.2.2 Localization and function of neuronal nAChRs	10
1.2.3 $\alpha 7$ nAChRs	12
1.3 The genetics of nicotine dependence	12
1.3.1 Linkage analysis	13
1.3.2 Association studies	15
1.3.2.1 Candidate-gene association studies.....	16
1.3.2.2 Genome-wide association studies (GWAS)	19
1.3.2.2.1 Results from GWAS on nicotine dependence	23
1.3.3 Targeted sequencing studies.....	25
1.3.4 <i>CHRNA7</i> and <i>CHRFAM7A</i> gene.....	26
1.3.4.1 Role of <i>CHRNA7-CHRFAM7A</i> loci in ND.....	29
1.4 Treatments for nicotine addiction	30
1.4.1 Behavioural counselling.....	31
1.4.2 Pharmacological therapy.....	31
CHAPTER 2 Cluster headache	34
2.1 Clinical features	34
2.2 Pathophysiology	35
2.3 The genetics of cluster headache.....	37
2.4 Molecular genetic studies of Cluster headache susceptibility	37
2.4.1 Linkage studies	40
2.4.2 Association Studies.....	40
2.5 Nicotine dependence in Cluster Headache	42
2.6 CH treatments	43
MATERIALS AND METHODS	45
CHAPTER 3 Materials and methods: Role of $\alpha 7$ nAChR in nicotine dependence	45

3.1	ND Study sample	45
3.1.1	Smokers sample.....	45
3.1.2	Controls samples	45
3.2	SNP Genotyping and CNVs detection by Illumina Infinium® PsychArray microarrays.....	46
3.3	Validation of <i>CHRNA7</i> CNVs by Real-Time PCR	49
3.4	Mutation screening of the <i>CHRNA7</i> proximal promoter.....	51
3.4.1	Primer design.....	51
3.4.2	Polymerase Chain Reaction (PCR) assay.....	51
3.4.3	PCR purification	52
3.4.4	Sanger Sequencing reaction	53
3.4.5	Ethanol-EDTA Precipitation of Sequencing Reactions.....	53
3.5	In vitro functional analysis of rs28531779 variant on <i>CHRNA7</i> promoter activity	54
3.5.1	Plasmid construction and cell transfection	54
3.5.2	Dual-Luciferase assay	55
3.6	CHRFAM7A Genotyping using ABI3730 and Gene-mapper v3.0 software	55
3.6.1	Primer design and PCR assays	55
3.6.2	PCR product analysis by ABI PRISM 3730 automatic sequencer.....	55
3.6.3	Analysis of CHRFAM7A Δ 2bp polymorphism and CNV by Genemapper v3.0 software	56
3.6.4	Analysis of CHRFAM7A copy number by real time PCR	57
3.7	Statistical analysis.....	58
3.7.1	Study sample analysis.....	58
3.7.2	Quantitative analysis	59
3.7.3	Categorical association analysis	59
3.7.4	Rare variants analysis	59
3.7.5	Luciferase assay	59
CHAPTER 4 Materials and methods: Genetic analysis of cluster headache		60
4.1	CH study sample	60
4.1.1	Cluster headache sample	60
4.1.2	Control sample	60
4.2	SNP Genotyping and quality control procedures.....	60
4.3	Association analysis.....	62
4.4	Gene-based association analysis.....	63
4.5	<i>MME</i> mutation screening.....	63
4.5.1	Primer design and PCR assay.....	63

4.5.2	Sanger Sequencing reaction and sequences precipitation	64
AIM AND RATIONALE OF THE PROJECT.....		66
CHAPTER 5.....		66
5.1	Role of $\alpha 7$ nAChR in nicotine dependence.....	67
5.2	Genetic analysis of cluster headache	69
RESULTS		72
CHAPTER 6 Analysis of <i>CHRNA7</i> and <i>CHRFAM7A</i> in nicotine dependence		72
6.1	Sample characteristics.....	72
6.2	<i>CHRNA7</i> copy number assessment by Illumina Infinium® PsychArray microarrays	74
6.3	Genotyping of <i>CHRFAM7A</i>	77
6.4	Case-control analysis of genetic variation in <i>CHRNA7</i> and <i>CHRFAM7A</i>	79
6.5	Quantitative analysis of <i>CHRFAM7A</i> variants	80
6.6	Quantitative analysis of <i>CHRNA7</i> variants	81
6.7	Analysis of rs28531779 effect on <i>CHRNA7</i> promoter activity by dual luciferase assay.....	84
6.8	Association analysis for smoking abstinence in the varenicline treated sample	85
CHAPTER 7 Genome-wide analysis of common and rare variants influencing risk for Cluster Headache		88
7.1	Sample characteristics.....	88
7.2	SNP genotyping by Illumina Infinium® PsychArray microarrays	88
7.3	Genome wide association analysis.....	89
7.3.1	Suggestive results from GWAS	91
7.4	Analysis of loci previously implicated in CH	95
7.5	Analysis of loci previously implicated in migraine.....	96
7.6	Analysis of loci previously implicated in smoking dependence	98
7.7	Gene based analysis	98
7.8	MME mutation screening.....	102
DISCUSSION.....		104
CHAPTER 8.....		104
8.1	Role of $\alpha 7$ nAChR in nicotine dependence.....	104
8.2	Genetic analysis of cluster headache	109
BIBLIOGRAPHY		114
APPENDIX.....		129

ABSTRACT

Genetic factors are known to play an important role in smoking behaviours. The work presented in this thesis was part of a research project aimed at investigating genetic factors involved in nicotine dependence (ND) and smoking cessation; more specifically, the aim of my work was to test the hypothesis that these complex traits may be influenced by genetic variation affecting $\alpha 7$ nicotinic acetylcholine receptors (nAChR) function. A secondary goal of my PhD project was to investigate genetic susceptibility to cluster headache (CH), a form of primary headache clinically well distinguished from other forms of migraine, and characterized by a very high prevalence of smoking addiction. Previous epidemiological studies indicated the importance of complex genetic factors in CH, but genetic studies were extremely limited and inconclusive; therefore, we decided to perform a genome-wide study to investigate genetic factors involved in this disorder, and their possible relationship to nicotine dependence.

- **Role of $\alpha 7$ nAChR in nicotine dependence:**

Numerous studies highlighted the role of nAChRs in nicotine addiction; genetic studies pointed to significant SNP associations within the *CHRNA5-CHRNA3-CHRNA4* and *CHRNA3-CHRNA6* gene clusters. *CHRNA7*, encoding the $\alpha 7$ subunit of homopentameric nAChR, has a still uncertain role in nicotine dependence, although it is implicated in a wide range of phenotypes and psychiatric conditions. *CHRFAM7A*, a hybrid gene containing a partial duplication of *CHRNA7*, is possibly involved in modulating $\alpha 7$ nAChR function. We conducted a genetic study in order to investigate the role of genetic variation at *CHRNA7* and *CHRFAM7A* in smoking phenotypes, as well as to test the hypothesis that $\alpha 7$ nAChR variation may modulate the efficacy of varenicline in smoking cessation. The study was performed on a collection of 408 regular tobacco smokers, recruited at smoking cessation centers, including a subgroup of 142 individuals treated with varenicline, a drug approved by US Food and Drug Administration for use as smoking cessation aid. We determined the copy number of both *CHRNA7* and *CHRFAM7A*, as well as the genotype of the *CHRFAM7A* exon 6 $\Delta 2$ bp polymorphism (rs67158670 -/TG), known to be associated to schizophrenia; in addition, we

resequenced the *CHRNA7* proximal promoter region in order to test the effect of common and rare variants involved in *CHRNA7* transcription regulation. Our results point to a role for *CHRNA7* promoter variants in tobacco addiction mechanisms; moreover, our study provides the first evidence that *CHRFAM7A* copy number variation could affect the response to varenicline treatment.

- **Genetic analysis of cluster headache:**

Family and twin studies have indicated a genetic component for CH, but its molecular genetic background is still largely unexplored. Smoking is the most consistent lifetime habit reported in CH patients, as over 80% of CH patients have a prolonged history of tobacco usage. However, it is still unknown if tobacco use could be an environmental trigger for CH in genetically predisposed subjects, or if specific genetic risk factors for CH may also predispose individuals to smoking addiction. Given the unknown CH pathophysiology, we decided to take a hypothesis-free genome-wide approach, using the Infinium PsychArray (Illumina); this particular SNP array combines both common highly-informative genome-wide tag SNPs and SNPs in coding regions of genes with an enrichment in genetic variants associated with common psychiatric conditions. Genotyping data from a sample of 99 CH cases and 359 controls were used to perform a genome wide case-control association analysis for common SNPs. Even if no genome-wide significant loci were reported, this analysis led to the identification of a suggestive association with a common variant of the PACAP receptor gene (*ADCYAP1R1*). No evidence for an overlap with the strongest and most replicated risk variants for migraine or nicotine dependence was detected. Furthermore, we performed a gene-based association analysis considering rare protein altering variants in 745 candidate genes with a possible role in CH. This analysis provided evidence of association for a rare potentially damaging missense variant in the *MME* gene, encoding for the metallo-endopeptidase neprilysin. *ADCYAP1R1* and *MME* both represent very interesting candidate genes for CH, as their gene products are known to have an important function in pain mechanisms; thus, our study provides the first evidence that genetic variation in genes related to pain processing might have a role in CH susceptibility.

INTRODUCTION

CHAPTER 1

Nicotine dependence

1.1 Biological mechanisms

Tobacco use is the main cause of preventable morbidities and deaths worldwide^{1,2}. Cigarette smoking is associated with increased risk of the four main death causes: lung cancer, cardiovascular diseases, cerebral infarction and chronic obstructive pulmonary disease. According to the World Health Organization (WHO), cigarette consumption causes more than 6 million deaths each year worldwide. The number of smokers, even if in decline, remains over 1.1 billion people around the world and Europe has the highest prevalence of tobacco smoking among adults (28%).

Despite cigarette smoking related risks are well known in Western countries, only about 30% of smokers attempt to quit smoking each year and, among these, only 5% maintain smoking abstinence within one year². The tobacco epidemic can be explained by the fact that tobacco use represents a form of drug dependence, and specifically, dependence to nicotine, which is the primary compound responsible for tobacco reinforcement³.

The process that leads to the development of nicotine addiction involves different areas in the brain in which several different nicotinic acetylcholine receptor (nAChR) subunits (Figure 1.1) are located.

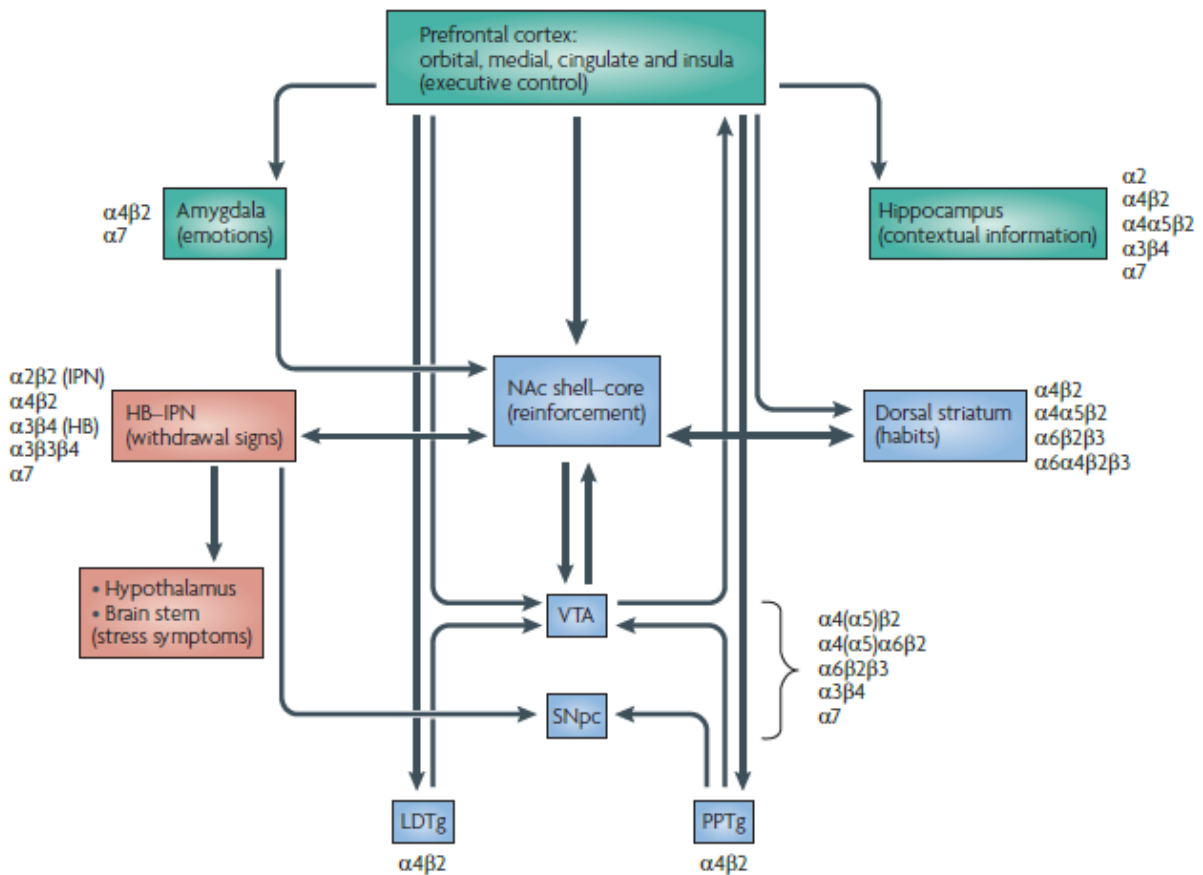


Figure 1.1: Model of neuronal mechanisms involved in smoking dependence. Nicotinic acetylcholine receptor (nAChR) subunits are located in different brain areas involved in ND mechanisms. Nicotine intake and reinforcement are caused by activation of VTA neurons in the midbrain that project to limbic areas (including the hypothalamus) and the prefrontal cortex. Cholinergic innervation from both the pedunculopontine tegmental nucleus (PPTg), in the caudal mesencephalic tegmentum, and the laterodorsal tegmental nucleus (LDTg) projects into VTA neurons. Withdrawal symptoms involve distinct neural circuits including the extended amygdala and brain stress systems, hippocampus, hypothalamus, substantia nigra pars compacta (SNpc), and/or the habenula–interpeduncular (HB–IPN) system. The transition from prefrontal cortex control (which regulates the hippocampus and amygdala) to dorsal striatum control determines the switch from voluntary to compulsive nicotine use (Changeux et al. 2010)3.

Nicotine binds and activates nicotinic acetylcholine receptors (nAChRs) and induces the activation of mesolimbic dopamine (DA) system neurons that trigger the process leading to tobacco addiction development. The activation of mesolimbic DA system is the principal cause of reward for both natural stimuli (for example drinks or food) and drugs⁴, and, thus, it is considered a major contributor to dependence development.

The mesolimbic DA system includes cell bodies in the ventral tegmental area (VTA) and their projections to the ventral striatum, which comprises the nucleus accumbens (NAc) as well as other telencephalic areas such as the amygdala, hippocampus and prefrontal cortex. The activation of nAChRs by nicotine binding causes the stimulation of dopaminergic neurons in the VTA leading to increased DA concentration in the NAc which is critical for the primary reinforcing effects of tobacco use, and contributes to the development of tobacco

addiction⁵. In vivo studies showed that blockage of dopamine release in the NAc with antagonist peptides or lesions reduces the rewarding effects of nicotine, as shown by decreased self-administration in animals⁶⁻⁸.

Withdrawal symptoms are regulated by different neural circuits including habenula, amygdala and the hypothalamus. Studies performed on animal models showed that neurons in the VTA receive inhibitory projections from the habenula and an elevated DA turnover is induced in Nac and prefrontal cortex after habenular lesion. It is supposed that cigarette consumption leads to increased habenular activity to compensate for elevated DA release. Withdrawal would then lead to non-compensated habenular hyperactivity, and therefore to a disappointment state, driving repeated cigarette consumption⁹.

Dependence represents the end point of a series of stages in which individuals seek and voluntarily smoke cigarettes owing to its reinforcing effects; this leads to loss of control of cigarette consumption and smoke becomes habitual and, ultimately, compulsive. Neuronal mechanisms underlying conscious control have been investigated and a model has been proposed: the global neuronal workspace (GNW) model. This model proposes that several cortical areas interact through a complex network of neuronal axons to maintain voluntary control. Under this hypothesis the hippocampus, amygdala and dorsal striatum are regulated by the prefrontal cortex (Figure 1.1) and this mechanism underpins the control and inhibition of behavior. It has been suggested that nicotine prolonged use could alter prefrontal cortex functions disrupting inhibitory control to resist cigarette consumption thus leading to compulsive cigarette smoke that characterizes the final step of ND³.

1.2 Nicotinic acetylcholine receptors

1.2.1 Protein structure

NACHRs are receptor proteins that are activated by the endogenous neurotransmitter acetylcholine and exogenous substance nicotine. They are expressed in the central and peripheral nervous system, muscle, and many other tissues of many organisms, including humans. NACHRs consist of 5 subunits assembled to delimit a central pore that allows cation flow down an electrochemical gradient (mainly influx of Na⁺ and Ca⁺⁺, and efflux of K⁺). The mammalian nervous system expresses twelve neuronal subunits, nine alpha (α 2– α 10) and three beta subunits (β 2– β 4), and five muscular subunits (α 1, β 1, γ , δ , and ϵ). The different

combinations of subunits lead to several pentameric receptor subtypes with different pharmacological properties, including binding affinity, and distribution in the nervous system⁵. Only the $\alpha 7$ and $\alpha 9$ subunits are capable of forming homomeric receptors.

Each subunit consists of one single polypeptide chain organized into transmembrane structure shared by all subunits. In particular, it is characterized by an amino-terminal glycosylated domain carrying one or more highly conserved cysteine bridges, facing the extracellular space; three transmembrane segments called M1, M2, and M3 linked by short loops, a large and variable intracellular domain and another transmembrane segment M4¹⁰ (Figure 1.2). The cysteine bridge, in the N-terminal fragment, is important in maintaining the correct folding of the chain and in the ligand binding^{11,12}. Furthermore, other two conserved amino acid, tyrosine and tryptophan, are involved in the ligand binding, establishing weak links with acetylcholine.

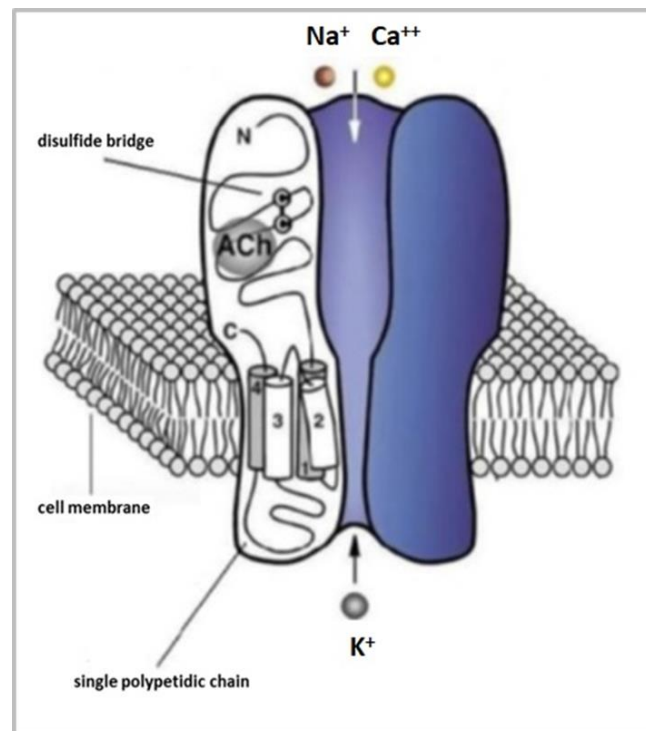


Figure 1.2: Neuronal nicotine receptor section.

The number of binding sites is different between homopentameric and heteromeric receptors: the first receptor type contains five identical acetylcholine-binding sites, while the heteropentameric receptors have only two acetylcholine-binding sites. In this case the two alpha subunits ($\alpha 2$ – $\alpha 4$ or $\alpha 6$) contain the main component of the acetylcholine-binding site while the binding site complementary component is carried by two beta subunits ($\beta 2$ or $\beta 4$).

The fifth subunit ($\alpha 5$, $\beta 3$, $\beta 2$ or $\beta 4$), is not directly involved in acetylcholine binding, but it influences receptor affinity for the ligand and receptor localization in the neuronal membrane.

Based on agonist exposure, the nAChR can be found in three different conformational states: closed, open and desensitized¹³. Agonist binding causes the activation of the receptor which changes its state from closed to open. In this state, the permeability to Na^+ and Ca^{++} increases, leading to neuronal depolarization and excitation. After this step, the receptor becomes closed again and it is desensitized. Only when the agonist dissociates from the receptor the activation-desensitization cycle can restart¹⁴⁻¹⁶.

1.2.2 Localization and function of neuronal nAChRs

Nicotine acetylcholine receptors are located both on the presynaptic, postsynaptic and the preterminal membrane. Presynaptically, nicotine acetylcholine receptors regulate different neurotransmission pathways, including the serotonergic and cholinergic pathways¹⁷⁻²¹. The activation of nAChRs at the presynaptic level initiates an intracellular Ca^{++} signal enhancing neurotransmitter release^{17,22-27}. Properly localized Ca^{++} signals lead to the start of intracellular signaling that alters synaptic transmission^{28,29}. Moreover, it was reported that timed presynaptic nAChRs activity, which precedes glutamatergic electrical stimulation, increases glutamate release and raises long-term synaptic potentiation^{30,31}.

nAChRs are also localized in the preterminal membrane where they regulate excitability along fibers as well as neurotransmitter release. Preterminal localization of nAChRs, just before the presynaptic membrane, indirectly modulates neurotransmitter release through activation of voltage-gated channels and induction of local action potentials^{32,33}. Dendritic and somatic location of nAChRs have a role in synaptic plasticity modulation. Postsynaptically, nAChRs have also a role in depolarization and in initiation of intracellular Ca^{++} signal^{30,31}.

In the central nervous system, nicotine acetylcholine receptors are widely distributed, therefore their activation influences several molecular mechanisms in different brain areas that could be involved in tobacco addiction³ (Figure 1.1). nAChRs share a common basic structure but they are also distinguished in different subtypes (based on different subunit combinations), with distinct functional and pharmacological properties³⁴.

In the central nervous system it is possible to discriminate 2 different classes of nAChRs based on their binding affinity: one class of receptors that binds nicotine and nicotinic agonists with high affinity (nM affinity) and another class of receptors that bind nicotine with low affinity (μM affinity) and the antagonist α -bungarotoxin with high affinity³⁵. Heteromeric receptors consisting of different combinations of $\alpha 2$ - $\alpha 6$ and $\beta 2$ - $\beta 4$ belong to the receptor class showing high affinity for nicotine but no sensitivity for α -bungarotoxin, while homomeric or heteromeric receptors consisting of the $\alpha 7$, $\alpha 9$, $\alpha 8$, $\alpha 7$ - $\alpha 8$, or $\alpha 9$ - $\alpha 10$ belong to the second class of receptors³⁶.

It was reported that nicotine, in the brain, causes a post-transcriptional up-regulation of high-affinity receptors, and this effect could be considered another mechanism through which nicotine leads to addiction development³⁷.

In the brain, the most expressed nicotine acetylcholine receptors are $\alpha 4\beta 2^*$ (the asterisk indicates the presence of other subunits in the pentameric receptor) and $\alpha 7$. The former are particularly expressed by dopaminergic neurons in the VTA^{18,34,35}. Generally, in these neurons, $\alpha 4$ and $\beta 2$ assemble with $\alpha 3$, $\alpha 5$, $\alpha 6$ or $\beta 3$ subunits, forming several nicotine acetylcholine receptor subtypes that differ in subcellular localization, activation rates, ligand affinity, ionic permeability, and pharmacological profile⁵. $\alpha 7$ receptors are localized in the hippocampus, cortex, and subcortical limbic areas, and to a lower extent, in the thalamus and basal ganglia regions³⁴.

Studies performed on animal models (rats and mice) revealed that the $\alpha 3$ subunit is located in the pineal gland, medial temporal lobes and cerebellum, while the $\alpha 5$ subunit is localized in the striatum and cerebral cortex³⁸⁻⁴¹. Both are also expressed in the ventral tegmental area, in the substantia nigra and in the hippocampus.

Given the different distribution of nAChRs subtypes in the central nervous system, nicotine binding causes several different effects depending on the brain region involved. In the prefrontal cortex and hippocampus nicotine binding enhances memory and concentration, while in the mesolimbic pathway nicotine modulates the positive reinforcement and gratification mechanisms that lead to the development of addiction^{3,34} (Figure 1.1).

1.2.3 $\alpha 7$ nAChRs

CHRNA7 encodes the $\alpha 7$ subunit of the neuronal nicotinic acetylcholine receptor, which forms a homopentameric chloride channel receptor. This receptor is characterized by fast activation, rapid desensitization, high Ca^{++} permeability, and specific binding for selective ligands which include the antagonist α -bungarotoxin⁴². *CHRNA7* is widely expressed in both the brain and periphery with many important roles in cognition and the immune system. $\alpha 7$ receptors are localized both pre- and post-synaptically; in the brain, presynaptic $\alpha 7$ nAChRs are found in glutamatergic and GABAergic terminals in the hippocampus and other regions, where Ca^{++} influx leads to the release of many different types of neurotransmitters¹¹. $\alpha 7$ nAChR are localized also in the postsynaptic density (PSD)^{43,44} where Ca^{++} influx modulates CREB phosphorylation, causing alterations in gene expression²⁹.

1.3 The genetics of nicotine dependence

Nicotine dependence (ND) is considered a multifactorial trait determined by a complex interaction of several genetic factors, each having a modest effect, and environmental influences⁴⁵. Family and twin studies highlighted the importance of genetics in tobacco addiction and in different aspects of smoking behavior (including the number of cigarettes smoked daily and the dependence level), estimating a heritability greater than 60%^{45,46}. Furthermore it has been shown that the ability to quit smoking is also influenced by robust heritable factors⁴⁷. It has been estimated that 50% of the risk for a failed attempt at smoking cessation can be attributed to genetic factors^{48,49}. Interestingly, it was also reported that heritable influence on ability to quit smoking overlaps only in part with genetic influences underlying tobacco addiction⁴⁷. Therefore, analysis of ND is complicated, since several genes and environmental factors are involved in smoking phenotypes, and the different smoking-related traits could be attributed to different genetic underpinnings. In recent years, researchers have used several approaches to investigate the contribution of genetic factors to ND. Experimental methods for genetic studies of ND have evolved from genome-wide linkage studies to candidate gene association studies and from genome-wide association studies (GWAS) to targeted sequencing. The first three approaches rely on genotyping of genetic markers, which are polymorphic variants with a known position in the genome, such as microsatellites and single base changes named Single-Nucleotide Polymorphisms (SNPs). In the next coming years, whole-exome and whole-genome sequencing studies are expected

to become the main methods to analyze the contribution of rare and common variants involved in complex disorders/traits⁵⁰.

To understand the complex aspects of tobacco addiction, researchers have used different measures of ND in genetic studies. One of these is the level of ND, calculated by Fagerstrom test for ND (FTND)⁵¹. It is a questionnaire, containing six items of which three are yes/no items with a score from 0 to 1 and three are multiple-choice items with a score from 0 to 3. The sum of each items represents the total score spanning from 0 to 10 and provides a measure of ND: 1-2 = low dependence, 3-4 = low to moderate dependence, 5-7 = moderate dependence, > 8 = high dependence⁵². Others nicotine addiction related phenotypes include smoking quantity, referred to the number of cigarettes smoked per day (CPD) and smoking cessation, based on success or failure of smokers that attempt to quit. Furthermore, some genetic studies have also considered the age of smoking initiation as an additional phenotypic trait⁵.

1.3.1 Linkage analysis

Genetic linkage analysis is a powerful method to identify the chromosomal position of genes related to disease. For several years, linkage analysis has been the main approach for genetic mapping of both Mendelian and complex disorders showing familial aggregation^{53,54}. Linkage analysis is the process of determining the approximate chromosomal location of disease-causing variants by looking for evidence of co-segregation across generations with other markers whose locations are already known. Co-segregation is a tendency for two or more genes to be inherited together, and hence for individuals with the same trait to share alleles at the marker locus. The degree of linkage is a function of how close the loci are to each other, with widely spaced loci on the same chromosome behaving as if they were unlinked, thereby making it possible to estimate the location of variant involved in a specific disease relative to one or more known markers.

Linkage studies are focused on related individuals of large multigenerational families or a consistent number of small nuclear families (including father, mother, and their children). This approach allows to detect large candidate regions (in the order of Mb), spanning many genes, and its success may be hampered by genetic and phenotypic heterogeneity of the trait.

The linkage analyses used to map genes for monogenic disorders are said to be *parametric*, and in this case the data can be analysed only if a specific genetic model is assumed. This type of linkage is used in the study of Mendelian diseases occurring within multigenerational families containing different affected individuals, from which it is possible to infer the inheritance model of the locus disease. Instead, to analyze complex diseases, *nonparametric* methods may be used, that do not require the pre-specification of a genetic model. Nonparametric linkage studies are usually based on the analysis of large samples of affected sib-pairs. The aim is to obtain genome-wide marker data and then identify chromosomal regions that have been shared by affected sib pairs more often than would be predicted by random Mendelian segregation.

In 2008, Li et al. published a comprehensive review including more than 20 genome-wide linkage analysis of smoking behaviors⁵⁵. The linkage studies were performed across several populations using different nicotine addiction phenotypes, CPD, FTND, ever-smoking, habitual smoking, or maximum number of cigarettes smoked in a day (24h). In this study 13 regions, located on chromosomes 3–7, 9–11, 17, 20, and 22, have been identified to be suggestively or significantly linked with various ND measures in at least two independent samples. Three genes that encode for nicotine acetylcholine receptors are located in these suggestive or significant regions: *CHRNA10* (11p15), *CHRNA2*(8p21–22), and *CHRNA4* (20q13.2–q13.3). In 2009, Hardin et al performed a genome-wide linkage study of nicotine withdrawal sensitivity in 158 pedigrees with 432 individuals⁵⁶. This study identified a linked locus in the same region previously reported to be linked to FTND⁵⁷. More recently, a meta-analysis of 15 genome-wide linkage scans of smoking phenotypes was performed⁵⁸. This study, including 3404 families with 10253 individuals, detected a genome-wide suggestive linkage on chromosome 17q24.3–q25.3. The same region has been also detected in one sample reported in Li et al. 2008⁵⁵. Furthermore, the metaanalysis performed by Han et al., provided a genome-wide suggestive linkage in 5q33.1–5q35.2, and a genome-wide significant linkage in 20q13.12–q13.32⁵⁸. These results confirmed the previous finding showed in Li et al. (2008), even if, in this metaanalysis, the regions detected on chromosomes 5 and 20 are larger.

1.3.2 Association studies

Linkage analyses have limited power to detect susceptibility factors in complex disease, and have been largely supplanted by the alternative of association studies. The purpose of association studies is to detect an allelic association between specific genetic variants and the studied trait in closely unrelated individuals within a population. For example, if allele A1 at locus A is found to be significantly more frequent in people affected by a specific disorder than would be expected from the individual population frequencies of A1 and the disease gene, the allele A1 is positively associated with disease and, thus, it is a disease susceptibility allele.

To investigate disease associations, case-control studies can be performed in which genetic variants are genotyped in affected individuals (cases) and controls. Different methods can be used to measure the disease risk for each tested genetic variant, notably the odds ratio (the odds of being affected of individuals carrying a specific variant divided by the odds of being affected of individuals without the variant). Association between genetic variants and disease could be interpreted in different ways. Genetic variants associated with disease might be directly involved in the disorder, or they may be in Linkage disequilibrium (LD) with the variant contributing to disease risk. The LD describes any non-random association of alleles at different loci in a specific population.

Notably, the association identified in case-control analysis could also represent a false positive caused by chance or problems related to the use of inappropriate statistical methods or population stratification. As a result of population stratification, different subgroups within a broad population often have significantly different frequencies of a genetic variant, and this can confound genetic analyses. To minimize problems arising from population stratification, cases and controls used in association studies should have the same population ancestry.

Generally, the density of SNPs required for association studies is higher compared to linkage studies, but association studies allow to detect a candidate genetic region with a better resolution. Association studies do not require large families with several affected members, but can be carried out on unrelated case and control individuals or using nuclear families (e.g. trios: a proband and parents). Furthermore, association approaches are more appropriate to identify susceptibility genes involved in common and complex traits in which the risk of any given susceptibility variant is relatively small⁵⁹.

Association studies results are normally expressed as P values or $-\log_{10}(P)$, a strong association is observed when p-value is very low. Generally, a p value < 0.05 is taken as the threshold of statistical significance. However, the significance threshold must be corrected by the number of independent statistical tests performed; thus, testing for association using a large number of markers increases the required number of tests and the significance threshold should be more stringent.

Genetic association studies may be focussed on testing for association between variants within pre-specified genes of interest and phenotypic traits (candidate gene approach), or they may be extended to the whole genome. Genome-wide association studies (GWAS) involve the analysis of a large number of SNP markers throughout the entire genome.

1.3.2.1 Candidate-gene association studies

Candidate gene studies are focused on the study of genes that could be related to the trait or disease. The first step of candidate gene analysis is the selection of a putative candidate gene and, generally, it is based on its known biological, physiological, or functional relevance to the trait being investigated. Furthermore, a positional-candidate approach can be used to further investigate a putative region of interest arising from genome-wide linkage mapping or GWAS.

In ND, some biological pathways that regulate the intake of nicotine, its effects in central nervous system, and its metabolism are well known, but others are not⁶⁰. Candidate genes studies have been carried out to investigate the contribution of genes involved in those pathways:

- **Dopaminergic system**

Several studies focused on the dopaminergic system, considered the main contributor in development of drug addiction. Different studies identified statistically significant association with several variants and haplotypes in regions encompassing the dopamine receptor genes *DRD2*, *DRD1*, *DRD4* and smoking-related behaviours⁶¹⁻⁶⁴. Significant associations with smoking cessation and others nicotine addiction traits, have also been reported for genes involved in dopamine metabolism, including dopamine β -hydroxylase (*DBH*)^{61,65-67} DOPA decarboxylase (*DDC*)^{68,69} and catechol-O-methyl transferase (*COMT*)^{70,71}. Interestingly these genes, except *DBH* and *DDC*, are within or close to a modest linkage peak

and received support from GWAS⁷². Furthermore, the dopamine transporter gene, *SLC6A3*, has been implicated in smoking cessation in a meta-analysis performed on 2155 subjects⁷³. However, a more recent meta-analysis, which assessed eight studies, didn't confirm this result⁷⁴. Several candidate gene studies also examined the *OPRM1* gene, encoding for the endogenous opioids receptor. *OPRM1* A118G variant seems to be involved in increasing susceptibility to smoking behaviours, especially to ND, but less to smoking initiation and cessation⁷⁵.

- **GABAergic systems**

Different candidate gene association studies were performed on the region on chromosome 9, showing a “suggestive” linkage results for smoking-related behaviour in previous studies⁷⁶⁻⁷⁹. Several candidate genes were analysed, and among these, the GABAB receptor subunit 2 (*GABBR2*) gene. Variants in this gene were significantly associated with ND, in subjects of European and African origin⁷⁷. Another candidate gene in the GABAergic system is the GABAA receptor-associated protein (*GABARAP*) gene, located on chromosome 17 in a “suggestive” linkage region for tobacco addiction⁵⁸. Lou et al. reported two polymorphisms in *GABARAP* (rs222843 and rs17710) showing association with ND in European-American smokers⁸⁰. Furthermore, variants in the GABAA receptor subunits alpha 2 (*GABRA2*) and 4 (*GABRA4*) located on the chromosome 4p cluster, have been associated to smoking behaviour and alcoholism^{61,81,82}.

- **Serotonergic systems**

The serotonergic system may be involved in tobacco addiction, since nicotine intake leads to an increased release of serotonin in the brain and nicotine withdrawal behaviours are related to a reduction of serotonergic neurotransmission⁸³. Candidate genes studies reported a statistically significant association for variants in genes encoding for serotonin transporter (*SLC6A4*)⁸⁴⁻⁸⁶ and serotonin receptor (*HTR3A – HTR5A*), with different smoking phenotypes^{61,87}.

- **Glutamatergic system**

The increase of glutamate release is very critical in drug dependence. Analysis of genes involved in the glutamatergic system showed that variants in *GRIN3A* and *GRIN2B*, encoding

for ionotropic glutamate receptors, are significantly associated with FTND^{88,89}. In a GWAS performed by Vink et al. in 2009⁹⁰, a suggestive association with smoking-related phenotypes was reported also in other genes of the glutamatergic system, including *GRIK2*, *GRIN2A*, *GRM8* and *SLC1A2* genes, however, candidate genes studies did not replicate this result⁹⁰.

The formation of glutamatergic synapses can be regulated by neurexins, cell-adhesion molecules that play a role in synapse formation and maintenance. Interestingly, genes encoding for Neurexin 1 (*NRXN1*) and neurexin 3 (*NRXN3*) have been both associated to nicotine addiction⁹¹⁻⁹³.

- **Nicotinic receptors**

Different candidate-gene studies have been performed to analyse the association with nAChR subunit genes with ND behaviours. These studies, carried out by either case-control or family-based designs, identified a prominent association between several neuronal nAChRs genes and tobacco addiction phenotypes⁹⁴. Statistically significant results were identified for gene clusters on chromosomes 15, encompassing *CHRNA5*, *CHRNA3*, *CHRNB4* and for gene clusters on chromosomes 8, including *CHRNB3* and *CHRNA6* with ND^{95,96}. These findings represent also the major discoveries from GWAS of ND^{97,98}. Candidate gene studies also identified significant association for variants in other genes encoding nicotine receptors subunits (*CHRNB1*, *CHRNA4*, *CHRNA2* and *CHRNB2*) with tobacco addiction^{89,99-101}. GWAS of ND did not find significant association for variants within these genes, however *CHRNB1* and *CHRNA4* are reported to be close to linkage peaks⁵⁰. Genetic variants in *CHRNA3* and *CHRNA5* have also been shown to have a role in smoking cessation and in response to pharmacological smoking cessation treatments¹⁰²⁻¹⁰⁴. In particular, the rs16969968 non-synonymous SNP in *CHRNA5*, the variant with strongest association to ND implicated by GWAS, has an effect on NTR efficacy but not on varenicline efficacy in smoking cessation¹⁰⁵

- **Nicotine metabolism pathway**

CYP2A6 is the enzyme involved in metabolic inactivation of nicotine to cotinine. Several studies found that variants in the *CYP2A6* gene, causing a reduced enzyme activity, are associated with CPD, FTND, and other smoking-related behaviours^{61,106,107}. Furthermore, *CYP2A6* variants, have also been shown to have an effect on smoking cessation maintenance

and on response to cessation pharmacotherapy. Genotypes related to fast nicotine metabolism are associated to decreased smoking cessation success and to a higher response to NRT compared to slow nicotine metabolism genotypes¹⁰⁸.

1.3.2.2 Genome-wide association studies (GWAS)

In contrast to candidate gene studies, genome-wide association studies (GWAS) are based on a 'hypothesis-free' approach.

GWAS began to really take off in the mid-2000s because of two technological developments. First, in the last years, the creation of public international projects, including the HapMap Project (<http://hapmap.ncbi.nlm.nih.gov/>) and the 1000 Genome Project (<http://www.1000genomes.org/>) allowed to determine the common patterns of human genome variation characterizing SNPs, their frequencies and the degree of LD in DNA samples from different populations. Knowledge of the LD pattern between SNPs has very important practical implications¹⁰⁹. By analysing a non-redundant group of representative SNPs (SNPs tags), it is possible to impute the genotype of the other common variants in high LD with them. All SNPs in high LD belong to a group of SNPs called "haplotype block" and the tag SNPs are the variants sufficient to discriminate between all the haplotypes in the block. The most widely used measure of LD is the square of the correlation coefficient (r^2), which can range from 0 to 1 (1 when the two SNPs are in complete LD and perfectly correlated with each other). Based on empirical studies, it has been shown that most of the information on common human variability, represented by ten million SNPs in the human genome, can be obtained by analysing 200000 up to 1000000 tag SNPs^{110,111}.

Secondly, an important contribution to the spread of the whole genome association studies was given by the development of microarray platforms. SNP arrays enable to genotype hundreds or thousands of SNPs across the human genome at the same time and provide information about both copy number and genotype. Currently, companies such as Illumina and Affimetrix produce standard SNPs panels, by which it is possible to generate millions of genotypes with only one hybridization reaction, obtaining good quality data in brief time. Furthermore, GWAS depend on the availability of large samples of cases and controls.

GWAS projects have been designed to identify common variants on the assumption that common complex disorders are often caused by common variants (the "common disease-common variants" hypothesis)⁵⁹. Under this hypothesis, different combinations of common

variants at multiple loci increase disease risk in specific individuals. It was supported by known associations of common variants with complex diseases, for example in the 1990s the Apoε4 allele was found to be a susceptibility factor for Alzheimer's disease¹¹² and the factor V Leiden was associated to venous thrombosis¹¹³.

The bulk of GWAS have focused on case-controls studies in which panels of affected individuals and matched controls are genotyped at hundreds of thousands of common SNPs (where the minor allele usually has a frequency of at least 0.05). SNPs in which allele frequencies are significantly different in cases than in controls are identified as associated with the studied trait (Figure 1.3).

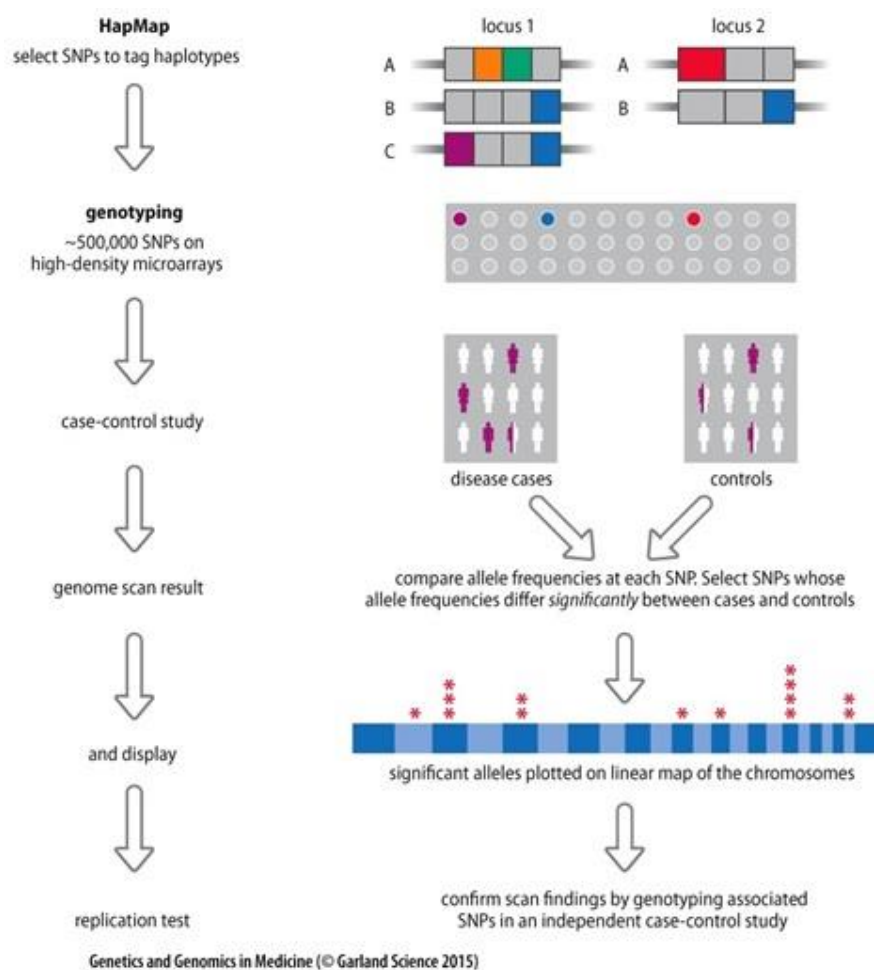


Figure 1.3: Outline of a genome-wide association (GWA) scan. Using HapMap data, representative SNPs are selected that will differentiate the common haplotypes at each locus. In this example, three common haplotypes (A,B and C) at locus 1 are tagged by four SNPs (with strong colour if present, or grey if absent). But just two SNPs (purple and blue) are sufficient to discriminate between the three haplotypes. Similarly, the two haplotypes at locus 2 can be distinguished by either the red or blue SNPs. Tag SNPs are then genotyped in case-control association study using microarrays, and the allele frequencies for each SNP are compared in the two groups. The significant results need then to be confirmed in an independent study.

In GWAS studies hundreds of thousands of common SNPs are investigated and therefore a huge numbers of association tests are carried out, hence stringent statistical significance thresholds are required to assess the significance of individual results. One way of setting a stringent genome wide significance threshold is to divide the standard p-value of 0.05 by the number of tests (Bonferroni correction). If one million of independent variants are tested in a GWAS, for example, a stringent P value would then be $0.05/1000000 = 5 \times 10^{-8}$. In any case, initial significant or promising GWAS results need to be confirmed by independent studies to gain additional confidence.

GWAS data can be visualized using two different types of plots (Figure 1.4):

- The Quantile-quantile (Q-Q) plot is used to explore the presence of systematic errors that may result in spurious association, such as stratification population. A Q-Q plot is a scatterplot created by plotting all observed p-values ranked from the smallest (the most significant) to the largest against the expected null distribution under the hypothesis of no disease association. Each p-value is converted to its negative log value. If there is no association, the plot of the observed versus expected results will form a 45° straight line. Deviation from the 45° reference line indicates a generalized shift of observed results from expected results for any level of statistical significance. Such a generalized shift indicates the presence of a systematic error such as population stratification, and these association results are likely spurious. A clean QQ plot, on the other hand, should show a straight line that sharply curves at the end (indicating few true association signals amongst thousands of unassociated variants) (Figure 1.4).
- The “Manhattan plot” is used to display GWA results according to their genomic position (x axis) and statistical significance (y axis, the negative log₁₀P scale helps reveal signals of particular interest) (Figure 1.4 B).

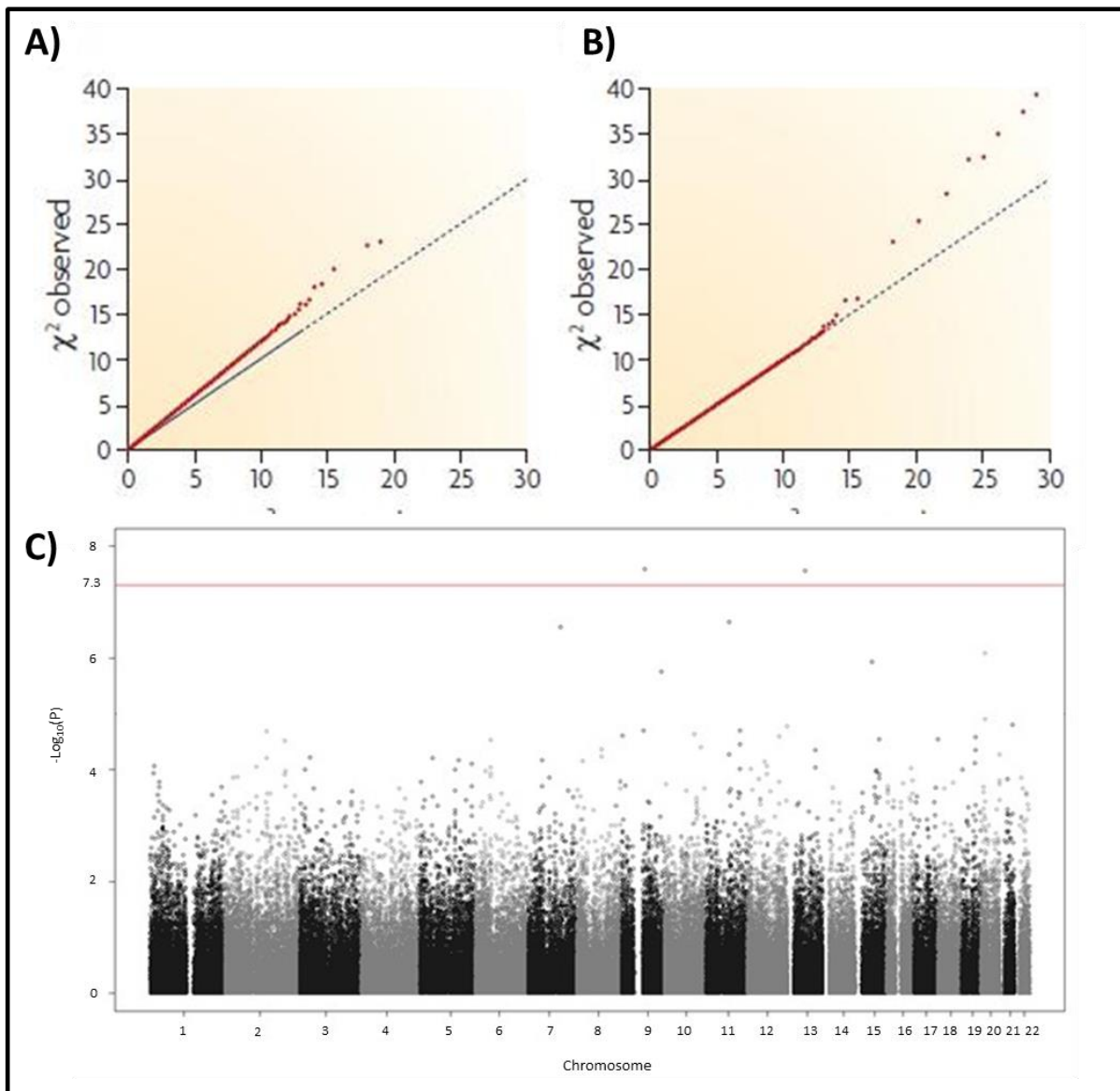


Figure 1.4: Visualizing genome-wide association (GWA) data. (A,B) Example of QQ plot visualizing observed GWAS results against theoretical expectation. The expected null distribution is a straight line (blue). (A) A problematic result showing a generalized shift of observed results from expected null results for any level of statistical significance. It indicates a systematic error such as population stratification. (B) The expected and observed results show similarity; for limited number of SNPs statistical significance values are higher than expected indicating true association. (C) An example of Manhattan plot summarizing GWAS results. The red horizontal line at position 7.3 on the vertical scale indicates the threshold of statistical significance in this particular example.

In recent years, a large number of GWAS have been performed, leading to the identification of hundreds of significantly associated variants to individual complex diseases (available in the GWAS catalog, <https://www.ebi.ac.uk/gwas/>). However, almost all of the identified susceptibility variants are of weak effect: even the cumulative contributions of the identified variants are usually quite small. That is, the available GWAS data can explain only a small proportion of the genetic variance of complex diseases. This observation has raised the issue of the “missing heritability”, that is the fact that SNPs associations cannot account for a large

proportion of the estimated heritability of a trait¹¹⁴. Several explanations have been put forward to justify the missing heritability. One of these is the evidence that GWAS with sample size of a few thousand cases and controls are well suited to identify susceptibility variants with odds ratio of 1.5 or more, but they are missing many true susceptibility factors of weaker effects (odds ratio ≤ 1.2). Much larger numbers of cases and controls are thus warranted to detect these weaker effect variants, either in single studies or in meta-analysis. Furthermore, a major limitation of GWAS is that they are focused only on the analysis of common variants. However, susceptibility to complex diseases could be also partly due to the contribution of a heterogeneous set of rare variants, individually with strong effects. In order to track down these specific rare variants whole-genome sequencing would be required. In addition, the proportion of heritability explained by known GWA variants does not take into account possible genetic interactions between loci and between genes and environmental components.

1.3.2.2.1 Results from GWAS on nicotine dependence

In recent years, several GWAS, using sets of about 500000 SNPs and including large numbers of participants, have shown that the strongest genetic contribution for smoking traits comes from variation in the nAChR subunit genes. The most prominent associations were found for variants in the *CHRNA5–CHRNA3–CHRNA4* gene cluster and in the *CHRNA3/CHRNA6* gene cluster, converging with previous candidate-gene studies results of nicotine receptors genes^{98,115-117}.

The importance of the *CHRNA5/A3/B4* gene cluster in several aspects of ND was highlighted by three GWAS meta-analyses^{72,97,118}. In this gene cluster three groups of risk variants for heavy smoking and ND have been identified. One group is marked by the non-synonymous SNP rs16969968 located in exon 5 of the *CHRNA5* gene, which causes a substitution of amino acid asparagine with aspartic acid at position 398 (D398N). Homozygous individuals for the rs16969968 minor allele (A) are about twice as likely to develop tobacco addiction, in a recessive model of inheritance⁶¹. rs16969968 is tightly linked to rs55853698, rs2036527, and rs1051730, which are also found to be significant associated to smoking phenotypes, including both CPD and FTND score. The second associated variant group is tagged by rs588765, located on *CHRNA5* intron 1. This polymorphism regulates *CHRNA5* expression: the C/C genotype is associated to low gene expression while the T/T genotype is related to

an increased expression of *CHRNA5* that is associated to higher risk for ND¹¹⁹⁻¹²¹. The third risk variants group is marked by rs578776, located on the 3'-untranslated region (UTR) of *CHRNA3*. The correlation between 16969968, rs588765 and rs578776 is very low, suggesting that they represent independent contributions to ND (Figure 1.5). The GWAS meta-analyses of smoking dependence did not identify SNPs in the *CHRNA4* receptor subunit gene that could contribute to the genetic association signal for heavy smoking^{72,97,118}. Therefore, to date, it is not clear if common variants in *CHRNA4* contribute to tobacco addiction, however, a possible role of this gene in ND can be hypothesized, given the high LD patterns existing across *CHRNA5*, *CHRNA3*, and *CHRNA4*.

The GWAS performed by Bierut et al. (2007) in 1050 cases and 879 controls, showed also a suggestive association for rs13277254 in *CHRNA3* with ND¹¹⁵. This variant is in LD with two other SNPs located on chromosome 8p11 (rs6474412, and rs13280604) that showed a statistically significant association with CPD in a genome-wide association meta-analyses performed in 31266 smokers by Thorgeirsson et al.⁹⁷ Furthermore, another variant on *CHRNA3* (rs1451240), has been associated to CPD in a GWAS of ND performed by Rice et al.¹²². All these variants (rs13277254, rs6474412, rs1451240, rs13280604) belong to the same LD block including *CHRNA3* and *CHRNA6* genes¹²². GWAS of tobacco addiction also detected statistically significant associations in the region on chromosome 19q13.2 encompassing the following genes: *CYP2A6*, *CYP2A7*, *CYP2B6*, *EGLN2*, *RAB4B*, and *NUMBL*¹²³. The association between *CYP2A6* and ND is also supported by candidate gene studies¹²⁴.

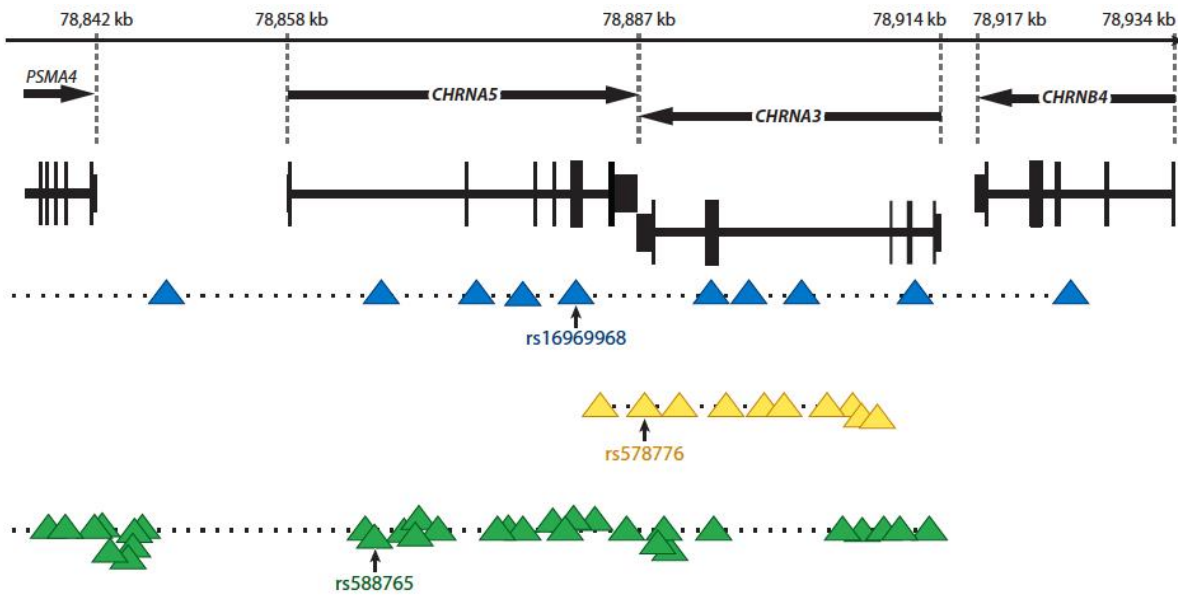


Figure 1.5: *CHRNA5-CHRNA3-CHRNB4* gene cluster on chromosome 15 in the human genome. Triangles represent SNPs: SNPs with the same colour are highly correlated with each other but not with SNPs in other colours. SNP position is not drawn to scale (Wang et al. 2012)¹²¹.

1.3.3 Targeted sequencing studies

Complex traits could be due to a complex interplay of several rare and common variants conferring different individual risk and collectively involving a large number of different genes¹²⁵. Rare genetic variants cannot be detected by GWAS and, thus, the use of next-generation sequencing approaches could help to understand the contribution of rare variants in complex traits susceptibility.

In the ND field, one of the first analysis of rare variants was performed by Wessel et al. in 2010⁹⁶. In this study, researchers tested the contribution of common and rare variants in 11 nAChR genes to severity of ND (FTND score) in 448 smokers. They observed a significant association for both common and rare variants in *CHRNA5* and *CHRNB2*, and only for rare variants in *CHRNA4* with the FTND score.

More recently, Olfson et al., reported that common and rare *CHRNA5* coding variants are independently associated with nicotine addiction susceptibility¹²⁶.

In order to investigate the role of *CHRNA4* rare variants on ND, Xie et al. sequenced all *CHRNA4* coding region in 209 smokers and 183 control subjects¹²⁷. The sequencing of *CHRNA4* exon 5 was also performed in additional 1000 smokers and 1000 control subjects. They identified that functional rare variants in *CHRNA4* could reduce the risk of ND.

Moreover, an effect in reducing risk for tobacco addiction has been also observed for missense rare variants at conserved residues in *CHRNB4*. In vitro study of the two variants

contributing most to *CHRNA4* association (T375I and T91I) and a variant in *CHRNA3* (R37H) in strong linkage with T91I reveals that the minor allele of each polymorphism increase cellular response to nicotine¹²⁸. Slimak et al. investigated the contribution of allelic variants of $\beta 4$ to nicotine receptor activity in the medial habenula (MHb) in mice¹²⁹. They found that 2 previously associated variants ($\beta 4A90I$ and $\beta 4T374I$), and another variant ($\beta 4D447Y$) in *CHRNA4*, significantly increased nicotine-evoked current amplitudes, while the variant $\beta 4R348C$, showed decrease nicotine currents. Moreover, they reported that habenular expression of the $\beta 4$ gain-of-function allele T374I resulted in strong aversion to nicotine in mice, while transduction with the $\beta 4$ loss-of function allele R348C do not induce nicotine aversion. More recently, a targeted sequencing study was performed in 30 candidate genes previously involved in tobacco addiction to test both the single and the cumulative effects of rare and common variants in 3088 African Americans and 1430 European American smokers¹³⁰. After Bonferroni correction, no common variant showed statistically significant association with FTND, indexed CPD and smoking status. However rare variants in *NRXN1*, *CHRNA9*, *CHRNA2*, *NTRK2*, *GABBR2*, *GRIN3A*, *DNM1*, *NRXN2*, *NRXN3* and *ARRB2* showed statistically significant association with smoking status in African American smokers. In European American smokers a significant increase of rare variants in *NRXN1*, *CHRNA9*, *TAS2R38*, *GRIN3A*, *DBH*, *ANKK1/DRD2*, *NRXN3*, and *CDH13* was reported. A significant cumulative effect of rare and common variants in ND susceptibility was identified in *CHRNA9* in European American smokers.

1.3.4 *CHRNA7* and *CHRFAM7A* gene

CHRNA7 is located on chromosome 15q13.3 which is one the most unstable regions of the human genome. The proximal region of the long arm of chr15 (15q11-q13) is a well-known hotspot for CNVs, given the existence of highly homologous low copy repeats (LCRs). The pathogenic role of 15q13.3 microdeletions has been proven for many neurodevelopmental and psychiatric conditions (including idiopathic generalized epilepsy, intellectual disability, autism and schizophrenia)¹³¹⁻¹³⁴. Strong evidence supporting *CHRNA7* as the major candidate gene responsible for the clinical phenotypes associated to the 15q13.3 deletion, derives from the identification of subjects with smaller deletions comprising only the entire *CHRNA7* gene, and conveying most or all of the phenotypic alterations associated with the larger 15q13.3 recurrent deletions¹³⁴⁻¹³⁶. Conversely, the reciprocal microduplication involving

CHRNA7 has a less certain clinical significance compared with the deletions, as it is identified across the same spectrum of neuropsychiatric phenotype observed with the microdeletions, but without the same high penetrance, and it is also common in the general population with an estimated frequency of 1 in 180¹³⁷.

A chimeric gene called *CHRFAM7A* is present at 1.6 Mb centromeric to *CHRNA7*; it derives from the fusion between a partial duplication of *CHRNA7*, including exons 5 through 10 and exons A–E of the *FAM7A* gene¹³⁸ (Figure 1.6). The formation of *CHRFAM7A* is human-specific and the duplication is evolutionary new: *CHRNA7* and *CHRFAM7A* are highly homologous in their duplicated portion (99.9%). *CHRFAM7A* is present in variable number of copies; some individuals have only one copy of *CHRFAM7A* and rare subjects have no copies. The translation start site of *CHRFAM7A* is in exon B and it is in frame through the *CHRNA7* sequence, leading to a peptide subunit, called dup α 7, that is a truncated form of *CHRNA7* missing the 5' acetylcholine binding site^{139,140}. The dup α 7 transcript has been identified in brain, immune cells, and the HL-60 cell line¹⁴¹, although its translation product and function are still unknown. In vitro studies indicate that *CHRFAM7A* assembles with α 7 subunits, causing a decrease of acetylcholine-stimulated current thus dup α 7 may act as a dominant negative regulator of α 7nAChRs function^{140,141}.

CHRFAM7A also harbors a polymorphic 2bp deletion within exon 6, rs67158670 -/TG (Δ 2bp), which is never observed in the homologous *CHRNA7* sequence and it is predicted to result in a truncated protein. However, since there are two methionine codons in exon 6, it is likely that translation could start from one of these methionine leading to a shorter dup α 7 peptide^{139,140}.

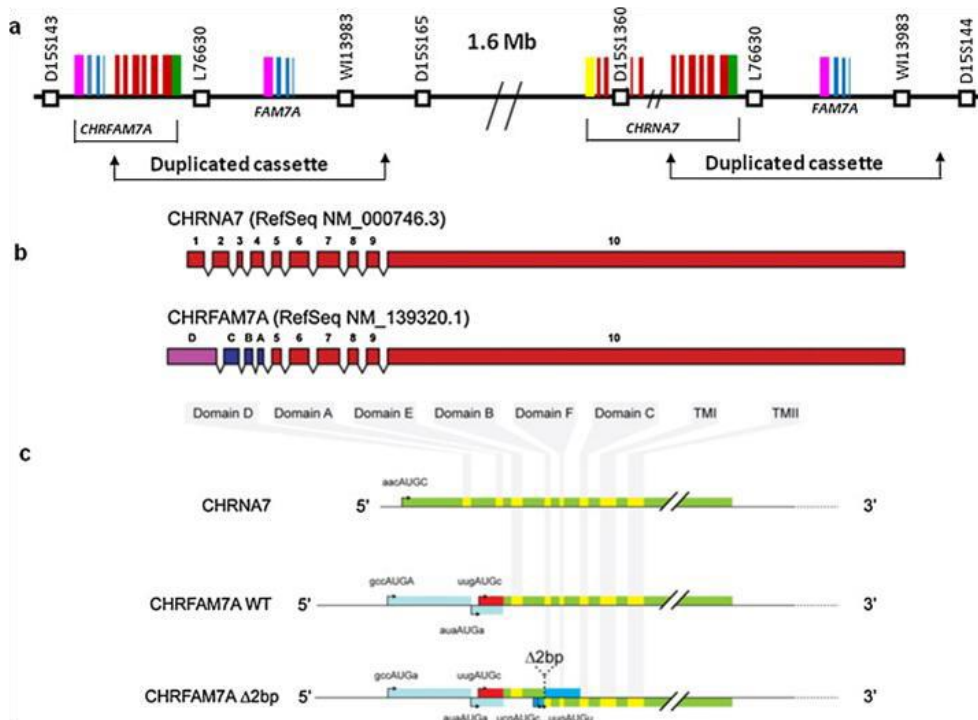


Figure 1.6: *CHRNA7/CHRFAM7A* gene cluster on human chromosome 15q13.3. a) Representation of *CHRNA7* and *CHRFAM7A* on 15q13.3: Exons 5-10 of *CHRNA7* are duplicated in a duplication of about 300kb at 1.6 Mb centromeric to *CHRNA7*. The duplication is fused to a partial duplication of a second gene, *ULK4*. b) Exon organization of the transcripts encoded by *CHRNA7* and *CHRFAM7A* RefSeq NM_000746.3 and NM_139320.1. c) Putative translation products from *CHRNA7*, *CHRFAM7A*, and *CHRFAM7A* $\Delta 2bp$ mRNAs. In green and yellow (the colour indicates the different domains) are represented the $\alpha 7$ amino acid sequence. In red and in blue are represented the alternative amino acids from *CHRFAM7A* and alternative amino acids from *CHRFAM7A* $\Delta 2bp$ respectively (Araud et al., 2011)¹⁴⁰.

The *CHRFAM7A* $\Delta 2bp$ allele has been associated to schizophrenia¹⁴² and to the P50 sensory gating deficit, a possible endophenotype for schizophrenia¹⁴³. The P50 is an electroencephalographic event-related potential wave occurring about 50 ms after a stimulus, that often is an acoustic click. The P50 response is used to measure sensory gating, by paired-click paradigm¹⁴⁴. This non-invasive technique consists in emitting an auditory click sound, followed by a successive click emitted about 500 ms after the first one. Usually, for an individual with normal sensory gating the second sound is redundant, and, thus, the response, related to the second click (measured by electroencephalographic wave amplitude), is decreased. Comparing the amplitude of the second auditory stimulus with the first one, it is possible to measure the reduction percentage. Normal subjects have an amplitude reduction of about 80%, while schizophrenic subjects show a reduction of only 10-20%¹⁴⁵.

Analysis of the frequency of the *CHRFAM7A* $\Delta 2bp$ allele in a cohort of schizophrenic individuals (N=70) and controls subjects (N=77) revealed that, while no difference was

detected among cases and control, the $\Delta 2\text{bp}$ allele seemed to confer risk to P50 sensory gating deficit, as genotypes with at least one $\Delta 2\text{bp}$ allele are more frequent in individuals with the P50 abnormality compared to individuals with normal P50¹⁴⁶. The association of $\Delta 2\text{bp}$ allele with P50 sensory gating deficit was also highlighted by a successive study on families with schizophrenia or bipolar disorder¹⁴³. Furthermore, association analysis in a Caucasian group (317 schizophrenic patients and 192 controls), in an African Americans group (66 schizophrenic patients and 60 controls), and in an Hispanic group (13 schizophrenic patients and 37 controls) confirmed an effect of the $\Delta 2\text{bp}$ variant with schizophrenia in Caucasian individuals and in African American subjects¹⁴². Another study also reported an association between the *CHRFAM7A* $\Delta 2\text{bp}$ allele and idiopathic generalized epilepsy¹⁴⁷. A mild effect of *CHRFAM7A* copy number with psychiatric disorder was also identified: the absence of *CHRFAM7A* showed a slightly association with schizophrenia and bipolar disorder when considered as a joint psychiatric phenotype¹⁴⁸.

Moreover, a study on a sample of patients with major psychiatric disorders (schizophrenia bipolar disorder and major depression) showed an altered ratio of *CHRFAM7A/CHRNA7* expression measured in postmortem prefrontal cortex, mainly due to overexpression of *CHRFAM7A* in this region¹⁴⁹.

Multiple independent studies have also suggested an important role of *CHRNA7* in schizophrenia. In particular, SNPs in the promoter region of *CHRNA7* have been associated to the P50 inhibitory deficit¹⁵⁰, and to schizophrenia^{151,152}. Interestingly, some of these variants have been reported to reduce *CHRNA7* promoter activity in in-vitro functional studies¹⁵⁰. Furthermore, several studies reported a decreased *CHRNA7* expression in multiple regions of post-mortem brain in schizophrenic individuals, including the hippocampus¹⁵³, cortex^{154,155}, and the reticular thalamic nucleus¹⁵⁶.

1.3.4.1 Role of *CHRNA7-CHRFAM7A* loci in ND

The genetic contribution of *CHRNA7* gene in ND has not been extensively studied, however, several neurobiological evidences support a significant role for the homomeric $\alpha 7$ nAChR in tobacco addiction.

As previously described, *CHRNA7* has been strongly associated with schizophrenia and with the specific schizophrenia endophenotype P50. Schizophrenic individuals have a very high risk for tobacco dependence, with a prevalence of around 80%, nearly three times the rate in

the general population and higher than the elevated rates of smoking in patients with other psychiatric disorders^{157,158}. A study performed on individuals with schizophrenia from Canada, showed a statistically significant association between the D15S1360 marker in *CHRNA7* intron 2 and smoking risk¹⁵⁹. However, no association was found between the polymorphism rs149637464 in *CHRNA7* promoter and smoking status among UK patients with schizophrenia¹⁶⁰.

In vivo studies in rodents have demonstrated that reductions in $\alpha 7$ nAChR function promote nicotine use, proposing that low expression of $\alpha 7$ nAChRs may act as a potential mechanism of a shared vulnerability to tobacco use and schizophrenia¹⁶¹. Furthermore, a study performed by Harenza et al., using pharmacological approaches, reported that *CHRNA7* contributes to nicotine conditioned place preference: the gain-of-function $\alpha 7$ mice did not show nicotine preference at all dose analyzed, in contrast to $\alpha 7$ knock-out mice that displayed nicotine place preference at a lower dose than normally required to show preference¹⁶². Preclinical studies using rodent intravenous nicotine self-administration also suggested that $\alpha 7$ nAChR might be involved in addiction mechanisms by modulating the activity of $\beta 2^*$ nAChRs¹⁶³. In fact, it has been reported that the activation of $\beta 2^*$ nAChRs facilitates nicotine self-administration, while the stimulation of $\alpha 7$ nAChRs seems to negatively modulate both nicotine reinforcement and $\beta 2^*$ nAChR function in the VTA.

Varenicline, a drug approved by US Food and Drug Administration for use as smoking cessation aid, is a $\alpha 4\beta 2$ nAChR partial agonist; although with lower affinity, varenicline is also a full agonist of $\alpha 7$ nAChRs¹⁶⁴. The same drug has been shown to provide some cognitive improvement in people with schizophrenia^{165,166}. It is thus possible that activation of $\alpha 7$ nAChRs can contribute to the action of varenicline as a treatment for smoking cessation and schizophrenia.

1.4 Treatments for nicotine addiction

Currently, treatment for smoking cessation includes various methods, from behavioural counselling to pharmacotherapy. The quitting success rate for cigarette smoke is higher in individuals that receive treatment consisting in behavioural and/ or pharmacotherapy than individuals who do not seek help¹⁶⁷. Several evidences support that the combination of medication and counselling or psychological therapies are more effective than their use alone¹⁶⁷. It was reported that smoking cessation rates increases of about 8% to 14% in

individuals that received both behavioural counselling and pharmacotherapy compared to individuals that did not received treatments or behavioural counselling only¹⁶⁷.

Given the elevated costs to society for cigarette smoking related diseases, the treatments aimed at smoking cessation are certainly among the most cost-effective interventions in health care^{168,169}.

1.4.1 Behavioural counselling

Behavioural counselling represents an integral component of comprehensive tobacco dependence treatment and it is based on advice, discussion, encouragement, and other activities aimed to help quit attempts succeed¹⁷⁰. Behavioral interventions includes individual or group therapy sessions, furthermore it is possible offer support by telephone counselling¹⁷¹.

Counselling usually uses behaviour change techniques addressing some factors, among which motivation, that has an important role in smoking abstinence success¹⁷⁰. It has been demonstrated that behavioural interventions are effective in helping smokers to quit, and moreover, it is reported that intensive behavioural counselling (10 minutes for session) are more effective on smoking cessation than brief interventions (3 minutes per session)¹⁷².

It was reported that the quitting success rate increases of about 11% to 15% in pregnant women that received behavioural counselling compared with controls (no interventions)¹⁷³.

1.4.2 Pharmacological therapy

Treating Tobacco Use and Dependence clinical practice guidelines divided pharmacological therapy for treatment nicotine addiction in two categories: first-line medication, including nicotine replacement therapy (NRT), bupropion, and varenicline; and second-line therapies, including nortriptyline and clonidine¹⁷².

The latter category of therapies are not approved by US Federal Drug Administration (FDA) and, given their side effects, are recommended only when first-line treatments are not effective or not tolerated.

Pharmacotherapy for ND acts through the reduction of craving and withdrawal symptoms and, moreover, it decreases the short-term reinforcing effects of tobacco.

The description of treatments included in the first-line category are listed below:

- **Nicotine replacement therapy (NRT)**

NRT is one of the most common treatment used to help smokers to quit¹⁷⁴. The main action mechanism is the replacement of nicotine effects obtained by tobacco consumption, and, through this, the reduction of the severity of withdrawal symptoms, cravings, and reinforcing effects of nicotine obtained from tobacco. Furthermore, it provides an alternative source of reinforcing and cognitive effects¹⁷⁵. NRT does not entirely eliminate all withdrawal symptoms since the delivery systems do not replicate the fast and elevated levels of nicotine obtained by inhalation of cigarette smoke^{176,177}.

Nicotine replacement therapy is available in different formulations, including patch, gum, nasal spray, inhaler, lozenge and, among all these formulations, there is no evidence for a differences in treatment efficacy¹⁷⁸.

The side effects depend on the formulation used, usually it is contraindicated in individuals with uncontrolled hypertension and myocardial infarction within the past 6 weeks.

- **Bupropion**

Bupropion is an antidepressant that it has been found to have a positive effect on smoking cessation. Its action mechanism in help smoker to quit is not comprehensively understood, however both dopamine and norepinephrine reuptake inhibition and a light nicotinic antagonist activity could lead to the reported decrease in the severity of nicotine cravings and withdrawal symptoms^{179,180}. Two different studies suggested that bupropion and NRT have similar effects on smoking cessation^{178,181}. The most common bupropion side effects are insomnia, occurring in 30-40% of individuals, and dry mouth, occurring in about 10% of individuals¹⁸¹.

- **Varenicline**

Varenicline, launched in 2006, is a drug approved by The United States Food and Drug (US-FDA) Administration for use as smoking cessation aid. In the last 10 years, varenicline has been the main prescription drug to treat smoking cessation. Among all pharmacologic treatments, varenicline is the intervention that provides the highest smoking cessation rate (28%). The quit success rate for individuals treated with bupropion is instead 19% and 17% for individuals using NRT¹⁸².

Varenicline has a receptor-dependent mechanism of action, acting as a $\alpha 4\beta 2$ neuronal nicotinic acetylcholine receptor partial agonist and, although with lower affinity, as a full

agonist of $\alpha 7$ nAChRs¹⁶⁴. Varenicline reduces the cravings and withdrawal symptoms in individuals attempting to quit smoking. Moreover, it could reduce the pleasurable effects of cigarettes, thereby potentially decreasing the relapse risk^{183,184}.

Two identically randomized, double-blind, multicentre trials have reported that varenicline is much more effective than placebo (odds ratio of 2.5) and it is more effective than bupropion (odds ratio of 1.7)^{185,186}.

The use of varenicline was approved for up to 12 weeks by US-FDA. However, if individuals maintain smoking cessation the use of varenicline can be prolonged for another twelve weeks¹⁸⁷.

Varenicline has never been tested in subjects under 18 years old or pregnant women and, thus, it is recommended to avoid the use in these two categories¹⁸². Furthermore, individuals should not have a history of psychiatric disorders before starting varenicline and medical staff should advise them to stop varenicline in case of agitation, depressed mood, or any other changes in behaviour not characteristic of nicotine withdrawal. The main varenicline side effects are nausea, insomnia, gastrointestinal upsets and headache; however, the incidence of adverse events leading to drug discontinuation is not different to that reported taking the placebo^{185,186}.

CHAPTER 2

Cluster headache

2.1 Clinical features

Cluster Headache (CH) is a rare primary headache with a mean prevalence of 0.1% among general population and 1% among Third Level Headache Centers. The term “cluster” originates from the tendency of attacks to cluster together into bouts that last several weeks followed by periods of remission, which can last for several months to years. CH shows a clear male predominance with a male:female ratio between 2.5-3.5:1¹⁸⁸.

The disease is characterized by a well-defined clinical picture and the diagnosis is made according to the International Classification of Headache Disorders (2013)¹⁸⁹. A patient with CH has to experience at least 5 attacks according to the criteria listed below:

- Unilateral retro-orbital or fronto-temporal pain, lasting from 15 to 180 minutes,
- Association with either one or both symptoms listed below:
 - at least one of the following signs, ipsilateral to the headache: a) conjunctival injection and/or lacrimation b) nasal congestion and/or rhinorrhoea c) eyelid oedema d) forehead and facial sweating e) forehead and facial flushing f) sensation of fullness in the ear g) miosis and/or ptosis
 - a sense of restlessness or agitation
- Attacks have a frequency ranging from 1 every two days to 8 times a day.
- Exclusion of other disorders.

CH attacks show a characteristic circadian periodicity (Table 2.1): they tend to occur at almost the same time every day especially at night, during the first REM sleep¹⁹⁰ and are also more frequent in spring and autumn¹⁹¹. Thus, CH displays both a typical circadian and a circannual rhythmicity.

Cluster headache can be distinguished in episodic, affecting 85-90% of patients, and chronic¹⁸⁹. The main difference between these two forms is in the remission period that in the first case must be at least one month while in the second case CH patients show continuous attacks and no remission periods.

During the attacks the patient is restless, unable to remain motionless, tends to isolate, refuses to be touched or comforted, walks nervously and writhes¹⁹². These behaviours highlight how the life quality of subjects with CH is strongly compromised and thus the primary need for patients is to suspend the attacks.

Most of CH attacks are spontaneous, however, in some cases may be triggered by different factors including alcohol intake and volatile substances such as solvents, oil-based paints NO-donors like nitroglycerin and histamine^{193,194}.

Features	Cluster headache
Pain location	Unilateral retro-orbital or fronto-temporal
Pain duration	15-180 minutes
CH periodicity	Circannual
Attacks periodicity	Circadian
Attacks frequency	1-8 times a day
Associated symptoms	Myosis, palpebral ptosis, conjunctival injections, tearing, nasal congestion and rhinorrhea
Behaviour during the attacks	Agitated, restless
Sex	Males: females = 2.5-3.5:1
Start age	20-50 years

Table 2.1 Main features of cluster headache

2.2 Pathophysiology

Despite its clear clinical presentation, the biology of CH is poorly understood. Because of the circadian and seasonal rhythmicity of attacks the involvement of the biological clock has been proposed. Furthermore, a possible role has been hypothesised for vasomotor changes, inflammation, immune changes, autonomic system imbalance and hypothalamic dysfunction. All these processes may also be interrelated, participating together in the genesis of CH symptoms¹⁹⁵.

Evidence for activation of the trigeminovascular system and the cranial parasympathetic nervous system, which are involved in controlling cranial vascular reactivity, has been reported^{196,197}. During the crisis, the concentration of CGRP (calcitonin gene related peptide) and VIP (vasoactive intestinal peptide) increases at the external jugular vein, indicating the

activation of the trigeminovascular and parasympathetic nervous system^{196,198}. This process leads to intracranial vasodilatation with consequent pain, sterile neurogenic inflammation, oedema and protein discharge at dural level^{195,198,199}. Neurogenic inflammation can activate trigeminal nerve fibres themselves, which transmit pain inputs to the spinal trigeminal nucleus (STN) and, via the ventral postero-medial nucleus of thalamus (VPMN), to the cortex²⁰⁰. Furthermore, the activation of trigeminal-parasympathetic reflex leads to onset of autonomic signs including tearing, nasal congestion, rhinorrhoea and sweating^{196,199}.

Nitric oxide (NO) has been suggested as a common mediator of vascular headache pathophysiology²⁰¹. In CH patients, increased levels of NO in the plasma have been found. Furthermore, several studies have shown that the administration of nitroglycerin, a NO donor, can trigger a headache attack during the active phase of cluster^{201,202}. NO acts as a potent vasodilator, but also it plays a role in central and peripheral modulation of nociception²⁰³, especially in both initiation and maintenance of hyperalgesia^{204,205}. These processes are probably associated with activation of the calcium dependent NO synthase (NOS) isoforms²⁰⁶.

NO is also involved in inflammation. It has been supposed that NO induces the release of CGRP, however other findings failed to support this suggestion^{207,208}.

CH patients seem to show alterations in melatonin metabolism compared to control. The melatonin production, normally follows a circadian rhythmicity with a minimum level during the day and a peak during the night. This hormone is a marker of pineal gland activity and it is involved in regulation of sleep-wake rhythmicity¹⁹⁴. Melatonin and its rhythmic secretion are regulated by the suprachiasmatic nucleus²⁰⁹.

Neuroimaging studies using PET (positron emission tomography) confirmed a dysfunction of chronobiological rhythms with the involvement of suprachiasmatic nucleus of the hypothalamus. These investigations, carried out during CH attack, demonstrated the activation of the ipsilateral hypothalamic grey matter²¹⁰.

Furthermore, functional magnetic resonance (fMR) studies have shown the activation of posterior hypothalamus during attacks²¹¹. Posterior hypothalamus is connected with the STN and its activation can activate both the trigeminal system and the parasympathetic reflex, inducing pain and autonomic symptoms²¹².

Based on these observations, CH can be considered a central nervous system disorder that is manifested by neurovascular mechanisms in which the hypothalamus is involved²¹².

The activation of both the trigemino-vascular and cranial parasympathetic systems provides the anatomical basis for the expression of the first division trigeminal pain and the ipsilateral autonomic symptoms that occur during cluster attacks¹⁹⁴. However, the primary trigger of the trigemino-vascular system activation remains still unknown.

2.3 The genetics of cluster headache

Twin and family studies have indicated the importance of genetic factors in CH¹⁸⁸. Twin data is scarce given the rarity of the disorder, however, monozygotic twins show a higher concordance rate for CH than dizygotic twins. Familial aggregation has been demonstrated by several studies: first-degree relatives of CH patients have a 5-to 18-fold increased risk and second-degree relatives a 1-to 3-fold increased risk (depending on the estimate of prevalence)¹⁸⁸. Despite the evidence of genetic factors in CH, the inheritance model is very complex. A putative autosomal dominant inheritance with low penetrance has been reported in some families, although in the majority of cases the inheritance is likely multifactorial, resulting from interactions between various genetic loci and environmental factors²¹³.

Nowadays, the molecular genetic background of CH is still largely unknown²¹⁴. The complex nature of the disorder and its low prevalence have hindered the genetic analysis of CH.

2.4 Molecular genetic studies of Cluster headache susceptibility

At the time our project started, only a limited number of small-scale linkage and candidate gene association studies have been performed in order to investigate the genetic risk factors involved in CH aetiology. These studies are summarized in table 2.2 and described more in detail in paragraph 2.4.1 and paragraph 2.4.2.

Study	Study design	Genes/variants investigated	Subjects	Results
Sjostrand et al. 2001	Case control association	An intragenic polymorphic (CA) _n -repeat (D19S1150) in <i>CACNA1A</i> and a (CAG) _n -repeat in the <i>CACNA1A</i> 3'UTR region	75 CH patients, 108 controls	No association
Sjöstrand et al. 2002	Case control association	Five polymorphic microsatellite markers in <i>NOS1</i> , <i>NOS2A</i> , <i>NOS3</i>	91 CH patients, 111 controls	No association
Aridon et al. 2004	Linkage analysis	The 6q23 region including <i>TAR1</i> , <i>TAR3</i> , <i>TAR4</i> , <i>TAR5</i> , <i>PNR</i> , <i>GPR58</i>	6 CH patients, 10 healthy subjects	No significant linkage
Rainero et al.2004	Case control association	-3250C>T (rs4796717), -1717C>T (rs8072081) in <i>HCRT</i> ; 264T>C (rs1056526), 1375C>T (rs2271933) in <i>HCRTR1</i> and 1246G>A (rs2653349), IVS4+12.564A>C (rs1027650) in <i>HCRTR2</i>	109 CH patients, 211 controls	Significant association between CH and the rs2653349 variant (1246 G>A)
Rainero et al.2005	Case control association	C282Y and H63D mutations in the <i>HFE</i> gene	109 CH patients, 211 controls	No association
Baumber et al. 2006	Genome-wide linkage analysis	400 markers, 9 cM spacing Additional markers around four markers with suggestive linkage from 5 Danish pedigrees	5 Danish pedigrees 33 Danish and Italian pedigrees, 82 members affected	Suggestive linkage: D2S1353, D2S1363, GATA151F02 (Chr 8), D9S2169 No significant linkage
	Case control association	1246G>A (rs2653349), rs3122169 in <i>HCRTR2</i>	259 CH patients, 267 controls	No association
Schurks et al.2006	Case control association	1246G>A (rs2653349) in <i>HCRTR2</i>	226 CH patients, 266 controls	Individuals with GG getotype had a twofold increase in risk for CH (OR 1.97; 95% CI 1.32 to 2.92; p = 0.0007)
Fourier et al. 2008	Case control association	rs1800759 and rs1126671 mutations in <i>ADH4</i>	390 CH patients, 389 controls	No statistically significant association for rs1800759C>A and rs1126671G>A
Cevoli et al. 2008	Case control association	T3111C variant (located in the 3' flanking region of the <i>CLOCK</i> gene)	101 CH patients, 100 controls	No association
Zhang et al. 2010	Case control association	<i>PER3</i> VNTR (variable number tandem repeat) polymorphism	149 CH patients, 432 controls	No association
Schurks et al. 2011	Case control association	rs1801133 in <i>MTHFR</i>	147 CH patients, 599 controls	No association

Study	Study design	Genes/variants investigated	Subjects	Results
Summ et al. 2010	Case control association	common polymorphism in <i>SERPINA1</i>	55 CH patients, 55 controls	No association with CH. Among CH patients, those heterozygous for M allele had more frequent attacks per day (median, 3) than those homozygous for M allele (median, 2; P=0.02).
Weller et al. 2015	Case control association	1246G>A (rs2653349) in <i>HCRTR2</i>	575 patients, 874 controls	No association
	Case control association (Meta-analysis)		1167 CH patients, 1618 controls	Significant association between CH and the rs2653349 variant (p = 0.006)
Zarrilli et al. in 2015	Case control association	G1246A mutation in <i>HCRTR2</i> , T3092C mutation in <i>CLOCK</i> , rs1800759 and rs1126671 mutations in <i>ADH4</i>	54 CH patients, 200 controls	rs1800759C>A and rs1126671G>A in <i>ADH4</i> showed significant association with CH

Table 2.2 Studies investigating the role of genetic variants in cluster headache

2.4.1 Linkage studies

A general description of linkage mapping approaches is reported in paragraph 1.3.1.

In order to identify chromosomal regions containing potentially susceptibility loci for CH, some research groups performed parametric linkage studies. The application of this methods, however, has been limited by the lack of large family pedigrees with many affected individuals.

In 2004, Aridon et al. studied two small families with CH in order to investigate the presence of linkage in the 6q23 region. In total 6 individuals with CH (two males and two females in the first family, and two affected first cousins in the second one) and 10 healthy subjects were included in this study²¹⁵. Four microsatellites from the 6q23 region were studied; this region encompasses a cluster of genes encoding G-protein-coupled receptors that bind and are activated by trace amines (*TAR1, TAR3, TAR4, TAR5, PNR e GPR58*), including tyramine, octopamine and synephrine. These neurotransmitters have been found increased in plasma and platelets of patients affected by CH, both in active and remission periods²¹⁶. Therefore, a possible involvement of such molecules in CH etiopathogenesis has been suggested. However, this study did not identify a disease segregating haplotype, suggesting that this specific region is not associated in the two studied families with CH²¹⁵.

A genome-wide genetic screen was carried out on 5 informative Danish CH families using approximately 400 microsatellite markers²¹⁷. Furthermore, further 111 individuals from Danish and Italian kindreds were analysed with additional markers in those loci showing suggestive evidence of linkage. Even if potential linkage has been detected at four possible disease loci in Danish kindreds, no single chromosome location reached statistical significance²¹⁷.

2.4.2 Association Studies

A general description of association studies is reported in paragraph 1.3.2

A case-control association study was performed in order to evaluate the contribution of different polymorphisms in the hypocretin/orexin system genes in 109 Italian patients affected by CH and 211 controls²¹⁸. This study identified a significant association between CH

and the rs2653349 variant (1246 G>A) in exon 5 of hypocretin receptor type 2 (*HCRTR2*). The hypocretins (orexins) are hypothalamic neuropeptides thought to have an important role in the regulation of sleep and arousal states²¹⁹. In particular, this study reported that homozygous individuals for G allele have an increased risk to develop disease (OR: 6.79, 95% CI, 2.25 to 22.99). The G allele causes a substitution of amino acid valine with isoleucine at position 308 (V308I). This amino acid change, that affect the receptor dimerization, could contribute to CH susceptibility²¹⁸.

The association between 1246 G>A variant in *HCRTR2* gene and CH was also confirmed in successive studies^{217,220,221}. In contrast, a more recent genetic association study did not show significant association between rs2653349 and CH in a cohort of 575 patients and 874 controls²²² ($p = 0.319$). However, in the same study, a meta-analysis performed on 1167 subjects with CH and 1618 controls from six study populations, identified association of the variant with CH ($p = 0.006$)²²².

In the study performed by Zarrilli et al. in 2015²²¹, researchers have also analysed variants in other two candidate gene: *CLOCK* gene, encoding for a transcription factor with a central role in the regulation of circadian rhythms, and *ADH4* gene, encoding for class II alcohol dehydrogenase 4 pi subunit, which is a member of the alcohol dehydrogenase family. This study was performed on 54 unrelated sporadic CH patients, in 200 controls in 8 families with CH. In *ADH4*, both variant tested (rs1800759C>A and rs1126671G>A) showed a significant association with CH ($p = 0.03$ in both cases). However, a recent replication study on rs1126671 and rs1800759 performed in a Swedish case-control cohort (390 unrelated patients with CH and 389 controls) did not support an association of *ADH4* variants with CH²²³.

No statistically significant association was identified for rs1801260 (T3092C) in the *CLOCK* gene and CH. This finding confirms the result obtained by a previous study in which association analysis of T3111C variant (located in the 3' flanking region of the *CLOCK* gene) among 101 CH patients and 100 healthy subjects did not provide significant results²²⁴.

The *PER3* gene, a member of the Period family genes expressed in a circadian pattern in the suprachiasmatic nucleus, has also been studied in CH. *PER3* transcription level is regulated by the *CLOCK* gene²²⁵ and variant in *PER3* has been associated to sleep disorders. The analysis of a *PER3* VNTR (variable number tandem repeat) polymorphism in CH, did not show statistically significant results²²⁶.

NO has been suggested as the common mediator in vascular headache pathophysiology²²⁷. NO is involved in vasodilation and inflammation²²⁸ and, thus, it could be a promoting factor for CH attacks. Several polymorphisms in genes encoding for NO synthases isoforms (*NOS1*, *NOS2A*, *NOS3*) have been studied in association to CH²²⁹. However, the case-control association study performed by Sjöstrand et al. in a Swedish population including 91 CH patients and 111 controls failed to show significant results for all tested variants in genes encoding for *NOS* isoforms²²⁹.

Furthermore, analysis of *CACNA1A* in CH did not reveal any statistically significant differences with regards to phenotype and allele frequencies between patients and controls²³⁰. *CACNA1A*, encoding for the alpha 1A subunit of the Cav2.1 calcium channel, has been implicated in several episodic neurological disorders, especially it is reported to have a critical role in familial hemiplegic migraine (FHM)²³¹.

Methylenetetrahydrofolate reductase (*MTHFR*) is an enzyme with a crucial role in the remethylation pathway converting homocysteine to methionine. The rs1801133 variant (677C>T) in *MTHFR*, which have an effect on enzyme activity leading to increased homocysteine levels, has been involved in vascular oxidative stress response²³² and has been linked to migraine^{233,234}. The effect of this variant was also tested in CH by a case-control association study among 147 CH patients and 599 controls. No significant difference between cases and control was identify for rs1801133 polymorphism²³⁵.

Finally, case-control association studies were also carried out for the *HFE* and *SERPINA1* genes, however, the polymorphisms tested did not show statistically significant association with CH^{236,237}. The *HFE* gene encodes for a protein that modulates iron absorption, and mutations in this gene are responsible for toxic iron overload in several body organs. Recent studies suggested that iron metabolism could be involved in the pathophysiology of primary headaches²³⁸. The *SERPINA1* gene encodes the alpha 1-antitrypsin, mutations in this peptide could predispose to pulmonary emphysema, a chronic obstructive pulmonary disease (COPD) that seems to be correlated with CH²³⁹.

2.5 Nicotine dependence in Cluster Headache

Smoking is the most consistent lifetime habit reported in CH patients. Over 80% of CH patients have a prolonged history of tobacco usage²⁴⁰. A recent study suggested that second hand cigarette exposure during childhood is also a risk factor for the development of CH²⁴¹.

However, the link between smoking and CH is unclear, and smoking cessation does not seem to alter the clinical course of the disorder. Since not all individuals who are smokers or are exposed to second hand smoke go on to develop CH, some other underlying factors must be involved in CH pathogenesis. Thus, tobacco use could be an environmental trigger for CH in genetically predisposed subjects; an alternative hypothesis is that the genetic risk factors involved in smoking-related traits might also have a role in CH susceptibility. As described in chapter 1, the $\alpha 5/\alpha 3/\beta 4$ nicotinic receptor subunit gene cluster on chromosome 15q25 (*CHRNA5*, *CHRNA3*, *CHRNA4*) is the strongest and highly replicated locus for smoking-related traits, and many independent studies demonstrated that rs16969968, a common non-synonymous variant in *CHRNA5*, is associated with nicotine dependence, smoking quantity (CPD), as well as smoking related diseases such as lung cancer and chronic obstructive pulmonary disease⁹⁸. Rare and low frequency coding variants in *CHRNA5* also contribute to nicotine dependence¹²⁶. The $\alpha 6/\beta 3$ nicotinic receptor subunit gene cluster (*CHRNA6*, *CHRNA3*) on chromosome 8p11, and more recently *CHRNA4* (chromosome 20q11) have also been correlated to smoking behaviours and its consequences^{97,242,243}. The role of nicotinic receptor genes in CH has never been investigated so far.

2.6 CH treatments

To date, there is no a specific drug for CH treatment; the drugs used have only the effect of reducing the pain associated with the disease. The main treatment for acute management of attacks have a vasoconstrictor effect with immediate action, including inhalation of oxygen and subcutaneous administration of triptans (serotonin [5-HT_{1B/1D}] receptor agonists)¹⁹⁴. However, about 20% of patients are non-responders and often prolonged use of these drugs causes side effects²⁴⁴. Only a limited number of studies have investigated the pharmacogenetics of triptan response in CH. A report has linked a common polymorphism in the gene coding for the G-protein $\beta 3$ subunit (*GNB3*) with triptan response²⁴⁵.

Octreotide, an injectable synthetic analogues of the brain hormone somatostatin, is another drug used for the treatment of acute CH attacks. The mechanism of action of these peptides is unknown, but it has been shown to inhibit the release of numerous vasoactive peptides, including CGRP²⁴⁶. Furthermore, neurons containing somatostatin are located in the regions of the central nervous system involved in nociception, including the hypothalamus, which have also been involved in CH etiopathogenesis²⁴⁷. The most frequent adverse reactions of

somatostatin are hyperglycaemia, nausea, abdominal pain and diarrhoea.

Furthermore, local anaesthetics, such as lidocaine, and the injectable form of dihydroergotamine (D.H.E.) have also been suggested to be effective in the acute treatment of CH²⁴⁸⁻²⁵¹.

In addition to acute treatments, there are also several preventive therapies for CH. They include, calcium antagonists (Verapamil) which interferes with slow calcium channels and it is the most widely used drug for preventing CH²⁵². Furthermore, effective preventive treatments are also inflammation-suppressing drugs (corticosteroids), lithium carbonate, used also to treat bipolar disorder, and melatonin¹⁹⁵.

A recent Japanese study has suggested the role of naratriptan as a preventive medicine for CH. In fact, the administration of naratriptan two hours before attacks seems to provide a good response in patients with CH²⁵³. In contrast to other triptans, naratriptan offers a long half-life and improved bioavailability²⁵⁴.

MATERIALS AND METHODS

CHAPTER 3

Materials and methods: Role of $\alpha 7$ nAChR in nicotine dependence

3.1 ND Study sample

3.1.1 Smokers sample

The collection of treatment seeking smokers was carried out in collaboration with Prof. M. Zoli and L.A. Pini at University of Modena and Reggio Emilia. The study sample includes 408 Italian smokers enrolled at 3 Smoking Cessation Centers (Modena, Parma and Imola) in Italy. Phenotypic data collected at baseline included sex, age, number of cigarettes per day (CPD), and Fagerström test for nicotine dependence (FTND). Additional information collected on each subject included self-reported drug treatment history, physical health or psychiatric problems, family history of tobacco use, reasons for starting tobacco use, smoking initiation age.

All participants received group or individual counseling; in addition, 142 subjects also received pharmacological treatment with varenicline. All individuals were followed up at 3 months and 6 months after treatment in order to assess maintenance of smoking cessation. The DNA from 380 smokers was extracted from blood with Blood/Cultured Cell Genomic DNA Extraction Mini kit (Fisher Molecular Biology). For 28 smokers, instead, the DNA was extracted from saliva with ORAcollect-DNA (OCR-100) and prepIT-L2P (DNAGenotek).

3.1.2 Controls samples

A healthy population control sample including 139 never smokers and 55 light smokers (FTND scores =0) was recruited among medical staff at Modena Policlinico hospital.

As a further comparison population sample, we used a group of 204 Italian individuals with ASD. These subjects were recruited at the Stella Maris Clinical Research Institute for Child and Adolescent Neuropsychiatry (Calambrone, Pisa, Italy). For ASD diagnosis, parents undertook the Autism Diagnostic Interview-Revised (ADI-R)²⁵⁵ that is a standardised, semi-structured clinical interview with the aim of obtaining an accurate development history from

caregivers of children, while probands were administered the Autism Diagnostic Observation Schedule (ADOS)²⁵⁶, that is a standardised protocol for direct observation of social interaction and communicative behaviours. A clinical evaluation was performed to exclude recognizable medical causes associated with autism. Karyotyping, molecular genetic testing for Fragile X syndrome, EEG and aCGH were obtained where possible for all probands.

ASD DNA samples were extracted from blood with the QIAGEN DNA Blood extraction kit. The control group DNA (never smokers and light smokers) were extracted from blood with the Blood/Cultured Cell Genomic DNA Extraction Mini kit (Fisher Molecular Biology).

All participants provided a written informed consent to participate. This study was approved by the local Ethical Committee and took place in observation of the declaration of Helsinki (protocol number 2224/2013).

3.2 SNP Genotyping and CNVs detection by Illumina Infinium® PsychArray microarrays

Genotyping was performed on Illumina Infinium® PsychArray microarrays (Illumina, San Diego, California, USA), using a standard protocol in two parallel stages, using Illumina PsychArray-24 v1.0 and PsychArray-24 v1-1 array, respectively²⁵⁷. We restricted the analysis to 566178 variants present on both versions of the array. Content for the Infinium PsychArray includes 265,000 validated tag SNPs, 245,000 exonic variants, and 50,000 additional markers associated with common psychiatric disorders: schizophrenia, bipolar disorder, autism-spectrum disorders, attention deficit hyperactivity disorder, major depressive disorder, obsessive compulsive disorder, anorexia nervosa, Tourette's syndrome. The genotyping is based on the Illumina Infinium high Throughput Screening (HTS) assay. Locus discrimination or copy number variation (CNV) determination results from sequence-specific hybridization capture and array-based, single-base primer extension. Briefly, the first step is whole-genome amplification to uniformly amplify the DNA amount of each sample. A controlled enzymatic process fragments the amplified product; after isopropanol precipitation, the precipitated DNA is resuspended in hybridization buffer and loaded to the BeadChip where it anneals to locus-specific 50-mers. The 3' end of the primer maps adjacent to or overlaps with the SNP site (according to Infinium II or Infinium I probe design). Extension occurs only in the presence of a perfect match and it is generated the signal which determines the genotype call for the sample. Allele-specific single base extension of the primer incorporates a labeled nucleotide (C and G are biotin labeled, while A and T are

dinitrophenyl labeled). The BeadChip is then scanned by the Illumina iScan, a laser system that excites the fluorophore of the single-base extension product on the beads and records the fluorescence signals. For each SNP, fluorescence signals specify the two alleles and the homozygous/heterozygous genotypes (red/red or green/green for homozygous , red/green (yellow) signals for heterozygous)(Figure 3.1).

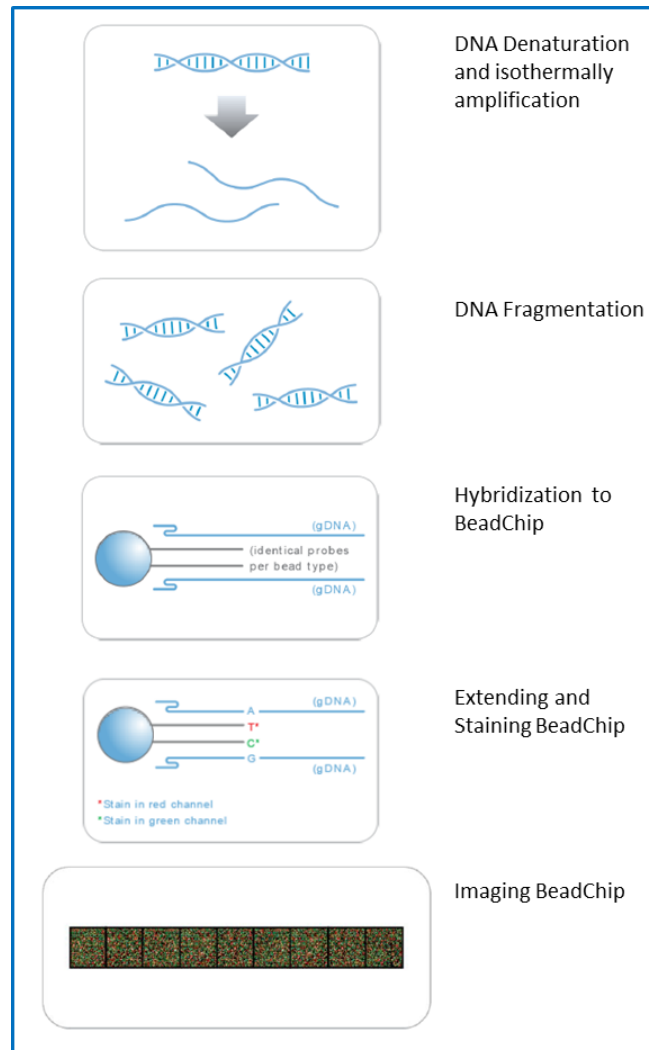


Figure 3.1: Schematic representation of the Illumina Infinium HTS Assay protocol.

SNP genotyping data can be analyzed and visualized with Illumina GenomeStudio software. This software includes algorithms designed for automated clustering and allele-calling. For each SNP the software clusters samples by genotype in three possible clusters (Figure 3.2). Each cluster can be moved manually so samples can be included or excluded from the clusters in each SNP.

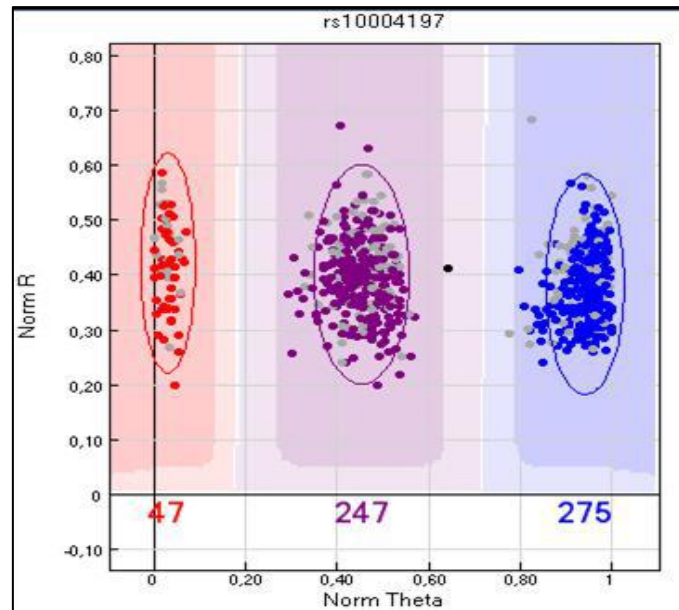


Figure 3.2: SNP genotypes graphical display in GenomeStudio (color code: red=AA; purple=AB; blue=BB). Norm-R represents the signal intensity (y-axis) while Norm Theta is the allele frequency (x-axis).

In GenomeStudio is also possible to visualize SNP data on a genome-wide scale using the Illumina Genome Viewer (IGV) tool. Different data plots can be displayed in IGV. In particular, to check the presence of a CNV it is very useful to visualize and combine genomic data plots of the logR Ratio and the B-allele frequency parameters.

LogR Ratio is the $\log_2(R_{subject}=R_{reference})$, a measure of the observed normalised total signal intensity of the subject sample compared to the expected intensity (which in turn is based on the observed allelic ratio of the canonical genotype clusters)²⁵⁸. The B-allele frequency is a normalised measure of the relative signal intensity ratio of both alleles. A duplication is identified when an upward deflection in the logR Ratio together with a split in the heterozygous allele frequencies (corresponding to a 2:1 and 1:2 allelic ratios or to AAB and ABB genotypes) in the B-allele frequency plot are detected (Figure 3.3). In turn, a deletion is identified when a downward deflection in the logR Ratio and a lack of heterozygous calls in the B-allele frequency plot are detected (confirming the reduction in copy number – Figure 3.3). It is possible to determine if the CNV in question is *de novo* or inherited, by looking at the same region in the respective parents.

All SNPs LRR and BAF values for each individual can be exported from GenomeStudio to identify CNVs using three different CNV detection algorithms: PennCNV²⁵⁹, QuantiSNP²⁶⁰ and CNVPartition (Illumina). In particular, CNVs required calling by at least two algorithms with one being PennCNV. It was not possible to assess *CHRFAM7A* copy number using genome-

wide array SNP data as no SNPs uniquely mapping the *CHRFAM7A* gene are present in most commercial arrays.

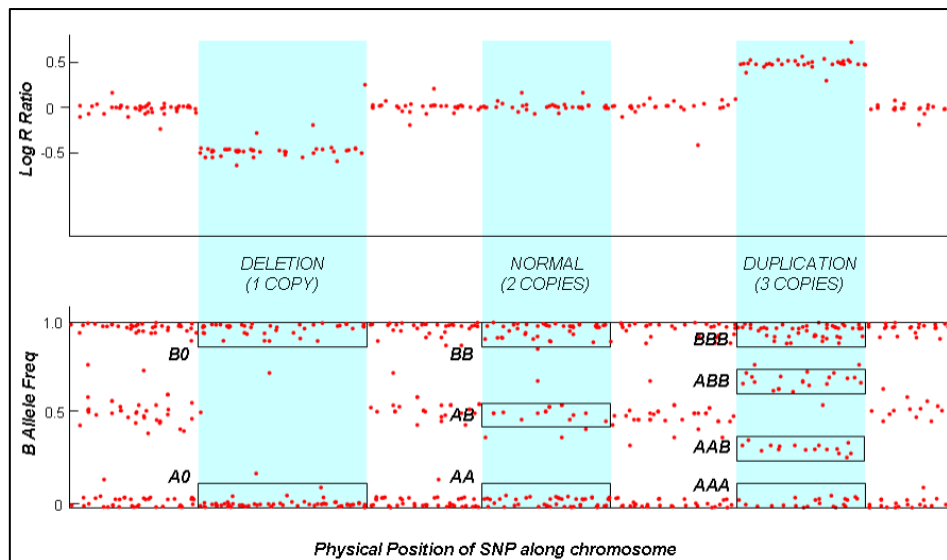


Figure 3.3: Examples of LRR and BAF plots for a deleted region, region with 2 normal copies and duplicated region. The decrease in the LogR Ratio and the lack of heterozygous calls indicates the presence of a deletion (1 copy, genotype B/- or A/-). The increase in the LogR and the split of the heterozygous cluster into two intermediate clusters indicates the presence of a duplication (3 copies, four possible genotypes for each SNP: AAA, AAB, ABB, BBB).

3.3 Validation of *CHRNA7* CNVs by Real-Time PCR

To validate the presence of *CHRNA7* duplications detected by SNP array we performed a real-time quantitative PCR (qPCR) using SsoAdvanced™ Universal SYBR® Green Supermix (Biorad). SYBR Green is a non-specific fluorescence dye that binds to the minor groove double-stranded DNA.

The analysis of qPCR data relies on the threshold Cycle (Ct), that is defined as the point at which the fluorescence rises appreciably above the background fluorescence. DNA quantification, based on fluorescence measure, always occurs during the exponential phase, when the amount of PCR product is taken to be proportional to the amount of input DNA.

Primers for qPCRs for CNV validation were designed from genomic DNA sequence using Primer3, (<http://bioinfo.ut.ee/primer3-0.4.0/primer3/>). For primers design, we used the following conditions:

- Product Size Range= 90-140bp
- Number to return = 10
- Primer Size = Min: 20; Opt: 22; Max: 30
- Primer GC%= Min: 40; Max: 50

- Max Self-Complementarity= 5.00
- Max 3' Self-Complementarity = 2.00
- Max Poly X = 3

The primer used to specific *CHRNA7* amplification are listed in the follow table:

Primer name	Sequence (5'-3')	Primer size (bp)	Product size (pb)	Fragment position (hg19)
CHRNA7_x3F	GGCTGCAAATGGTAAGTTAAGAG	23	111	chr15:32393540-32393650
CHRNA7_x3R	AACAGGACCTCTCAGAAGCAAG	22		

PCR efficiency was calculated using 4 dilution series of template DNA, and each was run in triplicate. For the relative quantification, a region of the *FOXP2* gene was amplified as internal control, with the following primers:

FOXP2 forward primer: 5'-TGCTAGAGGAGTGGGACAAGTA-3',

FOXP2 reverse primer: 3'-GAAGCAGGACTCTAAGTGCAGA-5'

Each reaction was set up in triplicate using the following conditions:

qPCR Reaction MIX	Amount (µl)
DNA template (5 ng/µl)	5
SsoAdvanced™ Universal SYBR®	7.5
Green Supermix 2X	
Primer F (10 µM)	0.75
Primer R (10 µM)	0.75
H2O	1
Final volume	15

A control subject predicted to have two normal copies of *CHRNA7* was included in all qPCR experiments. The qPCR reactions were run on the CFX Connect™ Real-Time PCR Detection System (Biorad) according to the following qPCR program, which includes three main stages:

- 1) Polymerase activation: incubation at 98°C for 3 minutes;
- 2) Anneal/extend: 40 cycles of incubation at 98°C for 10 seconds, at 60°C for 30 seconds;
- 3) Melting curve: incubation at 95°C for 1 minute, followed by an incubation at 65°C for 3 seconds, repeated for 61 times with an increase of 0.5°C each cycle.

Melting curve analysis of each PCR products were carried out to ensure specific amplification, as specificity of amplification is considered to be an important issue with intercalating dye assays.

Melting curve analysis is also called dissociation curve, because it is an assessment of the dissociation-characteristics of double-stranded DNA during heating. It consists in a step in which the temperature of the sample is incrementally increased, while the instrument continues to measure fluorescence. As the temperature rises enough, dsDNA denatures becoming single-stranded, and the SYBR Green dye dissociates, resulting in a decrease fluorescence.

Melting curve analysis permits the identification of primer-dimers or other non-specific PCR products that, giving spurious fluorescence signals, may decrease the PCR efficiency.

Serial DNA dilutions were used to calculate PCR efficiencies for *CHRNA7* assay.

Relative copy number was calculated using the comparative Ct method ($2^{-\Delta\Delta Ct}$ method)²⁶¹:

$$\Delta Ct \text{ sample DNA} = Ct \text{ fragment of interest} - Ct \text{ FOXP2}$$

$$\Delta Ct \text{ control DNA} = Ct \text{ fragment of interest} - Ct \text{ FOXP2}$$

$$\Delta\Delta Ct = \Delta Ct \text{ sample DNA} - \Delta Ct \text{ control DNA}$$

$$\text{ratio} = 2^{-\Delta\Delta Ct}$$

$$\text{Copy number} = 2 * \text{ratio}$$

3.4 Mutation screening of the *CHRNA7* proximal promoter

3.4.1 Primer design

CHRNA7 genomic sequence was retrieved from the UCSC genome Browser (hg 19). All the primers were designed using Primer3 (<http://bioinfo.ut.ee/primer3-0.4.0/primer3/>). Two different PCR amplicons were designed to amplify 740 bp upstream the *CHRNA7* start codon:

Amplicon	Foreword primer	Reverse primer	Lenght
Amplicon 1	5'-cattagggttaaccactgggaat-3'	5'- aggtgtgagcgggagggtact-3'	490 bp
Amplicon 2	5'-agtacctcccgctcacacct-3'	5-'gtgcagcccagacaagca-3'	480 bp

3.4.2 Polymerase Chain Reaction (PCR) assay

Optimisation of PCR conditions was carried out by altering the annealing temperatures,

MgCl² concentrations or cycle numbers, until achievement of the optimal conditions. Magnesium acts as a cofactor to the Taq polymerase and stabilized DNA base pairing, therefore variation in magnesium concentration influences the reaction specificity.

The PCR reactions were set up in a final volume of 15 µl using 30 ng of template DNA and with final concentrations of 0.2 mM of each dNTP, 0.05 u/ul AmpliTaq Gold DNA Polymerase (Life Technologies), 1.5-2.0 mM MgCl₂, 1X AmpliTaq Gold buffer, 0.2 mM of each primer (forward and reverse) and 30 ng of template DNA.

To deal with the GC rich sequences of the CHRNA7 promoter amplicons, 5% dimethyl sulfoxide (DMSO) and/or 0.1 mM 7-deaza-2''-deoxiguanosina-5''-trifosfato (Deaza GTP) were also added to the PCR mix, in order to improve the denaturation of the template DNA.

A "Touch-Down" PCR program (TD) was used for the amplification of both fragments²⁶²: starting with an initial higher temperature (T1) to ensure a specific primer annealing, then progressively decreasing the temperature until it reaching a second, lower temperature (T2), which is maintained constant for remaining amplification cycles.

Touch-Down PCR program	
Initial Taq Gold denaturation	95°C for 15 minutes
Touch-Down (10 cycles: Ta decreases 0,5°C at each cycle)	95°C for 30 seconds
	T1: 65°C for 30 seconds
	72°C for 30 seconds
Amplification (30 cyles)	95°C for 30 seconds
	T2: 60°C for 30 seconds
	72°C for 30 seconds

The PCR products were visualized with a UV transilluminator after electrophoresis on 2% agarose gel and GelRed staining (Biotium). The 100 bp and 1kb DNA ladders (NEB) were loaded to check the PCR fragment size.

3.4.3 PCR purification

After obtaining successful PCR products and confirming them on 2% agarose gels, products were purified prior to the sequencing reaction. The EXO/SAP (GE Healthcare) clean

up protocol was used, in order to digest primers and remove unused nucleotides. The reaction was performed adding 0.5 μl of SAP, 0.5 μl of exonuclease (for unused primer digestion) to 6 μl of each PCR product. The reactions were performed in the MJ Thermocyclers using caps and heated lids, with the following programme:

37°C x 15 minutes: Treatment step

80°C x 15 minutes: Enzymatic inactivation step

3.4.4 Sanger Sequencing reaction

Sequencing was carried out with the Sanger Method, using the BigDye Terminator kit v1.1 (Life Technologies) according to the following manufacturer's protocol:

Sequencing mix	Amount (μl)	Program	
Big Dye terminator buffer (5X)	1,75	Initial Denaturation	96°C for 1 minute
Big Dye terminator	0,5	Amplification (29 cycles)	96°C for 10 seconds
Primer (10 μM)	0,16		50°C for 5 seconds
H2O	variable		60°C for 4 minutes
PCR product	variable		
Final volume	10		

The primers used for the Sanger sequencing are:

Amplicon 1	5'-cattagggtaaccactgggaat-3'
	5'-agaattgtcccggctttctc-3'
Amplicon 2	5-'gtgcagcccagacaagca-3'

3.4.5 Ethanol-EDTA Precipitation of Sequencing Reactions

Once the amplification reaction was complete, sequencing products were precipitated using a reaction mix containing 1/10 of the volume of Sodium Acetate (3 M, pH 5.2) and 2.5 volumes of ice-cold 100% ethanol.

The steps of the precipitation protocol were:

1. The precipitation reaction mix was added to each sample,
2. The plate was spun at 3000 g at 4 °C for 30 min.

3. The seal was removed and the plate inverted on white paper towels (to remove the ethanol).
4. 70 µl of 70% ethanol was added to each well, and the plate was again spun at 1650 g at 4 °C for 15 min.
5. The seal was removed and the plate again inverted on white paper towels. The latter was spun inverted at 185 g for 10-15 sec (to remove remaining ethanol).
6. The plate was dried at room temperature.
7. 15 µl of Injection Solution (DNA Sequencing Reaction Cleanup kit, Millipore) was added to each well.

The sequencing reaction products were run on the ABI PRISM 3730 DNA analyser (Life Technologies). The sequences were analysed and compared to the reference sequence using the software Sequencher 5.0 (Gene Code Corporation).

3.5 In vitro functional analysis of rs28531779 variant on *CHRNA7* promoter activity

Two luciferase constructs containing *CHRNA7* core promoter were designed to analyse the effect of rs28531779 variant on *CHRNA7* promoter activity using dual luciferase assays.

3.5.1 Plasmid construction and cell transfection

Two different genomic DNA, one carrying G/G genotype (WT) for rs28531779 variants and one with C/C genotype (MUT) were used to amplify a region of 269 bp upstream to the *CHRNA7* start codon by PCR using forward primer 5'-tttgggtacc-gtacctcccgcctcacacctc-3' and reverse primer 5'-ttaaagctt-gttgagtcccggagctgca-3'. The WT and MUT PCR fragments were cloned into the luciferase pGL3-basic promoter vector: pGL3 WT or the pGL3 MUT (Promega Biosciences, Promega Corp., San Luis Oispo, CA). Both PCR products was ligated into pGL3-Basic vector by using T4 DNA ligase (NEB) and verified by sanger sequencing. The pGL3 basic (empty vector), pGL3 WT or the pGL3 MUT reporter vectors were transiently transfected using Lipofectamine LTX reagent (Invitrogen) in two different neuroblastoma cell lines: SK-N-BE-2(C) and SHSY-5Y. Renilla luciferase vector, TK-RL, was co-transfected as internal control. Luciferase assays were evaluated 48h post transfection. The experiments were performed in triplicate.

3.5.2 Dual-Luciferase assay

The Dual-Luciferase Assay (Promega) was used to measure differences in transcriptional activity of the *CHRNA7* promoter carrying G/G or C/C genotype. SK-N-BE-2(C) and SHSY-5Y transfected cells (see above) were washed twice in PBS and lysed in 100µl of “Passive Lysis Buffer” (PLB). Samples were analysed for both Firefly and Renilla luciferase activities by sequentially using 100 µl of “Luciferase Assay Reagent II” (Firefly activity) and “Stop and Glow” (Renilla activity) reagents. Firefly luciferase values were normalized to the renilla luciferase activities (normalized signals). Relative luciferase activity was calculated by the ratio between pGL3 WT (or pGL3 MUT) normalized signals and pGL3 basic empty vector normalized signals.

3.6 *CHRFAM7A* Genotyping using ABI3730 and Gene-mapper v3.0 software

Analysis of fluorescent labeled PCR products by ABI3730 and Gene-mapper v3.0 software allows to define the fragment size with high precision. Using this approach, it is possible to discriminate fragment length differences at single base pair resolution.

3.6.1 Primer design and PCR assays

DNA sequences and genomic organization of the *CHRFAM7A* gene are from the UCSC genome Browser (hg 19). The primers for the analysis of *CHRFAM7A* Δ2bp polymorphism were designed using Primer3 (<http://bioinfo.ut.ee/primer3-0.4.0/primer3/>) and map in intronic regions adjacent to exon 6. The primers amplify a region of 238 bases pair encompassing the polymorphism; the forward primer is labeled with a fluorophore at 5' position (forward: 5' [6-FAM] gtttccatcacccacacagg; reverse: 5' agcttgcccaggaataggaa). The use of 5' fluorescent labeled primer allows to analyze the PCR product by ABI PRISM 3730 and GeneMapper v3.0 software. *CHRFAM7A* exon 6 belong to the duplicated region deriving from *CHRNA7*. Therefore, primers used for the analysis of *CHRFAM7A* Δ2bp polymorphism amplify also the *CHRNA7* exon 6. However the Δ2bp polymorphism is specific for *CHRFAM7A* and it is never observed in *CHRNA7*.

Then the PCR assays were performed as previously described (3.4.2), using 2.5 mM MgCl₂.

3.6.2 PCR product analysis by ABI PRISM 3730 automatic sequencer

The PCR products were diluted 1:20 with water.

For each PCR product a mix containing 0.2 μ L of Size standard (LIZ 600) and 8.8 μ L of formamide was prepared. The LIZ 600 is a five dye-labelled high density size standard that allows to define the length of analysis fragment.

Nine μ L of the mix have loaded to a 96-well plate and, in each well, were added 1 μ L of diluted PCR product. Then the plate is loaded to ABI PRISM 3730 automatic sequencer to the electrophoretic run.

The capillary electrophoresis allows to separate fragments of different sizes. During the electrophoresis a laser excites the dye labelled PCR product and the fluorescence signal is detected. The analysis were then performed by Genemapper v3.0 software.

3.6.3 Analysis of *CHRFAM7A* Δ 2bp polymorphism and CNV by Genemapper v3.0 software

In Genemapper v3.0 software the fluorescent signal is represented by a peak in the graph: the Y axis reports the fluorescent intensity (RFU) and the X axis indicate the length of the product. The fragment length is calculated based on the size standard with which it co-migrates. The *CHRFAM7A* PCR product is 238 bp long for the wt allele and 236 for the Δ 2bp allele, thus, when both alleles are present we can observe the presence of two separated peaks representing fragments with 2 different sizes in Genemapper v3.0 (Figure 3.4).

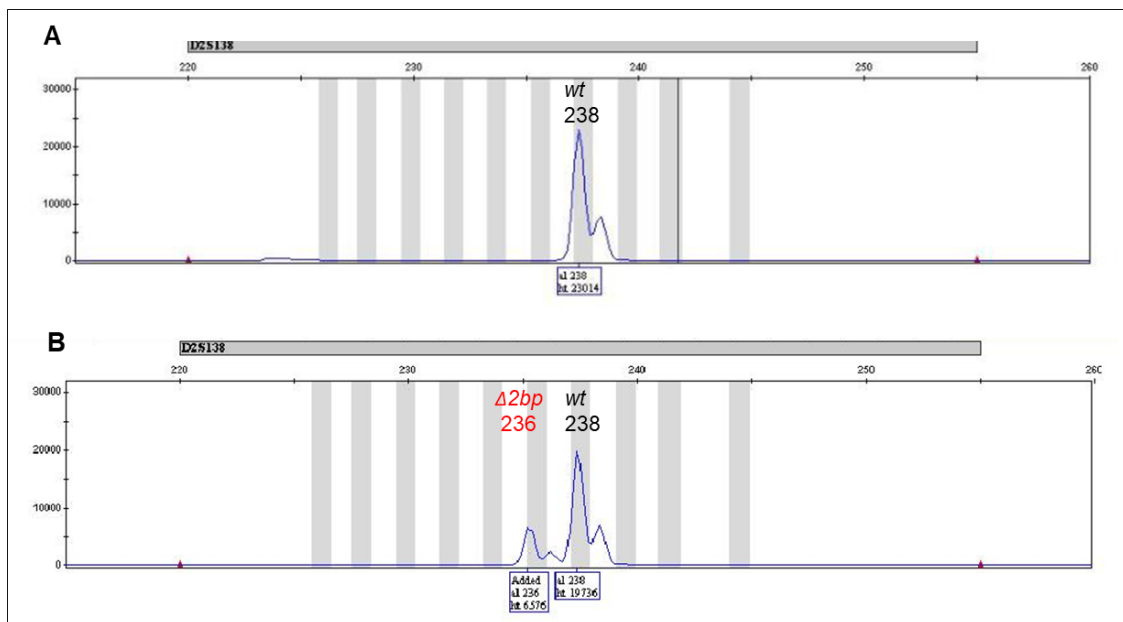


Figure 3.4: Fluorescence peak representation in Gene Mapper software, the Y axis reports the fluorescent intensity (RFU) and the X axis indicate the length of the product (base pair). **(a)** Graph with only one peaks indicating the 238 bp fragment; **(b)** Graph with two peaks indicating the 236 bp e 238 bp fragments

The peak height (fluorescence intensity) is proportional to the amount of DNA template, therefore, since the *CHRNA7* copy number is known (see paragraph 3.2 and 3.3) the ratio between the peak height of the 236 bp fragment and the 238 bp fragment allows to determine also the *CHRFAM7A* copy number (Table 3.1)

236 bp /238 bp (ratio)	Copy number		
	<i>CHRFAM7A</i> Δ2bp	<i>CHRFAM7A</i>	<i>CHRNA7</i>
1/4(0.25)	1	2	2
	or		
	1	1	3
1/3 (0.33)	1	1	2
	or		
	1	0	3
1/2 (0.50)	1	0	2
2/3 (0.66)	2	1	2
	or		
	2	0	3
2/2 (1.00)	2	0	2
3/2 (1.50)	3	0	2

Table 3.1: Evaluation of *CHRFAM7A* copy number by the peak height ratio between 236 bp fragment and 238 bp fragment (236/238)

The alleles were defined as follows: 0 = absence of the *CHRFAM7A* gene; 1 = wild type (TG) allele of rs67158670; 2 = Δ2bp allele of rs67158670 . Each assay was performed twice.

For all samples without the 2bp deletion in exon 6 of *CHRFAM7A* it is not possible establish the copy number with this method, therefore it was used a quantitative Real Time PCR (qPCR).

3.6.4 Analysis of *CHRFAM7A* copy number by real time PCR

To assess *CHRFAM7A* copy number in individual without the Δ2bp allele we performed a real-time quantitative PCR (qPCR) using SsoAdvanced™ Universal SYBR® Green Supermix (Biorad).

The selective amplification of *CHRFAM7A* is not easy since it derives from the fusion of *CHRNA7* partial duplication with a copy of *FAM7A*. Therefore to exclusively amplify

CHRFAM7A we designed a primer pair to amplify a region of 217 bp spanning the breakpoint between *FAM7A* exons D-A and *CHRNA7* exons 5–10 (Primer forward: 5' - tccttgccaatcaactttatga-3' and primer reverse: 5'- cacaccaccacacctggttaat-3') (Figure 3.5)

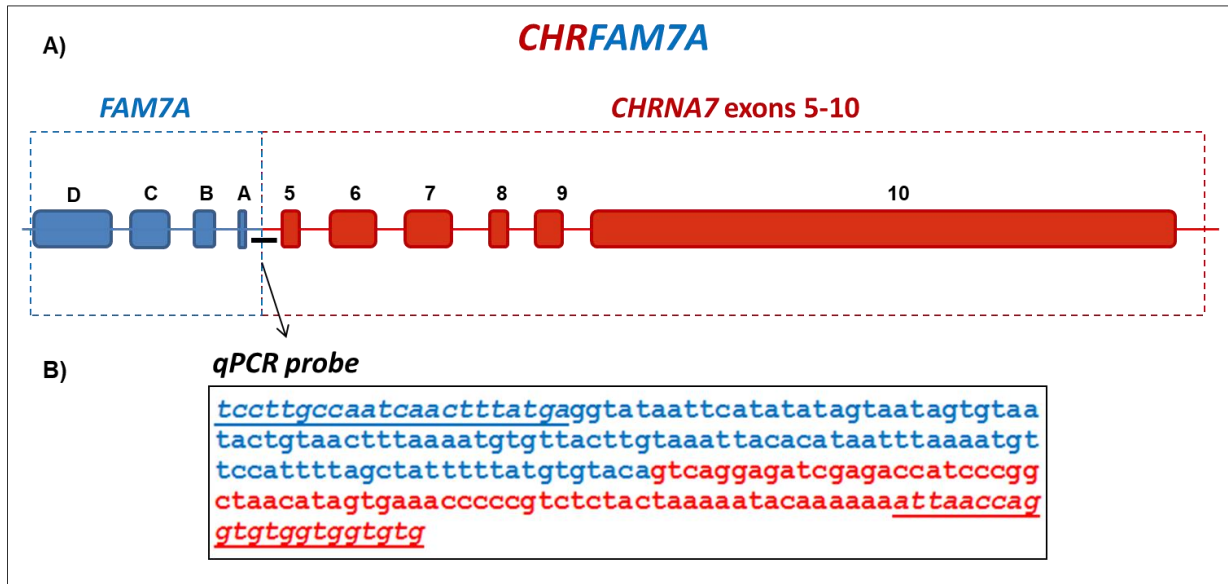


Figure 3.5: **A)** schematic representation of *CHRFAM7A* exonic organization, the blue genomic region derives from *FAM7A* duplication and the red genomic region derives from a partial duplication of *CHRNA7*. **B)** *CHRFAM7A* region amplified by qPCR primers: the forward primer (underlined in blue) maps in the homology region with *FAM7A* (blue), the forward primer (underlined in red) maps in the homology region with *CHRNA7* (red).

The Real time protocol used for the validation of *CHRNA7* duplication is described in paragraph 3.3.

3.7 Statistical analysis

All the analyses statistical analysis were performed using PLINK 1.9²⁶³ and STATA statistical software version 9.0.

3.7.1 Study sample analysis

Chi-square test and t-test were used to perform explorative analysis in the study sample. Specifically, possible gender difference among the pharmacological treatment group and the no pharmacological treatment group and between abstinent individuals and not-abstinent individuals were analyzed by Chi-square test. Difference in FNTD score between male and female and between abstinent subjects and not-abstinent subjects were tested using a t-test. T-test was also used to compare age and FNTD means among pharmacological and no

pharmacological treatment groups. To check if FTND score and CPD satisfied the assumption of normality we used Shapiro-Wilk test.

3.7.2 Quantitative analysis

We used linear regression to test the association of *CHRFAM7A* copy number, the *CHRFAM7A* Δ 2bp variant, and *CHRNA7* promoter variants with FTND score and CPD, including gender as covariate. Age was not included as a covariate in regression models as it did not show any influence on any of the smoking phenotypes in our sample. To test for the influence of the Δ 2bp polymorphism independently of *CHRFAM7A* copy number, regression analysis was conducted in the stratified sample of individuals with 1 or 2 copies of *CHRFAM7A*.

T-test and Mann-Whitney test were used to compare FTND and CPD means between subjects carrying different genotypes of the rs28531779 variant. Because only a single individual was homozygous for the minor allele, the heterozygous and minor allele homozygous individuals were collapsed into a single group and compared with the homozygous individuals for the major allele.

3.7.3 Categorical association analysis

Analysis of *CHRFAM7A/CHRNA7* copy number and *CHRFAM7A* genotypes in the sample of smokers and in the population control samples was performed by Fisher exact test.

Logistic regression analysis was conducted to investigate for an effect on quit success for *CHRFAM7A* and *CHRNA7* genetic variants, using nicotine dependence level (FTND score) and gender as covariates. As above, the additive effect of the Δ 2bp allele was tested by logistic regression analysis of abstinent/non-abstinent status by stratification of the sample according to *CHRFAM7A* copy number.

3.7.4 Rare variants analysis

Rare *CHRNA7* promoter variants were analyzed using the Sequence Kernel Association Test (SKAT)²⁶⁴, which aggregates individual score test statistics of a set of SNPs, as individually these SNPs are too rare for statistical analysis.

3.7.5 Luciferase assay

T-test was used to test differences in luciferase activity between cells transfected with the pGL3 MUT vector and cells transfected with the pGL3 wt vector.

CHAPTER 4

Materials and methods: Genetic analysis of cluster headache

4.1 CH study sample

4.1.1 Cluster headache sample

One hundred patients suffering from cluster headache (CH) were recruited at the Headache and Drug Abuse Research Centre, Policlinico Hospital, University of Modena e Reggio Emilia. CH diagnosis was made according the ICHD-III beta criteria (Headache Classification Committee of the International Headache Society 2013)¹⁸⁹. For each CH subject the following clinical data was collected: gender, age, headache history (age of onset, duration of the active phase, number of clusters per day and per month, triggering factors, exacerbating factors, autonomic symptoms associated, correlation with cigarette smoking in the active phase), drug treatment history and smoking status, including number of cigarettes per day (CPD), and Fagerström test. DNA was extracted from blood with the Blood/Cultured Cell Genomic DNA Extraction Mini kit (Fisher Molecular Biology).

4.1.2 Control sample

The control sample consisted of 360 age-matched healthy subjects who are cigarette smokers, with no history of CH and/or migraine, recruited at University of Modena as part of the study on the genetics of nicotine dependence (see paragraph 3.1.1). Control individuals were examined for tobacco dependence measures (CPD, Fagerström test) and to exclude a history of CH or migraine. Furthermore, all other information collected for these subjects are described in paragraph 3.1.1.

All participants are of self-reported European ancestry (Italian). DNA was extracted from blood with the Blood/Cultured Cell Genomic DNA Extraction Mini kit (Fisher Molecular Biology) and from saliva with ORAcollect-DNA (OCR-100) and prepIT-L2P (DNAGenotek).

4.2 SNP Genotyping and quality control procedures

The SNP genotyping was performed by Illumina Infinium® PsychArray microarrays (see paragraph 3.2).

The clustering algorithm implemented in GenomeStudio was used to cluster the data. GenomeStudio was also used to evaluate all genotypes using a quantitative genotype quality score called GenCall (GC) score ranging from 0 to 1 with 1 being the best. The GenCall scores generally decrease in the value the further a sample is from the centre of the cluster to which the data point is associated. The no-called threshold is the lower bound for calling genotypes relative to its associated cluster. The GC cutoff was set at 0.15, and the cutoff for sample genotyping success rate was 95%.

GenomeStudio allowed also to analyse the Log R Ratio (LRR) and B Allele Frequency (BAF) (See paragraph 3.2). Samples with standard deviation of Log R Ratio > 0.20 and standard deviation of the B Allele Frequency values > 0.13 were marked not suitable for CNV analysis. SNPs quality control (QC) was performed according to recommended guidelines²⁶⁵. Briefly, we manually edited or zeroed, all SNPs according to several GenomeStudio QC parameters: GenTrain scores (genotype clustering quality score < 0.6), low Custer Separation values, low Call Frequency, low or high AB R Mean values (mean normalized intensity of the heterozygote cluster), low or high AB T Mean values (mean of the theta values of the heterozygote cluster), low or high Het Excess (indicator of the quantity of excess heterozygote calls relative to expectations based on Hardy-Weinberg Equilibrium) and very low minor allele frequency (MAF), given that very rare SNPs could be mis-called by the GenCall algorithm. Probes mapping as "0" (no position), "Y" (Y chromosome) and MT (mtDNA) were excluded. The overall data quality was high: only one sample failed QC thresholds (one additional sample was subsequently removed because of not European ethnicity). The reproducibility of the assay was evaluated using 10 replicate samples: agreement of genotyping calls was 99.99% over all genotypes across these pairs.

After manual editing genotypes were exported to the PLINK 1.9 software^{263,266} for additional data cleaning, to remove SNPs deviating from Hardy-Weinberg equilibrium ($p < 0.001$), and markers with heterozygous haploid genotypes on the X. Principal component analysis (PCA) was performed using PLINK 1.9 on SNPs with MAF > 0.05 , pruned for linkage disequilibrium (200 kb window size, $r^2 > 0.5$). PCA is currently the most used method for the assessment of population substructure in a GWAS. The advantage of PCA is that the resulting correction is specific to the SNP variation in frequency across ancestral populations.

PCA plots were generated using the Genesis tool²⁶⁷. One outlying sample was identified and excluded from subsequent association analysis (Figure 4.1). We ruled out relatedness across

subjects (cases and controls) through identity-by-descent analysis, as implemented in PLINK, for all possible pairs of individuals. 556485 variants pass filters and QC, of these 211927 are monomorphic and were excluded from association analysis.

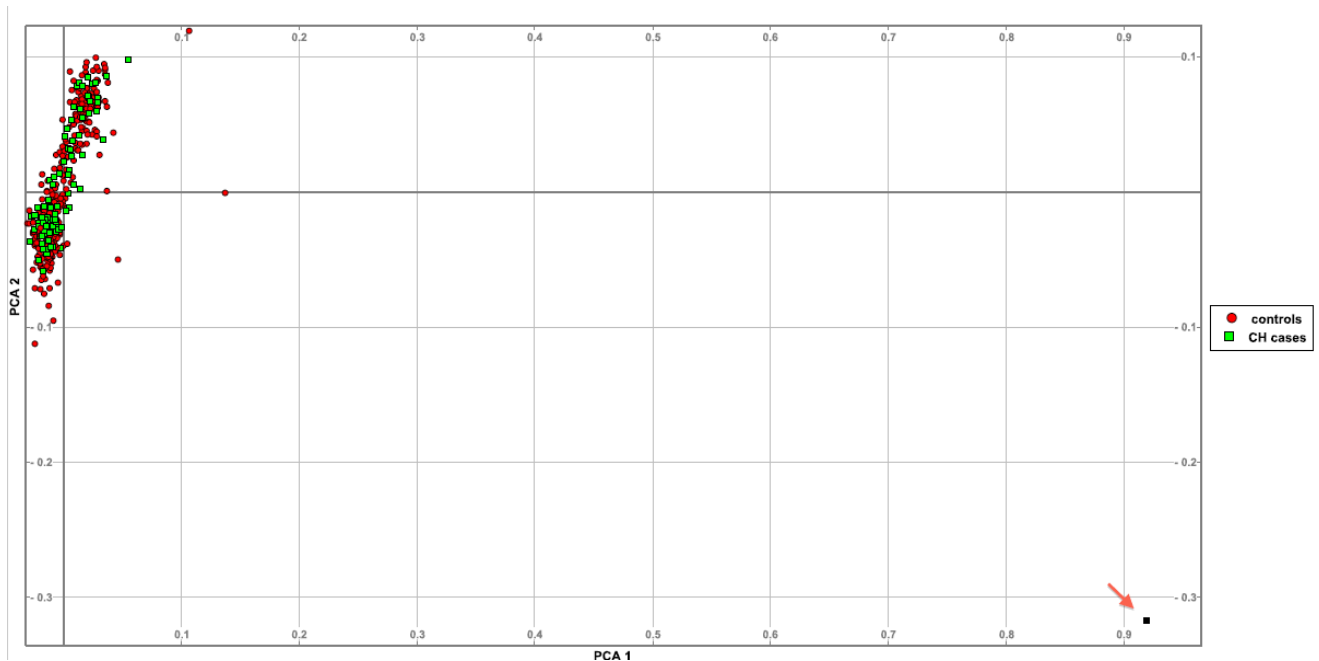


Figure 4.1: Principal component analysis (PCA) plot. The red arrow indicates the outlying sample excluded from genetic analysis.

4.3 Association analysis

Single SNP association analysis was performed using the PLINK v 1.9 software²⁶³. On 290505 SNPs that passed QC and MAF > 0.01 a basic case-control analysis was performed using Fisher's exact test.

In order to aggregate all SNPs in LD with each others, results from the association analysis were clumped according to P-value using PLINK. Each clump is represented by an index variant (that with the lowest P-value in the clump), and contains all SNPs with P-value < 0.01 in linkage disequilibrium with it ($R^2 > 0.5$, within 250 kb of the index SNP).

Plink was also used to carry out logistic regression analysis. Bonferroni correction was applied to correct for multiple tests ($P < 1.7 \times 10^{-7}$, corresponding to $0.05/\text{number of analysed SNPs}$).

Quantile-quantile (Q-Q) plot for test statistics was performed using the R package. Q-Q plot is a probability plot, in which the observed and the null distributions under the assumption of no association, are compared by plotting their quantiles against each other.

LocusZoom²⁶⁸ was used to create the regional association plot, in which for each SNP is represented the p-value (in the Y axis) and the localization in the genome (in the X axis).

4.4 Gene-based association analysis

The Sequence Kernel Association Test (SKAT)²⁶⁴ was used to perform gene-based association analysis. It is an efficient regression method to test for association between rare genetic variants in a region and a continuous or dichotomous trait while adjusting for covariates. SKAT aggregates individual score test statistics of a set of SNPs and easily computes gene-level p-values. After quality control, all non-monomorphic SNPs were mapped to RefSeq genes (downloaded from the UCSC Table Browser, GTCh37/hg19). A collection of 1038 candidate genes with a putative role in cluster headache pathogenesis was selected according to Gene Ontology (GO) biological process annotations (<http://geneontology.org/page/download-annotations>), including 66 GO terms. These 1038 genes are implicated in circadian rhythm, pain perception and response, blood pressure regulation and vasodilation/vasoconstriction, alcohol metabolism, neuropeptide signaling, ion channels, tumor necrosis factor (TNF) signalling, nicotinic acetylcholine receptors (Appendix: Table S1 and Table S2).

Gene-based analysis was performed only on protein altering variants (nonsynonymous and splicing variants) with MAF <0.05 within these candidate genes. In total, 2568 variants in 745 candidate genes were analysed. These included 2497 missense, 11 frameshift, 40 stopgain, 3 stoploss, and 17 splicing variants. A Bonferroni correction which considers the number of the evaluated genes was used to define the significance threshold of the gene-based test results ($p < 6.7 \times 10^{-5}$).

We used two freely available bioinformatic tools to functional annotation of variants: **Polymorphism Phenotyping**, (PolyPhen - <http://genetics.bwh.harvard.edu/pph2/>)²⁶⁹ and the Combined Annotation–Dependent Depletion method (CADD)²⁷⁰. Polyphen-2 is an algorithm that predicts the impact of the non-synonymous change, combining sequence conservation data and protein structure annotations; the output is a score ranging from 0 (neutral) to 1 (damaging). CADD is a scoring algorithm that predicts the deleteriousness of variants in the human genome by integrating multiple annotation algorithms a variety into one metric score (C score).

4.5 *MME* mutation screening

4.5.1 Primer design and PCR assay

DNA sequences and genomic organization of the *MME* genes are from the UCSC genome

Browser (hg 19). All coding exons, intron-exon boundaries were sequenced by Sanger method. All the primers were designed using Primer3 (<http://bioinfo.ut.ee/primer3-0.4.0/primer3/>).

Region	Foreward primer (5'-3')	Reverse primer (5'-3')	lenght
Exon 2 (first coding exon)	cagccacattaagcatttgg	cgttggatagatggtaaagca	326
Exon 3	ggggcttcggtgtagaga	caactacatggcaagctcca	559
Exon 4	atgcaatcaaaaggagcaa	tggtggtgtacacaaatcct	399
Exon 5-6-7	tgtacctccagaaaagcaagg	ccaggtattaggacagagca	797
Exon 8	atggtcacccataaacagc	gaatgaaaaacatcagagggcta	300
Exon 9	gaatctgtgcaggtcatttctta	aaaagcggttgacattattcagt	344
Exon 10	cccacagccaaatctcaataa	cggcacaataagagagcaca	351
Exon 11-12	tgaggaagaatcccaagttaa	tgcaaagttcacctatgtcct	556
Exon 13	gccttgtaggagaagtgatg	ttagccaaatgatggagaactg	347
Exon 14	tttaatcaagagtgtcgataatagcaa	acatattgaaggagcttacaagttttt	430
Exon 15	aattgctagtcatgggcagatt	atttcaggcaccccatagc	246
Exon 16	tgctctctttaactttattgactga	ggagggaagacctgcttct	271
Exon 17	ttcatctaggaatggtaataatgctt	tgcttgtttagaggtattgtaattgg	247
Exon 18	aagcctgccatcactgaataa	aattgaaagtgtggtgaaaattagag	400
Exon 19-20	gacagtctctctcatgctctgc	gaaacactctaaatcactaaaatggaa	489
Exon 21-22	tggcatgatctttacataggttt	agcaccttgattgctgttca	605
Exon 23	ggctccagtgtggtatgga	tgatggtgccctctctgtta	300

Then the PCR assays were performed as previously described (3.4.2), using 2.5 mM MgCl₂. For the PCR products purification protocol see the paragraph 3.4.3.

4.5.2 Sanger Sequencing reaction and sequences precipitation

The primers used for Sanger sequencing are the same used for PCR amplification. Moreover, for PCR fragment including *MME* exons 5-6-7 an addition sequence primer was designed, as well as for the sequencing of PCR fragment including *MME* exons 21-22. Primers sequencing are shown in the following table:

Additional Sequence primers	
Exons 5-6-7	tccaagaagcacctaaagcaa
Exons 21-22	atgttcctggttgcctttca

For the Sanger Sequencing reaction and sequences precipitation protocols see the paragraph 3.4.4 and paragraph 3.4.5.

AIM AND RATIONALE OF THE PROJECT

CHAPTER 5

In recent years, multiple studies highlighted the importance of genetic factors in several smoking related phenotypes, including nicotine dependence, cigarette consumption quantity and smoking cessation. Despite the clear heritability of smoking behaviours (estimated to be >50%), their genetic determinants still remain not completely understood, due to the complex architecture of these traits, in which several genes and environmental factors interact with each other.

The work presented in this thesis, was carried out within Prof. Elena Maestrini's research team, and was part of a project aimed at investigating genetic factors involved in nicotine dependence and smoking cessation. To this purpose, we recruited 408 nicotine dependent smokers from 3 different Smoking Cessation Centres of the Emilia Romagna region in Italy, who were enrolled on a smoking cessation program, and were followed up for a period of at least six-months to collect data on smoking abstinence after treatment.

During the recruitment of smokers for this project, we identified a group of strong smokers who were also affected by cluster headache (CH), a form of headache that is clinically well distinguished from other forms of migraine. Previous epidemiological studies indicated the importance of complex genetic factors in CH susceptibility, but existing genetic studies were extremely limited and inconclusive; therefore, we decided to perform a genetic study to investigate genetic factors involved in this disorder, and their possible relationship to nicotine dependence. Therefore, alongside the recruitment of treatment seeking smokers, a clinically homogeneous sample of 100 patients with CH, regardless of their smoking status, was collected at the Division of Toxicology and from Clinical Pharmacology, Headache Centre, University of Modena and Reggio Emilia; this sample was studied independently from the rest of the smokers.

The specific aims of these two related projects are outlined below (paragraphs 5.1 and 5.2).

5.1 Role of $\alpha 7$ nAChR in nicotine dependence

The aim of this study was to investigate the contribution of genetic variation in the *CHRNA7* and *CHRFAM7A* genes to nicotine dependence and smoking cessation in a sample of 408 smokers recruited at smoking cessation centers.

In recent years, multiple genome-wide association studies (GWAS) for smoking behaviors and ND have been performed on thousands of smokers; these studies have implicated genes encoding for different nicotinic acetylcholine receptor (nAChR) subunits, including the gene clusters on chromosomes 15q25 (*CHRNA5-CHRNA3-CHRNA4*) and 8p11 (*CHRNA3-CHRNA6*)^{5,98}, as well as the *CHRNA4* gene²⁴³.

CHRNA7, the gene encoding the $\alpha 7$ subunit of homopentameric nAChR, has a still uncertain role in nicotine dependence, although it is implicated in a wide range of phenotypes and neuropsychiatric conditions^{131,139}. *CHRNA7* is partially duplicated in a chimeric gene called *CHRFAM7A*, including *CHRNA7* exons 5-10 and exons A–E of the *FAM7A* gene. *CHRFAM7A* is present in a variable number of copies and it harbours a polymorphic 2bp deletion within exon 6, rs67158670 -/TG ($\Delta 2$ bp), never observed in the *CHRNA7* sequence. The *CHRFAM7A* $\Delta 2$ bp allele, as well as SNPs in the proximal promoter of *CHRNA7*, have been associated to schizophrenia, and to the P50 sensory gating deficit^{142,143,150,151}. Interestingly, individuals with schizophrenia have a very high risk of tobacco dependence¹⁵⁸, suggesting that $\alpha 7$ nAChRs abnormal function may act as a shared vulnerability mechanism to smoking and schizophrenia.

GWAS studies for smoking related traits have not identified significant association in *CHRNA7*, but this lack of association could be due to the complex genetic architecture of this genetic region. Indeed, the presence of a duplication giving rise to the *CHRFAM7A* chimeric gene, together with the very high C+G content of the *CHRNA7* promoter region, has hampered genetic analysis of this region by standard genotyping arrays or next generation sequencing. In particular, the most commonly used commercial SNPs arrays (including Illumina 1M, Illumina Omni1-Quad and Affymetrix 6.0 array), do not contain SNP probes in *CHRNA7* exon1 and in the 1200 bp 5' to exon 1. This genomic region is predicted to harbor *CHRNA7* core promoter, a region of 231 bp immediately 5' to start site, reported to be sufficient to regulate transcription levels in vitro¹⁵⁰ (Figure 5.1). Likewise, the $\Delta 2$ bp *CHRFAM7A* variant (rs67158670) is not represented in commercial SNPs arrays. Moreover

SNPs located in the duplicated portion of *CHRNA7* and *CHRFAM7A* cannot be univocally mapped to a gene or the other, and thus they are not reliable.

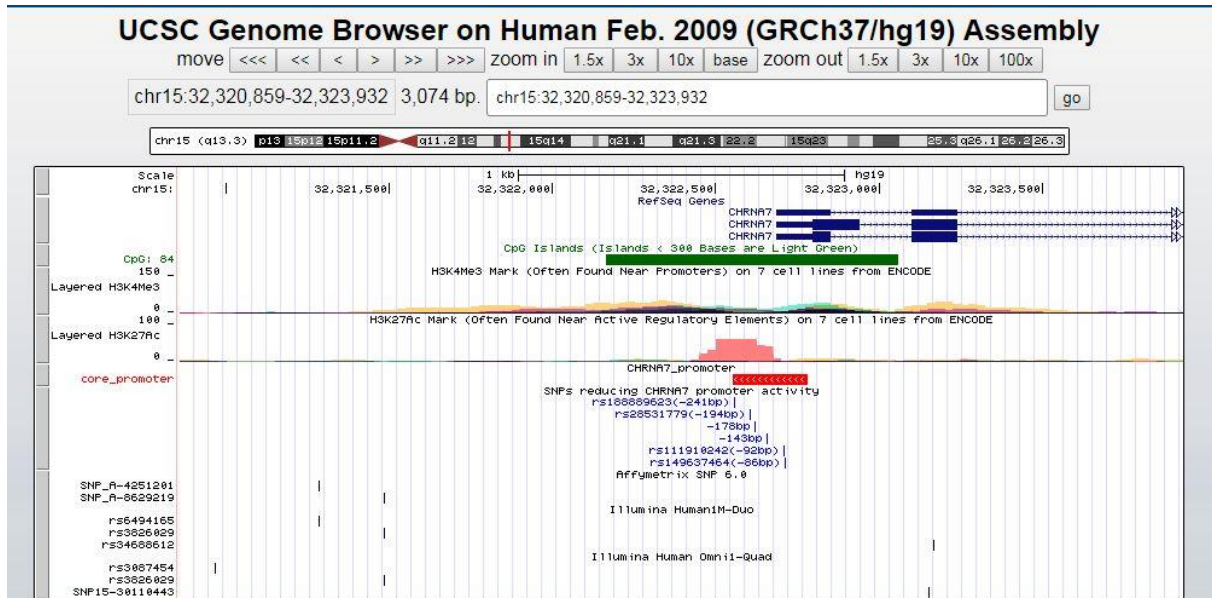


Figure 5.1: 3 kb region on chromosome 15q13.3 spanning *CHRNA7* promoter region (UCSC, hg19). The *CHRNA7* core promoter, as defined in Leonard et al. 2002¹⁵⁰ is indicated as red bar. The SNPs located on *CHRNA7* core promoter, reported to reduce *CHRNA7* promoter activity in vitro¹⁵⁰, are written in blue. Encode regulator tracks are indicated: H3K4Me3 track shows a histone mark associated with promoters, H3K27Ac tracks show where modification of histone proteins is suggestive of enhancer and other regulatory activity. SNP probes present in Illumina 1M, Illumina Omni1-Quad and Affymetrix 6.0 array are indicated.

SNPs in *CHRNA7* proximal promoter, described to reduce *CHRNA7* promoter activity in vitro, have been significantly associated to schizophrenia¹⁵⁰, and to a specific schizophrenia endophenotype, the P50 sensory gating deficit¹⁵¹. Interestingly, no genome-wide significant association was reported for the *CHRNA7* locus in the recent GWAS for schizophrenia performed on tens of thousands of cases and controls²⁷¹. These contrasting results may suggest that commercial SNPs arrays used in GWAS do not comprehensively assess genetic variation in this gene, pointing out the importance of a specific analysis of the *CHRNA7* promoter and the *CHRFAM7A* region.

Even if genetic association studies have not yet reported significant associations for *CHRNA7* variants and nicotine dependence, recent functional studies have suggested that $\alpha 7$ nAChRs may be involved in addiction mechanisms^{161,162}, possibly by modulating the activity of $\beta 2^*$ nAChRs in the VTA¹⁶³. The $\alpha 7$ subunit is widely expressed in the brain with the highest expression level in the cortex and hippocampus³⁴.

Based on these lines of evidence, $\alpha 7$ nAChRs has been considered a promising therapeutic target for the treatment of tobacco addiction, as well as for improving cognition in complex disorders such as schizophrenia.

Over the last few years, varenicline has become the most widely used drug for treating nicotine dependence. It is an $\alpha 4\beta 2$ nAChR partial-agonist and, although with lower affinity, it is an $\alpha 7$ nAChR full-agonist¹⁶⁴. Varenicline has also been shown to provide some cognitive improvement in people with schizophrenia^{165,166}. It is thus possible that activation of $\alpha 7$ nAChRs can contribute to the action of varenicline as a treatment for smoking cessation and schizophrenia.

We conducted a genetic study in order to investigate the possible role of $\alpha 7$ nAChR genetic variation in smoking phenotypes, as well as to test the hypothesis that $\alpha 7$ nAChR variation may modulate the efficacy of varenicline in smoking cessation. The study was conducted on the collection of 408 treatment seeking smokers, which included a subgroup of 142 individuals who were treated with varenicline. More specifically, the aims of this study were: i) to investigate the association of genetic variants in the *CHRNA7* and *CHRFAM7A* genes with smoking quantity and ND in the whole sample of 408 smokers; and ii) to test the effect of *CHRFAM7A* and *CHRNA7* genetic variants on smoking cessation in varenicline treated smokers, by contrasting individuals who successfully maintained smoking cessation at six months after treatment versus those who did not quit smoking.

5.2 Genetic analysis of cluster headache

The aim of this project was to investigate the genetic background of CH by performing a genome-wide association study (GWAS) in a cohort of 100 Italian patients with CH and 360 matched controls.

Cluster headache (CH) is the most severe primary headache displaying a very typical clinical picture with severe, unilateral attacks pain, often accompanied by ipsilateral autonomic symptoms, showing a typical circadian and circannual rhythmicity^{190,191}. These specific symptoms allow to discriminate CH from other forms of migraine. Over 80% of CH patients have prolonged history of tobacco usage, making smoking the most consistent lifetime habit reported in CH patients²⁴⁰. However, it is still an unsolved issue if tobacco use could be an environmental trigger for CH in genetically predisposed subjects, or specific genetic risk factors for CH may also predispose individuals to tobacco smoking. Family and twin studies

have indicated a genetic component for CH¹⁸⁸, but at present, its genetic background is largely unexplored. Prior to our study, only small-scale genetic studies have been completed, which investigated the involvement of variants in single candidate genes thought to be involved in the pathophysiology of CH^{217,218,220,222,226,229,230,235,239}. Among these, the only evidence of association has been reported for a common variant in the *HCRTR2* gene²³⁹. Hence, as for most complex disorders, the candidate gene approach has not been successful in the identification of risk genes. By contrast, GWAS have now yielded hundreds of significant results for numerous complex disorders, including migraine, providing a substantial contribution to our understanding of the genetic determinants of many disorders. For example, genome wide significant risk loci have been identified for migraine, implicating genes expressed in vascular and/or smooth muscle tissue into migraine pathophysiology²⁷².

So far, most GWAS have been performed to identify association with common variants in the general population (> 5%), each having a modest effect on risk, hence requiring very large numbers of cases and controls. However, low frequency and rare variants have been shown to play a significant role in the aetiology of several complex diseases; in particular, exonic functional variants, such as nonsynonymous SNPs lying in the coding regions of genes, are expected to have a greater impact on the disease phenotype. These variants are not typically interrogated by the widely-used SNP genotyping platforms. Exome sequencing technology has provided the means to comprehensively assess coding variation, including the discovery of very rare and private variants. Recently, “exome” genotyping arrays have been developed as a cost-effective alternative to exome sequencing, in order to allow genotyping of rare coding variants identified by exome sequencing studies in samples of thousands of individuals.

Given this framework, we decided to carry out an hypothesis-free GWAS in a sample of 100 CH cases and 360 controls, using the Infinium PsychArray (Illumina)²⁵⁷, which combines both common highly-informative genome-wide tag SNPs and SNPs in coding regions of genes, with an enrichment in genetic variants associated with common psychiatric conditions. Given the unknown genetic architecture of CH, this approach represents the most powerful and cost-effective design to simultaneously investigate the contribution of both rare and common variants to CH susceptibility. Moreover, this approach allows to test the association of genetic variants previously implicated in migraine and in ND.

Specifically, the aims of this study were: i) to test genome-wide association for common SNP; ii) to investigate the possible genetic overlap between CH and migraine;; iii) to test the hypothesis that genetic factors involved in smoking dependence might also predispose to CH, in order to clarify the observed link between smoking and CH; iv) to perform a gene-based analysis, limited to rare protein-altering variants (PAVs) in a subset of 745 candidate genes involved in molecular pathways with a plausible role in CH pathogenesis.

Finally, it should be noted upfront that our sample is very small and lacks power to detect significant associations for variants conferring low or moderate risk. Our results therefore should be considered as preliminary and warrant replication in much larger and independent samples in order to achieve an adequate statistical power. However, we think that this study is worthy of note as it represents the first attempt at a comprehensive genome wide analysis in CH, for which genetic studies are still very limited.

RESULTS

CHAPTER 6

Analysis of *CHRNA7* and *CHRFAM7A* in nicotine dependence

6.1 Sample characteristics

The study sample consisted of 408 Italian regular smokers enrolled at three Smoking Cessation Centers (Modena, Parma and Imola) in Italy. Baseline phenotypic data was collected on all participants recruited in the smoking cessation program, including sex, age, number of cigarettes per day (CPD), and Fagerström test for nicotine dependence (FTND). All participants received group or individual counseling; in addition, a subgroup of 142 treatment seeking smokers also received a pharmacological treatment with varenicline. All individuals were followed up at six months after treatment in order to assess maintenance of smoking cessation.

The demographic and phenotypic characteristics of the total cohort of smokers are shown in Table 6.1, and the distribution of smoking measures (CPD, FTND) are shown in Figure 6.1.

	All smokers	Varenicline treatment	No pharmacological treatment
N	408	142	266
<i>Sex M/F</i>	235/173 (1.36)	94/48 (1.96)	141/125 (1.13)
<i>Age (ys) mean ± sd</i>	49.13 ± 11.59	48.87 ± 11.33	49.27 ± 11.74
<i>CPD (mean ± sd; median)</i>	21.79 ± 9.74; 20	22.69 ± 7.14; 20	21.30 ± 9.78; 20
<i>FTND (mean ± sd)</i>	5.8 ± 2.15	6.38 ± 1.99	5.50 ± 2.17
<i>Abstinence rate</i>	129/408 (31.62%)	53/142 (37.32%)	76/266 (28.57%)

Table 6.1: Sample characteristics

The FTND score is an ordinal variable ranging from 0 to 10, which satisfied the assumption of normality (Shapiro-Wilk test; $p= 0.11$); thus, we modeled the FTND score as a normal continuous variable in subsequent statistical analysis. The distribution of CPD did not satisfy the assumption of normality (Shapiro-Wilk test $p < 0.0001$), possibly because most smokers

tend to round off the number of daily cigarettes to multiples of 10, thus introducing some bias (Figure 6.1). Nevertheless, the FNTD score and CPD are significantly correlated in our sample ($r=0.60$; $P < 10^{-5}$).

We identified an association of gender with FTND (T-test $p=0.02$) and CPD (T-test $p < 0.0001$), with males having a higher mean FTND (6.02, sd 2.27) and mean CPD (23.6, sd 10.78) compared to females (mean FTND: 5.52, sd 1.95; mean CPD: 19.37, sd 7.51). Age did not show any association with either CDP or FNTD, therefore this variable was not included as covariate in subsequent regression analysis.

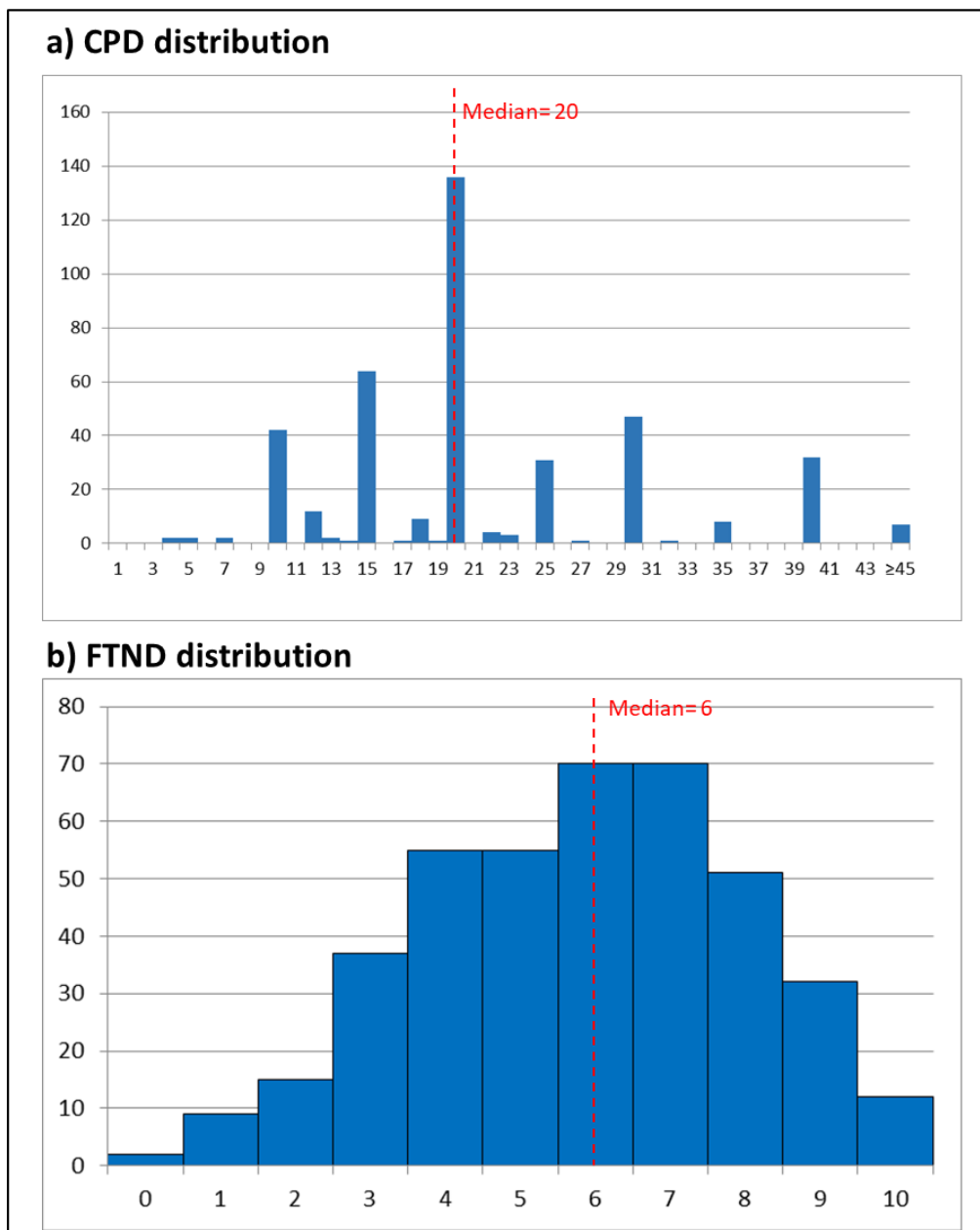


Figure 6.1: CPD and FTND distribution in the entire sample of smokers (N=408). The mean CPD is 21.80 ± 9.74 , the mean FTND score is 5.8 ± 2.15 .

Maintenance of abstinence at six months after treatment was investigated in the whole sample and in the subgroup of varenicline-treated subjects (Table 6.1). The abstinence rate was 31.6% in the whole sample and 37% in the varenicline-treated group. This result is in agreement with the current literature¹⁶⁷ showing the highest cessation rates with varenicline treatment, compared to other pharmacological and behavioural interventions; however, our study design did not involve a randomized controlled trial and testing the efficacy of pharmacological treatment was beyond the scope of the study.

By comparing the group of successful quitters to unsuccessful quitters, we observed a significant difference in nicotine dependence (FNTD) ($p < 0.0001$) and CPD ($p = 0.002$), while there was no difference for gender and age (Table 6.2). Thus, the FNTD score was included as a covariate in our regression model to test the effect of genetic variants on smoking cessation (paragraph 6.8).

	Abstinent smokers	Not abstinent smokers
N	129	279
<i>CPD (mean \pm sd; median) **</i>	19.64 \pm 8.77; 20	22.78 \pm 10; 20
<i>FTND (mean \pm sd)***</i>	5.12 \pm 2.05	6.12 \pm 2.13
<i>Sex M/F</i>	76/53 (1.43)	159/120 (1.325)
<i>Age, ys (mean \pm sd, range)</i>	50.23 \pm 11.57	48.63 \pm 11.58

Table 6.2: Analysis of abstinence in the sample

** T-test $p = 0.002$; Mann Whitney test $p = 0.0015$

*** T-test $p < 0.0001$

6.2 *CHRNA7* copy number assessment by Illumina Infinium® PsychArray microarrays

CHRNA7 copy number was established in the entire sample of smokers, in a control group including 194 light smokers (FTND= 0) or never smokers and in a cohort of 204 ASD individuals, using SNP array data from the Illumina Infinium® PsychArray microarrays (Illumina, San Diego, California, USA). Three CNV prediction algorithms, namely, QuantiSNP²⁶⁰, PennCNV²⁵⁹ and CNVPartition (Illumina), were used to obtain high-confidence CNV call and to minimize the number of potential false discoveries. Array data of each individual were exploited by manual inspection of Log R ratio and B allele frequency in Illumina's GenomeStudio software, as described in Materials and Methods.

Five *CHRNA7* microduplications were identified in the sample of smokers, one in the control sample and one in the ASD sample (Figure 6.2A). Although the frequency of *CHRNA7*

microduplications is slightly higher in the smokers sample compared to controls and to individuals with autism, this difference is not significant.

This CNV includes exon 1 of the longer isoform of *OTUD7A* and the entire *CHRNA7* gene (chr15:32049125-32514341 NCBI build 37 coordinates). The duplication was also validated by quantitative PCR in all 7 individuals. As shown in Figure 6.2B, five smokers (20150; 10116; 10061; 10471; 10058), one ASD individual (SM_60.3) and 1 control subject (10315) have 3 copies of *CHRNA7* gene. In the graph is also represented a subject (CTR) with 2 copies of *CHRNA7* gene, including in the qPCR experiment as control DNA.

No *CHRNA7* deletions were found in our sample, and this is not surprising given the rarity and highly penetrant association of this microdeletion with different neuropsychiatric disorders¹³²⁻¹³⁴.

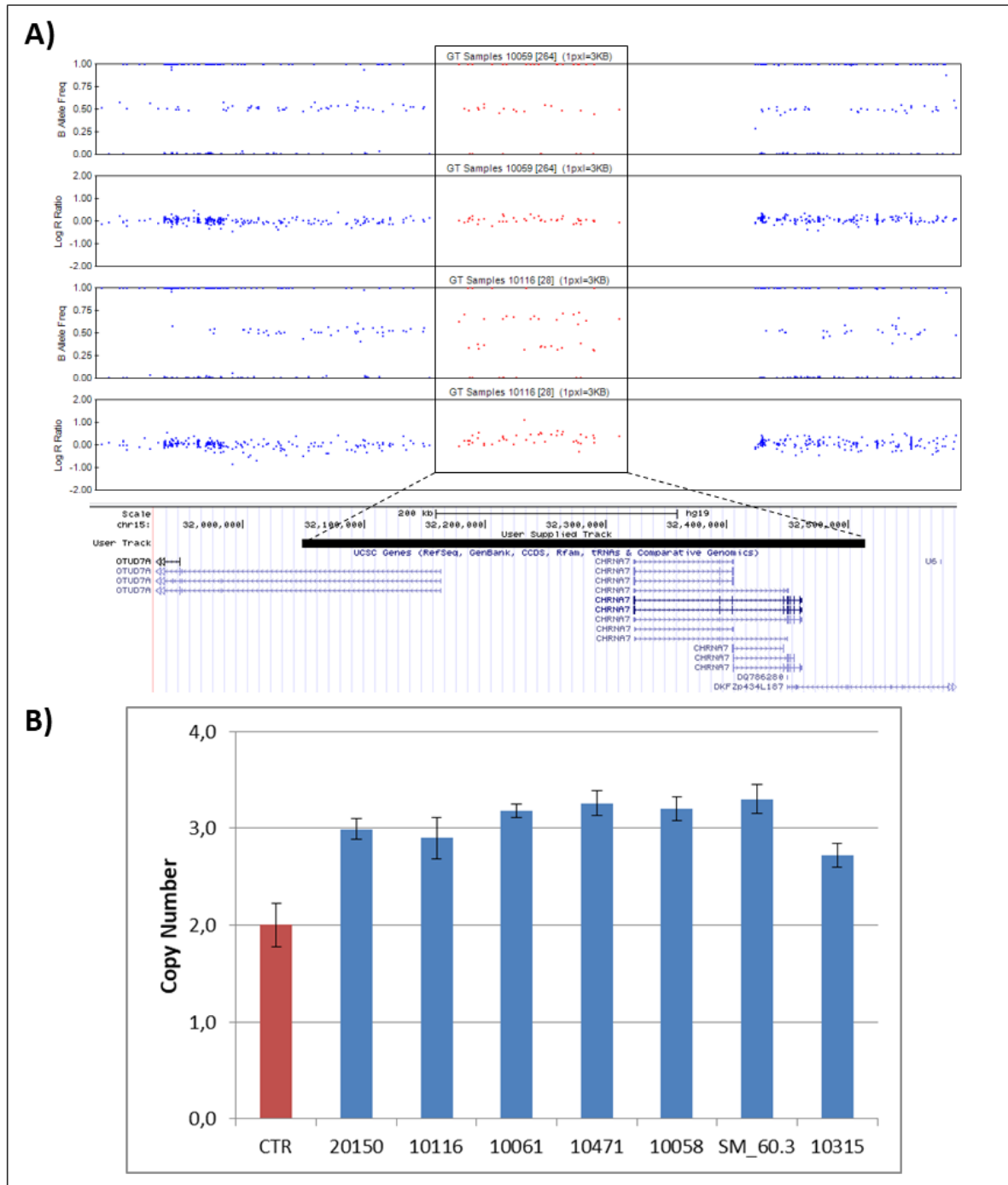


Figure 6.2: A) GenomeStudio screenshot showing B-allele frequency and log R ratio for an individual without CNVs (10059) and an individual carrying the microduplication involving *CHRNA7* (10116). The duplication results in an increase of the Log R ratio and a deviation of the allelic ratio. The SNPs included in the duplication are boxed. **B)** qPCR results for the *CHRNA7* copy number in 5 smokers, 1 ASD individual and 1 control subjects.

6.3 Genotyping of *CHRFAM7A*

The genotypes of the *CHRFAM7A* Δ 2bp polymorphism (rs67158670) was determined by analysis of exon 6 labeled PCR-product using Genemapper v3.0 software. This polymorphism is specific of *CHRFAM7A* and it has not been observed in *CHRNA7* exon 6.

Briefly, to assess rs67158670 genotype, a fragment of 238-236 bp encompassing *CHRFAM7A* and *CHRNA7* exon 6 was amplified by 5' fluorescent labelled PCR primers and PCR products were resolved by capillary electrophoresis on the ABI PRISM 3730 automatic sequencer. In Genemapper v3.0 software the PCR product fluorescent signal is represented as a peak in the graph: the Y axis reports the fluorescent intensity (RFU) and the X axis indicate the length of the product in bp (see materials and methods, paragraph 3.6.3). The presence of a 2bp deletion allele in *CHRFAM7A* gives rise to a PCR product which is 2 bp shorter than the wt allele in *CHRNA7* and/or *CHRFAM7A*, leading to two separated peaks representing fragments of 236 bp and 238 bp. In this case, considering that peak height (fluorescence intensity) is proportional to the amount of DNA template, the ratio of the two peak heights allows to determine the relative copy number of wt alleles compared to Δ 2bp alleles; given that the Δ 2bp allele is specific for *CHRFAM7A*, and that *CHRNA7* copy number has already been determined for each sample (see paragraph 6.2), from this analysis we can infer the number of copies of the *CHRFAM7A* gene.

The allelic status of *CHRFAM7A* was defined according to the deletion of the whole gene ("allele 0"), or presence of a copy of *CHRFAM7A* with the wt (TG) allele for rs67158670 ("allele1"), or the Δ 2bp allele ("allele2").

In total, 553 individuals were found with at least one copy of *CHRFAM7A* allele 2 and for these individuals it was possible to establish also the gene copy number of *CHRFAM7A*. The ratio between the fluorescence peak height representing *CHRFAM7A* allele 2 and the fluorescence peak height representing *CHRNA7* and/or *CHRFAM7A* allele 1 allowed to define six different genotype states for *CHRFAM7A* in our sample (Figure 6.3).

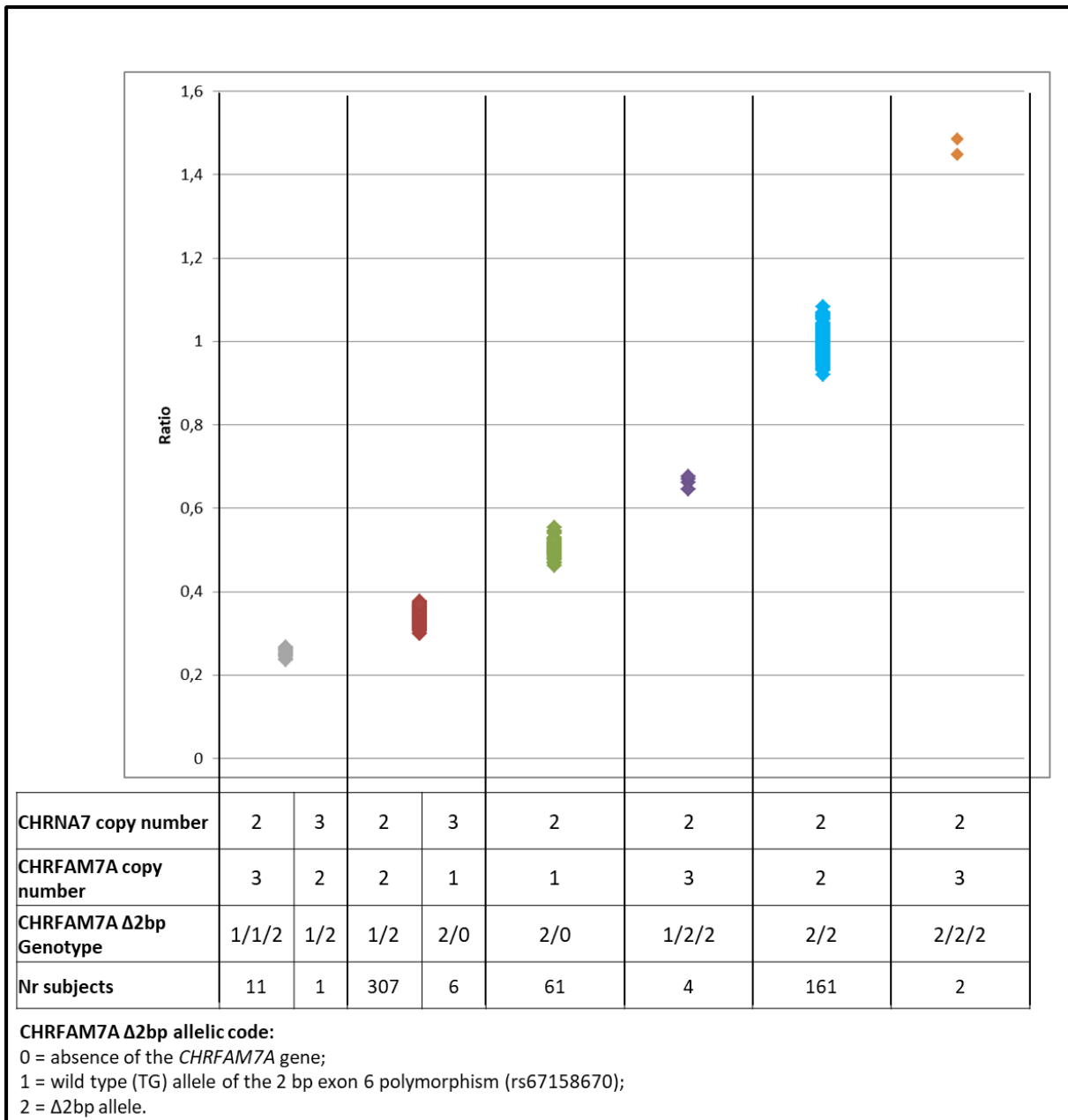


Figure 6.3: Graphical representation by scatter plot of *CHRFAM7A* genotype states (according to rs67158670) for 553 subjects with at least one copy of *CHRFAM7A* allele 2. The Y axis represents the ratio between peak heights of *CHRFAM7A* allele 2 and *CHRFAM7A* allele 1 obtained by analysis with Gene Mapper software. In the X axis are reported the copy number of both *CHRNA7* and *CHRFAM7A*, and the different *CHRFAM7A* genotypes inferred by the ratio of fluorescence peaks heights, taking into account the *CHRNA7* copy number (for example a ratio=0.25 indicates 1 copy of *CHRFAM7A* allele 2, 2 copies of *CHRFAM7A* allele 1 and two copies of *CHRNA7*: $\frac{1}{2}$ =0.25, grey dots). The number of individuals found for each genotype state is reported.

Instead, for 253 individuals carrying only the wild type allele, the *CHRFAM7A* copy number was established by real time PCR using *CHRFAM7A* specific primers (see material and methods paragraph 3.6.4). We detected 4 additional possible genotype states at *CHRFAM7A* according to the copy number of allele 1 (Figure 6.4).

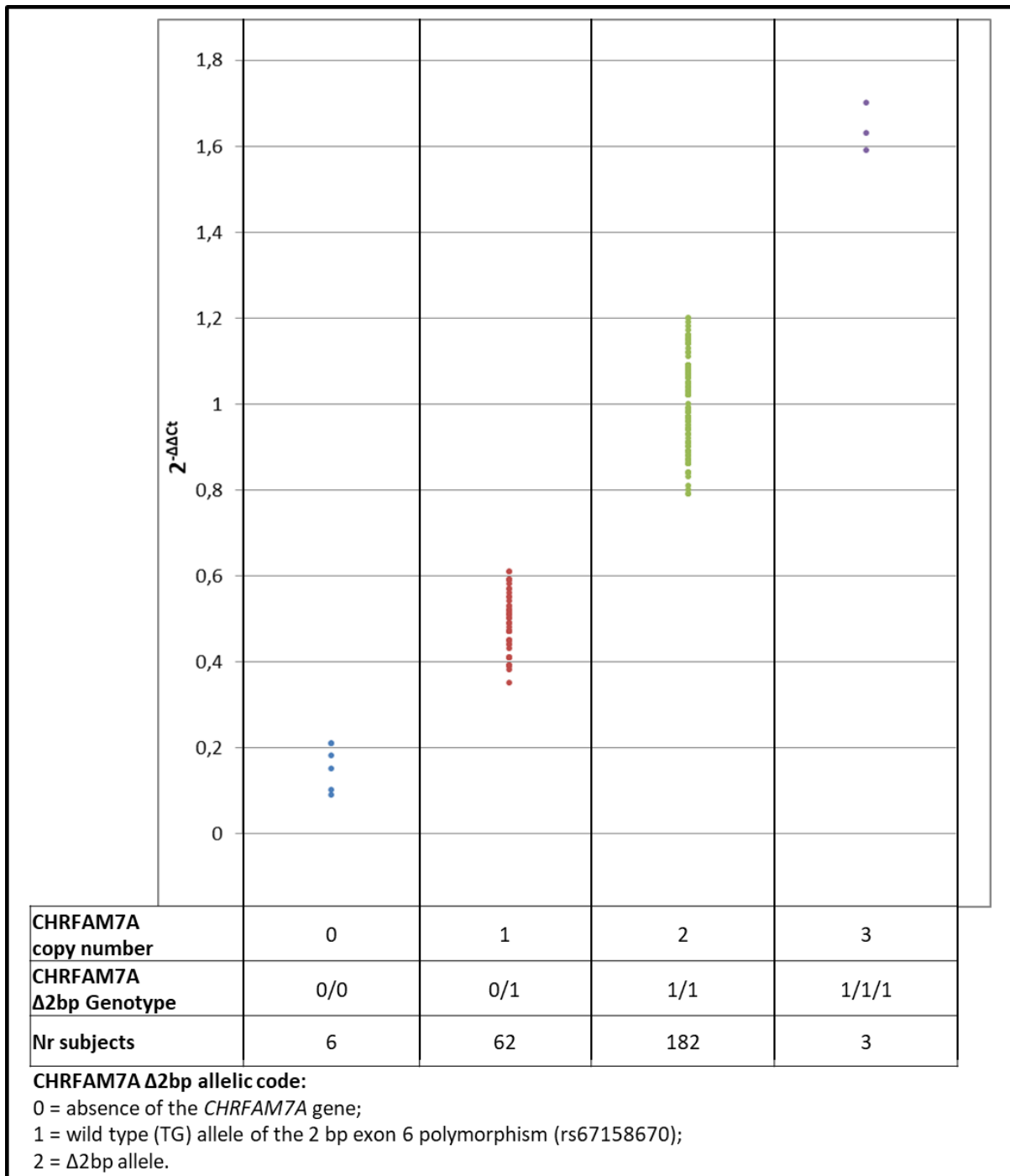


Figure 6.4: Graphical representation by scatter plot of *CHRFAM7A* copy number for 253 subjects found without the *CHRFAM7A* allele 2. The Y axis represents the $2^{-\Delta\Delta ct}$ value obtained from real time PCR analysis. The X axis shows *CHRFAM7A* copy number, the rs67158670 genotypes according to *CHRFAM7A* copy number and the number of subjects found in each category. All these subjects have 2 copy of *CHRNA7*.

6.4 Case-control analysis of genetic variation in *CHRNA7* and *CHRFAM7A*

We performed a case control analysis (Fisher test) to test if *CHRNA7* and *CHRFAM7A* copy number genotypes differ between smokers, controls and ASD subjects. No statistically significant difference was detected in this analysis ($p = 0.651$). Furthermore, the copy number

genotypes distribution observed in our sample is comparable to previously reported data in other European populations¹³⁹. (Table 6.3).

	Copy number (%)						Total
	CHRNA7(2)/ CHRFAM7A(0)	CHRNA7(2)/ CHRFAM7A(1)	CHRNA7(2)/ CHRFAM7A(2)	CHRNA7(2)/ CHRFAM7A(3)	CHRNA7(3)/ CHRFAM7A(1)	CHRNA7(3)/ CHRFAM7A(2)	
<i>Smokers</i>	3 (0.74)	58 (14.22)	333 (81.62)	9 (2.21)	4 (0.98)	1 (0.25)	408
<i>Controls</i>	1 (0.52)	34 (17.53)	148 (76.29)	10 (5.15)	1 (0.52)	0 (0)	194
<i>Autism</i>	2 (0.98)	31 (15.20)	166 (81.37)	4 (1.96)	1 (0.49)	0 (0)	204
<i>Total</i>	6 (0.74)	123 (15.26)	647 (80.27)	23 (2.85)	6 (0.74)	1 (0.12)	806

Table 6.3: . CHRNA7/ CHRFAM7A copy number in smokers, controls and individuals with autism

The majority of individuals carry two copies of each gene (80%), while approximately 16% of individuals have only one copy of *CHRFAM7A*, and only 0.74 % has no copies. A minority of subjects have three copies of *CHRNA7* (0.86%) or *CHRFAM7A* (2.85%).

Next, we analyzed the allelic status of *CHRFAM7A* according to presence of either the wt (TG) allele for the exon 6 polymorphism (“allele1”), or the Δ 2bp allele (“allele2”), or deletion of the whole gene (“allele 0”), (Table 6.4). There was no significant difference in allele frequency between the three samples of smokers, controls, and ASD (Chi2, p-value=0.72).

	Allele¹ (%)			Total
	0	1	2	
<i>Smokers</i>	68 (8.24)	404 (48.97)	353 (42.79)	825
<i>Controls</i>	37 (9.30)	185 (46.48)	176 (44.22)	398
<i>Autism</i>	35 (8.5)	186 (45.14)	191 (46.36)	412
<i>Total</i>	140 (8.56)	775 (47.4)	720 (44.04)	1635

Table 6.4: *CHRFAM7A* Δ 2bp allele frequency distribution in smokers, controls and autistic individuals
¹“0” = absence of *CHRFAM7A*; “1” = wild type (TG) allele; “2” = Δ 2bp allele

6.5 Quantitative analysis of *CHRFAM7A* variants

Given the availability of quantitative smoking measures on the sample of smokers, we performed linear regression analysis to investigate the effect of genetic variants on smoking

quantity (CPD) or nicotine dependence (FTND). Linear regression analysis with adjustment for sex as covariate, did not identify a significant effect for *CHRFAM7A* copy number on either smoking measures (Table 6.5).

Furthermore, we tested the effect of $\Delta 2\text{bp}$ polymorphism on CPD or FTND. In order to test for the influence of the $\Delta 2\text{bp}$ polymorphism independently of *CHRFAM7A* copy number, regression analysis was conducted in the stratified sample of individuals with 1 or 2 copies of *CHRFAM7A* (Table 6.5). In individuals carrying 2 copies of *CHRFAM7A* we observed a mild association of $\Delta 2\text{bp}$ allele with CPD, but this result was not confirmed in regression analysis with FTND (Table 6.5).

FTND				
Variants	Coef.	Std. Err.	95% C.I.	P (FTND)
<i>CHRFAM7A</i> copy number	-0.09	0.25	-0.57 - 0.39	0.715
$\Delta 2\text{bp}$ allele (<i>CHRFAM7A</i> copy number=1)	0.32	0.56	-0.80 - 1.46	0.562
$\Delta 2\text{bp}$ allele (<i>CHRFAM7A</i> copy number=2)	0.16	0.16	-0.16 - 0.48	0.333
CPD				
Variants	Coef.	Std. Err.	95% C.I.	P (CPD)
<i>CHRFAM7A</i> copy number	-1.16	1.10	-3.34 - 1.00	0.29
$\Delta 2\text{bp}$ allele (<i>CHRFAM7A</i> copy number=1)	0.37	2.31	-4.25 - 5.00	0.87
$\Delta 2\text{bp}$ allele (<i>CHRFAM7A</i> copy number=2)	1.86	0.73	0.41 - 3.31	0.012

Table 6.5: Linear regression analysis of *CHRFAM7A* copy number and $\Delta 2\text{bp}$ polymorphism stratified by copy number, with adjustment for sex

6.6 Quantitative analysis of *CHRNA7* variants

The region encompassing 740 bp upstream the *CHRNA7* start codon, containing the *CHRNA7* core promoter region¹⁵⁰ was sequenced in the sample of smokers by Sanger sequencing. We identified a total of thirteen polymorphism listed in Table 6.6, of which 2 are common variants (MAF > 0.01) and 11 are rare variants (Table 6.6).

POSITION (hg19)		SNP ID	Nr het/Nr hom N=408 smokers (MAF)	Nr het/Nr hom N=129 abstinent smokers (MAF)	Nr het/Nr hom N=279 not abstinent smokers (MAF)
chr15:32322094	-704 T/C	rs576919947	1/- (0.001)		1/- (0.002)
chr15:32322464	-334 C/T	rs182726713	4/- (0.005)		4/- (0.007)
chr15:32322476	-322 C/T	rs377300328	1/- (0.001)		1/- (0.002)
chr15:32322482	-316 C/A	rs139231762	3/- (0.004)		3/- (0.005)
chr15:32322557	-241 A/G	rs188889623	6/- (0.007)	1/- (0.004)	5/- (0.009)
chr15:32322604	-194 G/C	rs28531779	27/1 (0.036)	9/1 (0.043)	18/- (0.032)
chr15:32322607	-191 G/A	rs553179500	2/- (0.002)	1/- (0.004)	1/- (0.002)
chr15:32322632	-166 C/T	-	1/- (0.001)		1/- (0.002)
chr15:32322643	-155 G/A	-	1/- (0.001)		1/- (0.002)
chr15:32322706	-92 G/A	rs111910242	5/- (0.006)	2/- (0.008)	3/- (0.005)
chr15:32322712	-86 C/T	rs149637464	43/2 (0.055)	15/- (0.058)	28/2 (0.058)
chr15:32322750	-48 C/G	rs201089931	1/- (0.001)		1/- (0.002)
chr15:32322752	-46 G/T	rs145180415	4/- (0.005)	2/- (0.008)	2/- (0.004)

Table 6.6: *CHRNA7* promoter variants. Common variants (MAF > 0.01) are indicated in bold.

Focusing only on the two common variants rs28531779 and rs149637464 (MAF > 0.01), we carried out a linear regression analysis, to test for association of these SNPs with smoking measures. As above, sex was included as covariate in our regression model. This analysis revealed a statistically significant association for the rs28531779 SNP with both FTND ($p=0.026$) score and CPD ($p=0.006$) (Table 6.7).

FTND						
Index SNP	CHR	BP	Coef.	Std. Err.	95% C.I.	P value
rs28531779	15	32030401	-4.82	1.73	-1.67 -0.11	0.02639
CPD						
Index SNP	CHR	BP	Coef.	Std. Err.	95% C.I.	P
rs28531779	15	32030401	-0.89	0.4	-8.22 -1.42	0.006

Table 6.7: Linear regression analysis of *CHRFAM7A* copy number with adjustment for sex

Specifically, individuals carrying the minor allele for rs28531779 have a higher FTND score and CPD than homozygotes individuals for the G allele (Figure 6.5). Mean CPD for rs28531779 GG genotype were 21.37 ± 9.13 , and 26.50 ± 13.10 for the GC and CC genotypes (Ttest; p-value= 0.003); while mean FTND score for GG genotype was 5.73 ± 2.13 , and for the GC and CC genotypes was 6.71 ± 2.40 (Ttest; p-value= 0.01)

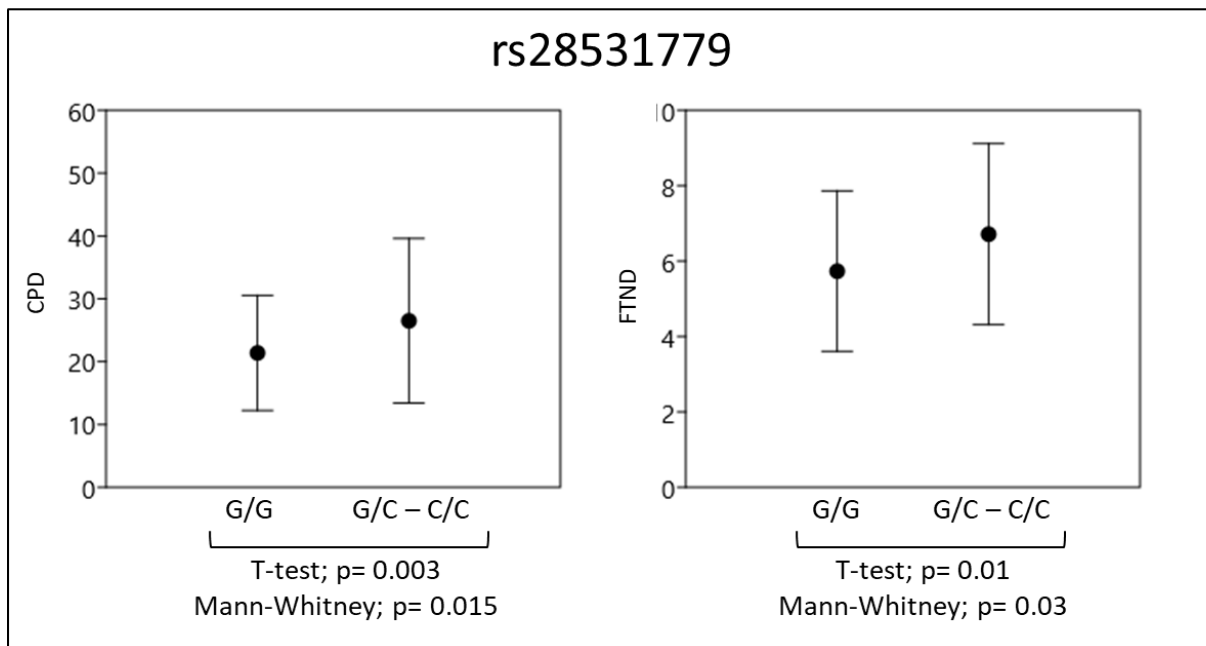


Figure 6.5 The boxplots display the distribution of CPD (A) and FTND (B) among individuals homozygous for rs28531779 G allele and carrying the C allele.

Then, we also evaluated the cumulative effect of 11 rare (MAF < 0.01) promoter variants on smoking measures (FTND, CPD). Using the SKAT method, we performed a burden analysis that allows to increase the power to identify variants effect on phenotype than testing each variant individually. The SKAT analysis provides a cumulative p-value indicating the degree of

enrichment of rare variant associations within a genetic region. This analysis did not detect a statistically significant result.

6.7 Analysis of rs28531779 effect on *CHRNA7* promoter activity by dual luciferase assay

A previous functional study using luciferase assay, suggested that several common variants in the *CHRNA7* core promoter region, including rs28531779, decrease *CHRNA7* promoter activity *in vitro*. In order to confirm this result, we replicated *in vitro* functional analysis for rs28531779 by dual luciferase assay in two neuroblastoma derived cell lines, BE-2(C) and SHSY-5Y. A region of 269 bp including the *CHRNA7* core promoter was amplified by PCR from two different genomic DNA samples: one carrying the G/G genotype (WT) for rs28531779 and one carrying the C/C genotype (MUT). The fragments were cloned into pGL3 Basic vector (pGL3 WT or the pGL3 MUT), and analyzed for luciferase reporter gene activity as described in material and methods (see paragraph 3.5). In both cell lines tested, reporter assays showed a slightly lower luciferase activity in cells transfected with the pGL3 MUT vector compared to the pGL3 WT, however this difference was not statistically significant (Figure 6.6).

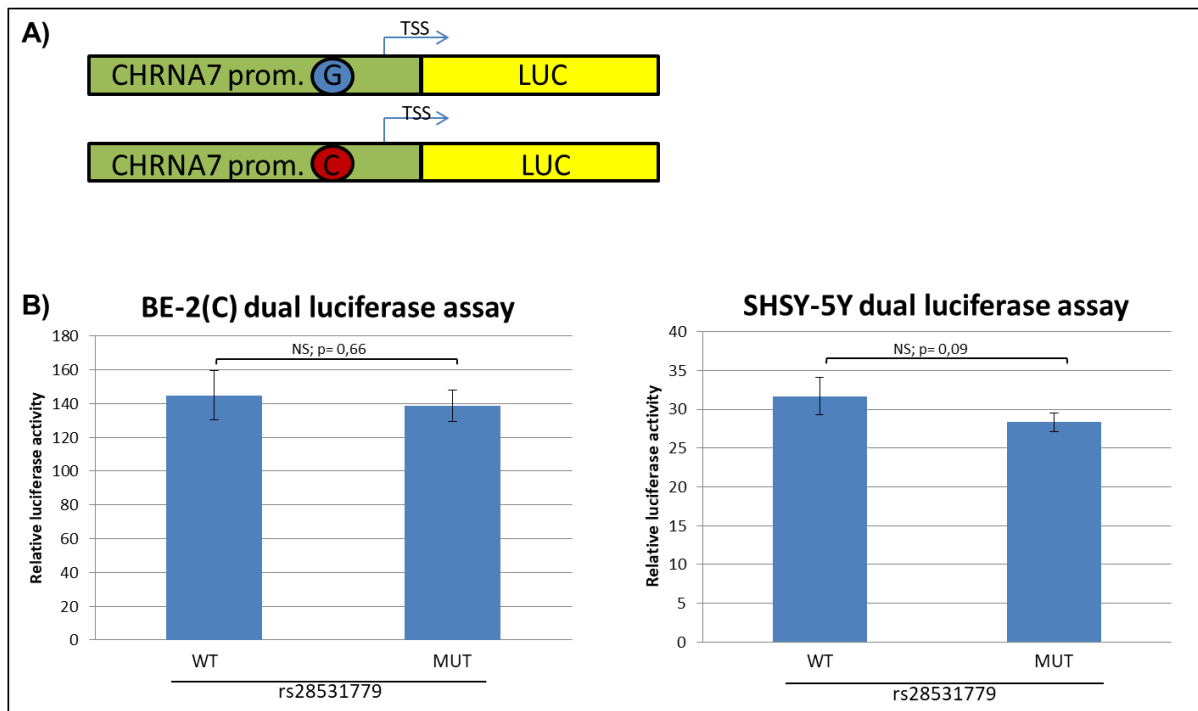


Figure 6.6: **A)** Schematic representation of the "pGL3_wt" and "pGL3_MUT" recombinant plasmids, used in dual luciferase assays to verify the effect of rs28531779 on *CHRNA7* promoter activity. **B)** Luciferase activity of *CHRNA7* promoter constructs measured in Dual luciferase assays using two different cells lines. Firefly luciferase data are normalized to renilla luciferase activity. Relative luciferase activity was calculated by the ratio between pGL3 WT or pGL3 MUT signals normalized to renilla and pGL3 basic empty vector (normalized to renilla). The experiment was set up in triplicate; error bars represent SD.

6.8 Association analysis for smoking abstinence in the varenicline treated sample

We performed a logistic regression analysis, with adjustment for sex and FTND score as covariates, in order to test for an effect of *CHRFAM7A* copy number, the Δ 2bp allele (rs67158670) and *CHRNA7* promoter variants on smoking abstinence in the group of 142 subjects treated with varenicline. This analysis identified a possible effect of *CHRFAM7A* copy number on abstinence (OR= 3.18, 95% CI= 1.09 – 9.30, p= 0.035); while no statistically significant results were observed for rs67158670 and *CHRNA7* promoter variants (rs28531779, rs149637464) (Table 6.8).

Abstinance (varenicline treated group N=142)					
Variants	Coef.	Std. Err.	95% C.I.	P value	
rs28531779	-1.21	0.69	-2.57 -0.14	0.079	
rs149637464	-0.41	0.60	-1.59 0.76	0.49	
CHRFAM7A copy number	3.17	1.74	1.09 - 9.30	0.035	
Δ2bp allele (CHRFAM7A copy number=1)	1.09	1.27	-1.40 - 3.59	0.39	
Δ2bp allele (CHRFAM7A copy number=2)	0.45	1.45	-0.16 - 1.06	0.146	

Table 6.8: Logistic regression analysis to test the effect of *CHRNA7* common promoter variants and *CHRFAM7A* variant (Δ 2bp allele and copy number), on abstinence with adjustment for sex and FTND. Δ 2bp polymorphism was stratified by copy number.

The significant result from logistic regression analysis is also supported by a higher quit success rate in smokers carrying 2 or 3 copies of the *CHRFAM7A* gene compared to smokers carrying 0 or 1 copies (1 sided Fisher exact test $p= 0.048$) (Figure 6.7 A).

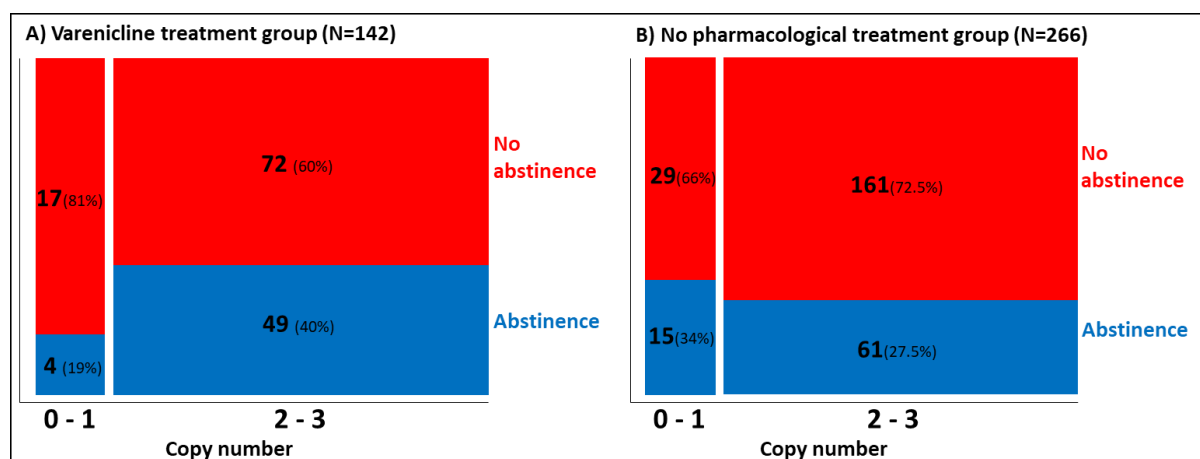


Figure 6.7: The mosaic plot displays the *CHRFAM7A* copy number among abstinent and not abstinent subjects in: **A)** the varenicline treated group (N=142), 1 sided Fisher exact test: $p= 0.048$, **B)** in the No-pharmacological treatment group (N=266), 1 sided Fisher exact test $p= 0.23$. The blocks width indicates the sample size in the two categories (Copy number 0-1 and 2-3), while the blocks heights indicate the percentage of subjects (abstinent individuals or not abstinent individuals) in each categories.

The logistic regression analysis was repeated on the remaining sample of 266 smokers who did not receive varenicline treatment to detect a possible effect of *CHRFAM7A* copy number on abstinence. This analysis did not reveal a statistically significant effect (Table 6.9).

To support the hypothesis that *CHRFAM7A* copy number may interact with varenicline in modulating the effectiveness of varenicline treatment as a smoking cessation aid, a logistic

regression analysis was performed in the entire sample of smokers including the “varenicline treatment X *CHRFAM7A* copy number” interaction term in the model. As expected, the interaction term yields a mild statistically significant p-value ($p = 0.044$).

CHRFAM7A Copy Number	Odds ratio	95% C.I.	P value
Varenicline treatment N=142	3.18	1.09 - 9.30	0.035
No pharmacological treatment N= 266	0.88	0.47 - 1.66	0.705

Table 6.9: Logistic regression analysis to test the effect of CHRFAM7A copy number variants on abstinence with adjustment for sex and FTND in the varenicline treatment group and in the no pharmacological treatment group.

CHAPTER 7

Genome-wide analysis of common and rare variants influencing risk for Cluster Headache

7.1 Sample characteristics

The genome wide analysis was performed on 99 subjects with cluster headache (CH) and 359 controls. All phenotypic and demographic information collected for these 458 individuals is described in Table 7.1.

	CH patients	Controls
N	99	359
Gender (N,%)		
Male	85, 83.84%	204, 56.82%
Female	16, 16.16%	155, 43.18%
Age, ys (mean \pm sd, range)	47.39 \pm 13.12, 23-81	48.96 \pm 11.91, 18-70
CH attacks		
Age at onset, ys (mean \pm sd, range)	30.04 \pm 12.65, 6-80	
Chronic (N, %)	14, 14.14%	
N attacks/year (mean \pm sd, range);	1.29 \pm 0.77, 0.17-4	
N attacks/day (mean \pm sd, range);	2.85 \pm 1.68, 1-9	
Smoking		
Ever smoking (N,%)	88, 89.11%	359, 100%
N. cigarette/day (mean \pm sd)	19.17 \pm 10.83	21.77 \pm 9.13
Fagerström test (mean \pm sd); N	4.60 \pm 2.54 (N=72)	5.95 \pm 2.21

Table 7.1: Sample characteristics

7.2 SNP genotyping by Illumina Infinium® PsychArray microarrays

Genotyping was performed on Illumina Infinium® PsychArray microarrays (Illumina, San Diego, California, USA), in two batches, the first using Illumina PsychArray-24 v1.0, the second using PsychArray-24 v1-1 array²⁵⁷. The Infinium PsychArray combines common highly-informative genome-wide tag SNPs (265000 variants), exome-focused markers (245000 variants) and 50000 additional polymorphism associated with common psychiatric disorders. For the analysis, only SNPs present on both versions of the array (566178 variants) were used.

After quality control filtering (as described in paragraph 4.2), 211927 monomorphic SNPs were excluded from the analysis. A total of 344558 SNPs passed the filters and they were used for genetic associations analysis for CH disease susceptibility.

In particular, common SNPs with minor allele frequency (MAF) > 0.01 were used in the genome wide association analysis (paragraph 7.3), while rare (MAF < 0.05) protein altering variants (PAVs) were used to perform a gene-based association analysis (paragraph 7.7).

7.3 Genome wide association analysis

We performed a single marker case-control association analysis on high quality SNPs with minor allele frequency (MAF) > 0.01 (290505 variants) in the study population, using the Fisher exact test. In order to exclude the hypothesis that in our sample the statistics results could be inflated by artificial differences in allele frequencies caused by population stratification or cryptic relatedness and genotyping errors, we calculated the genomic inflation factor (λ), defined as the ratio of the observed and expected medians of the test statistic distribution, and we carried out a Q-Q plot, showing the expected distribution of association test statistics compared to the observed values. In our sample the λ score is 1, indicating that no overall inflation of the genome-wide statistical results exists. In addition, the Q-Q plot showed no global deviation of the observed distribution from the expected null distribution (Figure 7.1) indicating that the inflation of the genome-wide association results due to population stratification is negligible.

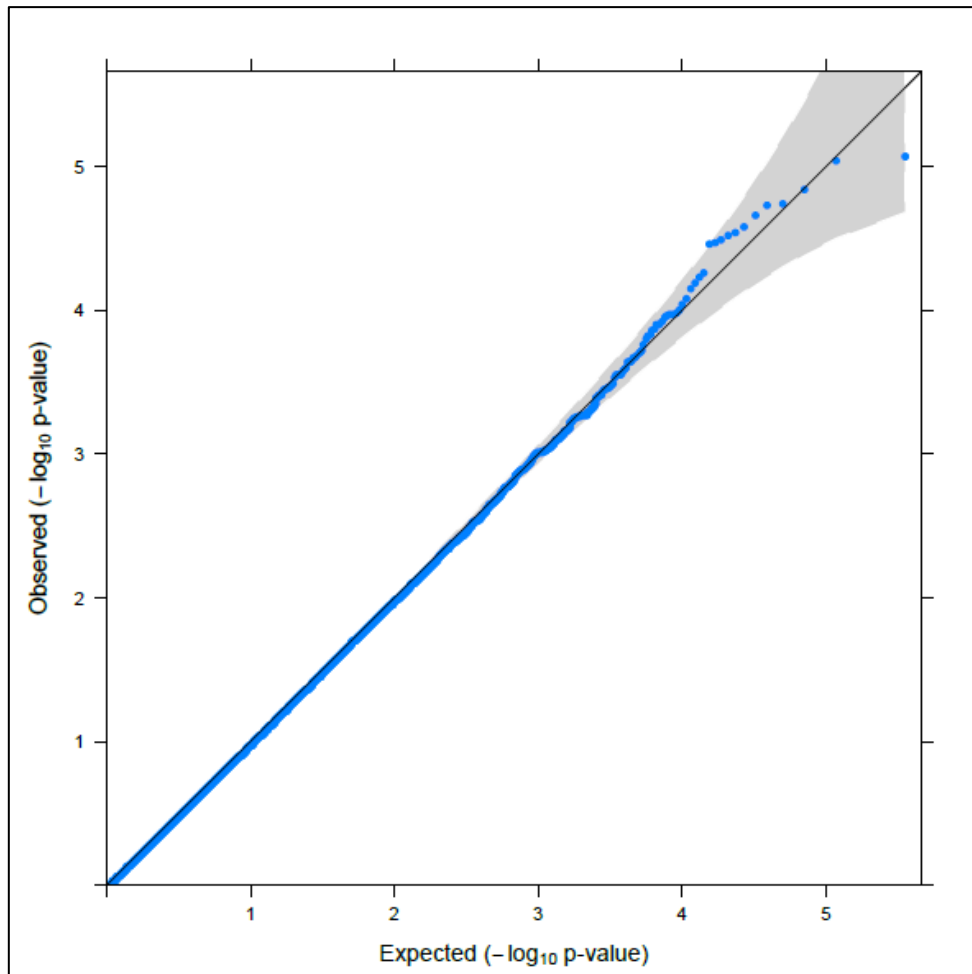


Figure 7.1: Quantile-quantile (Q-Q) plot of Fisher's exact test P-values for association with CH. X-axis shows P-values expected under the null distribution; Y-axis shows observed data. Grey region shows 95% confidence interval.

The genome wide association results are represented in the Manhattan plot (Figure 7.2). This scatter plot displays the SNPs genomic localization along the X-axis with different colours for each of the 23 chromosomes and the $-\log_{10}$ of the association P-value for each SNP on the Y axis.

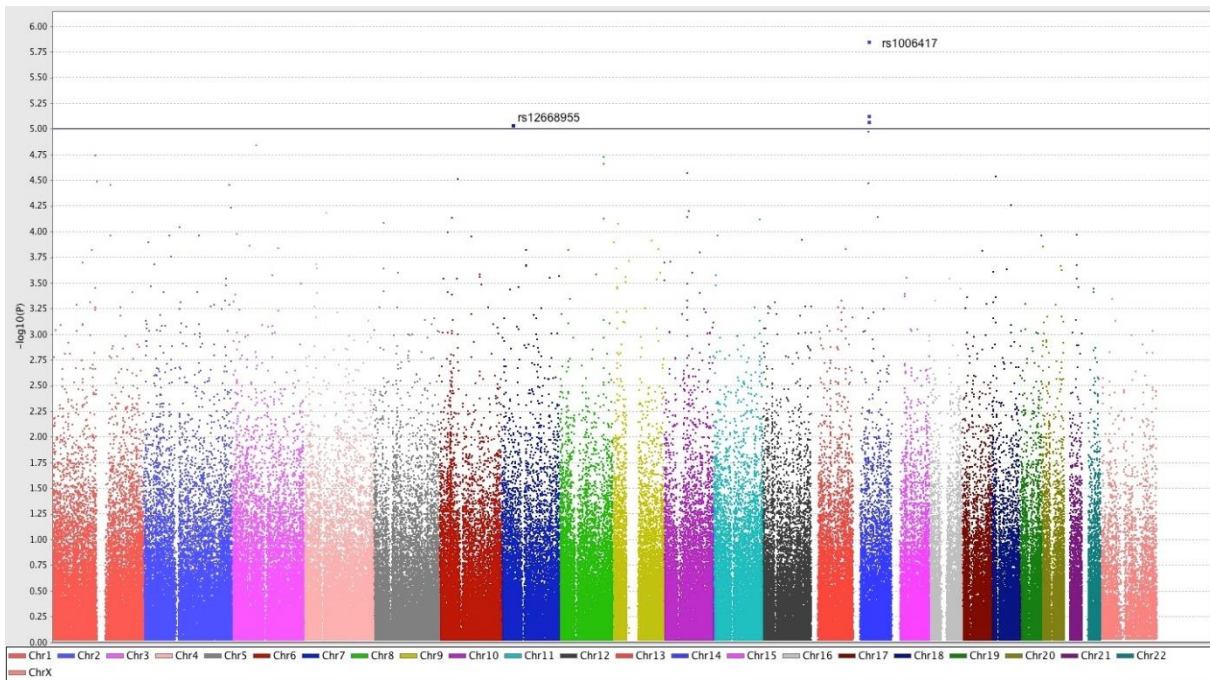


Figure 7.2: Manhattan plot of genome-wide association P-values. The y axis represents the $-\log_{10}$ Fisher's test P-values; the horizontal line indicates the threshold for suggestive significance ($P < 10^{-5}$)

In this study, the genome-wide threshold for statistically significant association, calculated by the Bonferroni correction for multiple testing, is $P < 1.7 \times 10^{-7}$. No variant reached this genome-wide significance level; however some SNPs showed suggestive associations (p value $< 10^{-5}$, the threshold is indicated with a grey line in the Manhattan plot).

7.3.1 Suggestive results from GWAS

The SNPs with the most significant p-values identified in our study and their chromosomal localization are listed in table 7.2. Furthermore, all variants included in the study in LD with the index SNPs are also reported.

Suggestive results (p value $< 10^{-5}$) have been identified for the 2 polymorphisms listed at the top of the table. Genotypes for these 2 variants are represented in the Genoplots in Figure 7.3. For each variant, the genotypes are grouped in two different Genoplots based on different batches of Illumina Infinium® PsychArray microarrays (v1.0 and v1.1) used for SNPs genotyping.

Index SNP	Position	Other SNPs in clump	Gene	A 1	A 2	A1-F case/controls	A1-F 1000G_all (1000G_EUR; 1000G_TSI) ^a	P-value	OR (95% CI)
rs1006417	14:41803291	rs1782180, rs1779522, rs1778408, rs11157219, rs715334, rs12433558		G	A	0.11/0.26	0.19 (0.19; 0.22)	1.40×10^{-6}	0.34 (0.21-0.55)
rs12668955	7:31116168		<i>ADCYAP1R1</i>	G	A	0.34/0.52	0.55 (0.50; 0.47)	9.10×10^{-6}	0.48 (0.34-0.66)
rs1495452	3:65834076		<i>MAGI1</i>	A	G	0.55/0.38	0.39 (0.45; 0.49)	1.43×10^{-5}	2.03 (1.48-2.79)
rs2182605	1:117463537		<i>PTGFRN</i>	G	A	0.32/0.50	0.51 (0.48; 0.45)	1.80×10^{-5}	0.49 (0.35-0.68)
rs16895584	8:122518935			A	G	0.24/0.04	0.070 (0.054; 0.051)	1.85×10^{-5}	3.50 (2.03-6.02)
rs6469999	8:122415207	rs13255877, rs7833779		A	G	0.31/0.17	0.46 (0.16; 0.17)	2.16×10^{-5}	2.23 (1.56-3.19)
rs1509957	10:64610718	rs224308, rs10822065		G	A	0.60/0.43	0.43 (0.49; 0.42)	2.66×10^{-5}	1.99 (1.44-2.74)

Table 7.2: Genome wide association analysis results of SNPs with the most significant p-values.

Abbreviations: A1 = minor allele in study sample; A2 = major allele; A1-F = A1 frequency; OR = odds ratio for minor allele; CI = confidence interval

^a Allele 1 frequency in 1000 Genomes phase 3, all populations (1000G_all), european population (1000G_EUR) and Tuscans from Italy (1000G_TSI)

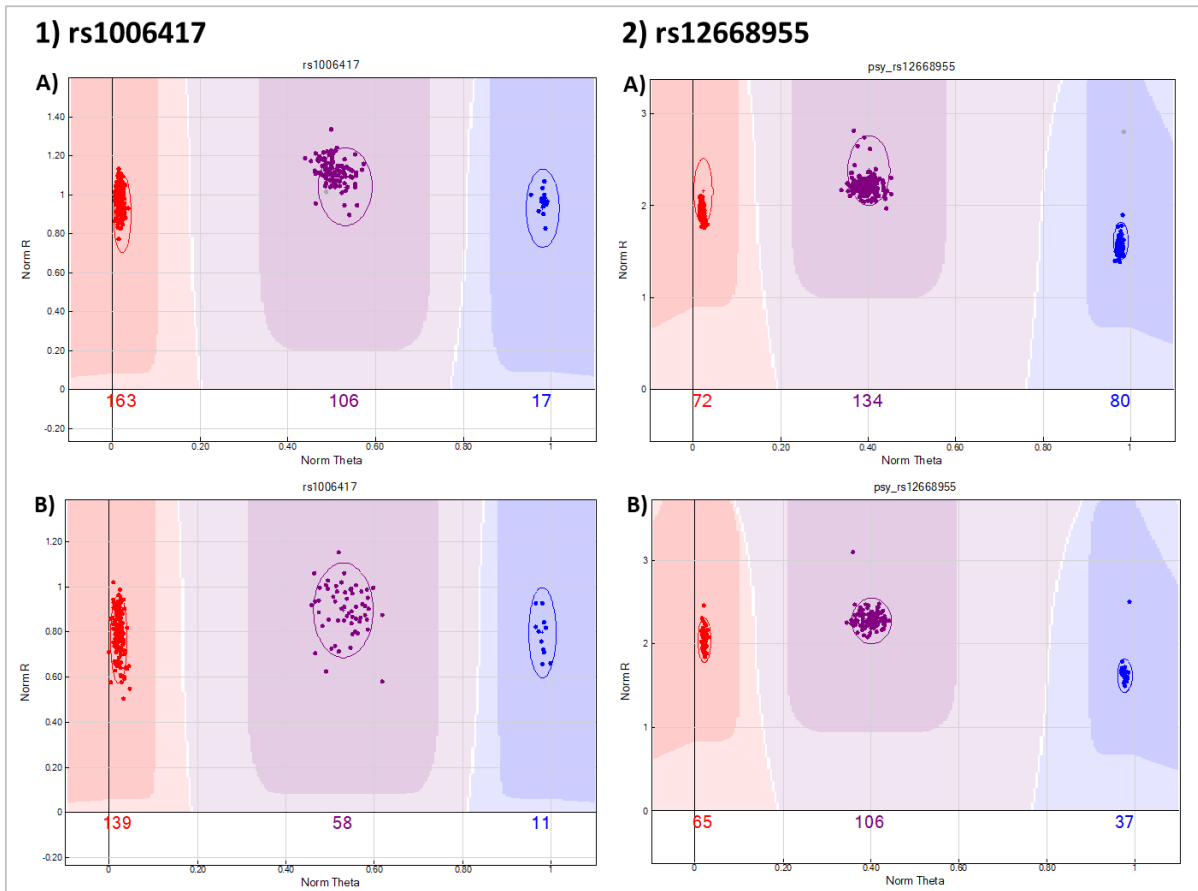


Figure 7.3: Plots for variants rs1006417 and rs12668955 in CH and control samples genotyped by PsychArray-24 v1.0.(A) and by PsychArray-24 v1.1 (B). The colours indicate the genotype: red= CC, purple= GC and blue= GG.

The most significant hit is a SNP cluster tagged by rs1006417 located on chromosome 14 ($p=1.4 \times 10^{-6}$). This SNP maps in a chromosomal region with no known genes. The second suggestive results is for SNP rs12668955 located on chromosome 7, in an intronic region of the *ADCYAP1R1* gene encoding for the pituitary adenylate cyclase-activating polypeptide (PACAP) receptor ($p=9.10 \times 10^{-6}$). Figure 7.4 displays the local association plots for both the suggestive results loci.

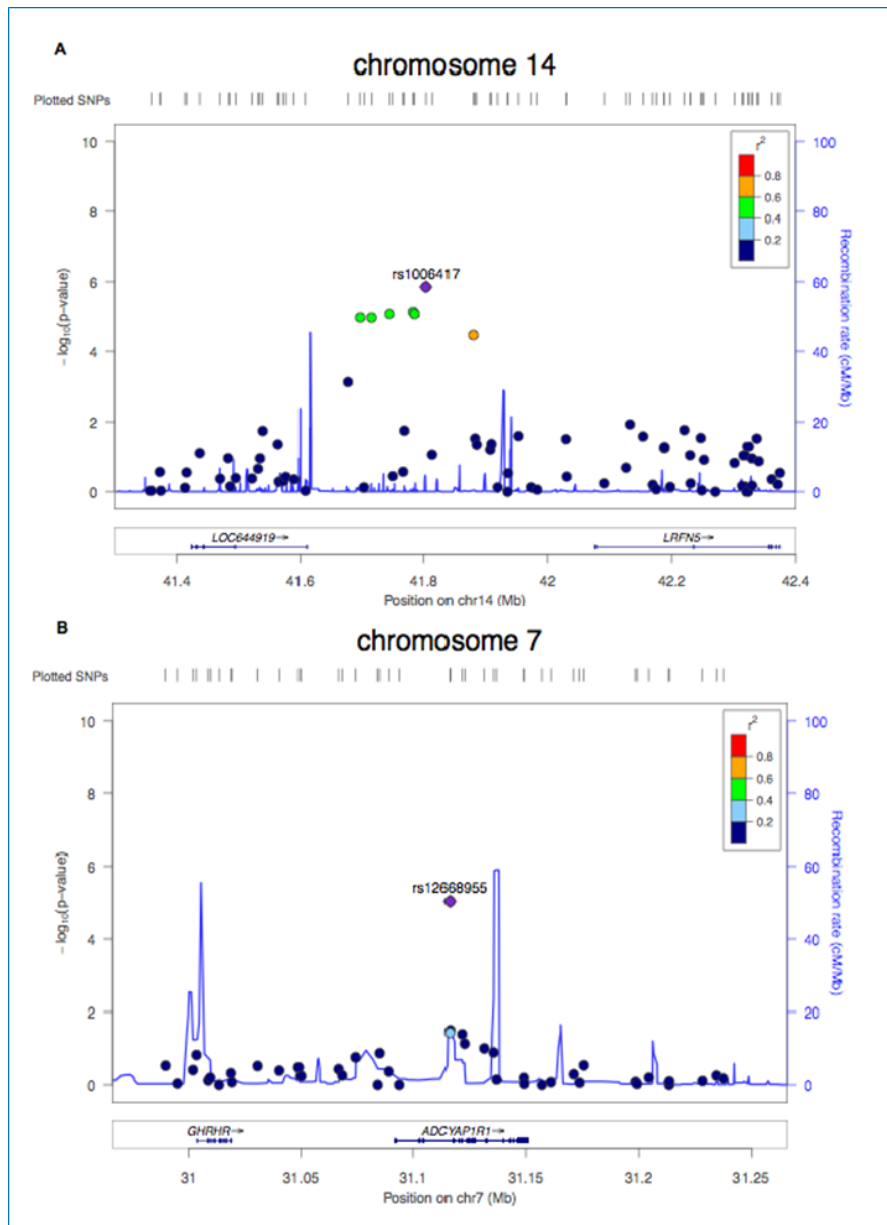


Figure 7.4: Local association plots for chromosome 14 locus (A) and the chromosome 7 locus (B). Association results are shown for genotyped SNPs, colored according to their level of linkage disequilibrium of the each SNP with the index SNP (purple diamond). The blue line shows the estimated recombination rates from the 1000 Genomes Project November 2014 release. The genomic locations of genes are shown below the plot based on GRCh37/hg19 assembly.

Given the high prevalence of males suffering from CH, the ratio between males and females is very different among CH patients and controls individuals. In order to take into account this gender distribution difference, we performed a logistic regression analysis for the most significant SNPs from GWAS, adding sex as covariate. In this analysis, rs1006417 was confirmed to be the most significant result ($P = 4.18 \times 10^{-6}$). However, for rs12668955, linear regression analysis identified a reduction of significance ($p = 0.000138$), suggesting a possible sex effect at this locus. In the logistic regression analysis we have also included CPD and age as covariates, but we did not find a significant effect of these variable at each locus tested. The logistic regression results are listed in table 7.3.

Index SNP	CHR	BP	P value
rs1006417	14	41803291	4.18E-06
rs12668955	7	31116168	1.38E-04
rs1495452	3	65834076	7.25E-06
rs2182605	1	117463537	2.87E-04
rs16895584	8	122518935	9.95E-05
rs6469999	8	122415207	3.22E-04
rs1509957	10	64610718	1.05E-04
rs117202318	18	10613697	6.15E-06
rs1324523	6	50080330	2.19E-04

Table 7.3: logistic regression analysis. P-values for additive effect of SNPs controlling for sex as a covariate.

7.4 Analysis of loci previously implicated in CH

We investigated if our dataset could provide some support to previously reported putative association signals for CH in the *HCRTR2* and *ADH4* genes. 21 polymorphic SNPs genotyped on the PsychArray (18 common variants and 3 rare variants) map in *HCRTR2*: no common SNP provided a significant single marker P-value (Fisher test), including the previously implicated variant rs2653349 (G1246A) (Table 7.4). Only a very rare missense variant (rs41271312) reached a nominally significant P-value ($P = 0.03$) (Table 7.4).

ADH4 contained 13 polymorphic SNPs (12 common variants including the reported SNPs rs1126671 and 1 rare missense variants) none of which was nominally significant (Table 7.4).

SNP rsID	Position (hg19)	Locus	F_A	F_U	P	OR
rs7766546	chr6:55006253	HCRTR2	0.4192	0.3841	0.4108	1.157
rs9475176	chr6:55014872	HCRTR2	0.383	0.3641	0.671	1.084
rs13200042	chr6:55033223	HCRTR2	0.2424	0.2019	0.2375	1.265
rs9382460	chr6:55037484	HCRTR2	0.1919	0.1894	0.9188	1.016
rs41271312	chr6:55039416	HCRTR2	0.0151	0.0014	0.0335	11,03
rs10456181	chr6:55040696	HCRTR2	0.3889	0.4248	0.372	0.8617
rs6927478	chr6:55044386	HCRTR2	0.3698	0.4286	0.1609	0.7824
rs9370399	chr6:55045025	HCRTR2	0.4343	0.3942	0.3264	1.18
rs3122148	chr6:55065989	HCRTR2	0.2062	0.2207	0.6959	0.9173
rs6937878	chr6:55067627	HCRTR2	0.1566	0.1894	0.3493	0.7944
rs9396060	chr6:55079046	HCRTR2	0.1263	0.1685	0.1877	0.713
rs3122156	chr6:55082807	HCRTR2	0.2626	0.2947	0.4249	0.8524
rs9357849	chr6:55092069	HCRTR2	0.3081	0.3259	0.6681	0.921
rs7771240	chr6:55093831	HCRTR2	0.3081	0.3245	0.731	0.9268
rs9357851	chr6:55097163	HCRTR2	0.2424	0.273	0.4148	0.8522
rs9382471	chr6:55107267	HCRTR2	0.2677	0.2911	0.5356	0.8902
rs77680302	chr6:55110524	HCRTR2	0.1162	0.07521	0.08148	1.616
rs41381449	chr6:55120108	HCRTR2	0	0.00696	0.591	0
rs2653349	chr6:55142337	HCRTR2	0.1616	0.1453	0.5734	1.134
rs146899452	chr6:55147138	HCRTR2	0	0.00139	1	0
rs2653350	chr6:55144102	HCRTR2	0.404	0.4513	0.258	0.8244
rs3828541	chr4:100042262	ADH4	0.3776	0.3855	0.8686	0.967
rs1139490	chr4:100045141	ADH4	0.3131	0.3482	0.3972	0.8534
rs1042365	chr4:100045500	ADH4	0.2879	0.3273	0.3027	0.8309
rs1139490	chr4:100045141	ADH4	0.3131	0.3482	0.3972	0.8534
rs1042365	chr4:100045500	ADH4	0.2879	0.3273	0.3027	0.8309
rs1126673	chr4:100045616	ADH4	0.2929	0.344	0.2014	0.79
rs1126672	chr4:100047812	ADH4	0.2879	0.3273	0.3027	0.8309
rs1126671	chr4:100048414	ADH4	0.2929	0.344	0.2014	0.79
rs1126670	chr4:100052733	ADH4	0.2929	0.344	0.2014	0.79
rs6532798	chr4:100054827	ADH4	0.2929	0.344	0.2014	0.79
rs13110764	chr4:100062466	ADH4	0.2879	0.3273	0.3027	0.8309
rs61734620	chr4:100062814	ADH4	0	0.0029	1	0
rs2032349	chr4:100062819	ADH4	0.005051	0.01671	0.319	0.2986

Table 7.4: Fisher's exact test P-values for all tested SNPs mapping on the *HCRTR2* and *ADH4* genes

7.5 Analysis of loci previously implicated in migraine

To explore a possible genetic overlap between migraine and CH, we also inspected association results in our dataset for confirmed hits which have emerged from recent large scale GWAS for migraine²⁷². A recent meta-analysis reported association for 45 independent

confirmed SNPs located on 38 different loci²⁷². In our study, 29 of these SNP have been directly genotyped or detected by a tag SNP. The Fisher test was used to investigate difference between cases and controls for these variants. Only rs9349379 located in *PHACTR1*, encoding for phosphatase and actin regulator 1 showed a nominally significant P value (P = 0.034) (Table 7.5)

SNP	POSITION (hg19)	locus	Tag SNP	Tag SNP bp	r2	P-value
rs11172113	chr12:57527283	LRP1	rs11172113	57527283	1.00	0.1979
rs10218452	chr1:3075597	PRDM16	rs7518255	3086464	0.90	1
rs12135062	chr1:3103312	PRDM16	rs2651927	3101762	0.87	0.7834
rs67338227	chr6:97042147	FHL5	rs11153058	97012746	0.73	0.6399
rs2223239	chr6:96767685	FHL5	rs2205760	96786690	0.74	0.6747
rs7775721	chr6:97056979	FHL5 (MO)	rs2273621	97058553	0.96	0.4564
rs10166942	chr2:234825093	TRPM8	rs10166942	234825093	1.00	0.3681
rs566529	chr2:234756811	TRPM8	rs13384669	234759800	0.76	0.5703
rs6724624	chr2:234820578	TRPM8 (MO)	rs10166942	234825093	1.00	0.3681
rs9349379	chr6:12903957	PHACTR1	rs9349379	12903957	1.00	0.03442
rs1925950	chr1:156450740	MEF2D	rs3790455	156456301	1.00	0.3186
rs4814864	chr20:19469817	SLC24A3	rs6081613	19465907	0.92	0.3828
rs1024905	chr12:4518140	FGF6	rs10849061	4523456	0.88	0.688
rs186166891	chr7:40406876	C7orf10	rs12533531	40418721	0.71	0.6179
rs10786156	chr10:96014622	PLCE1	rs2274224	96039597	0.99	0.1271
rs7961602	chr12:57273481	PLCE1	rs4237805	57249600	0.65	0.7452
rs4910165	chr11:10674044	MRVI1	rs4909945	10673739	0.99	0.865
rs10456100	chr6:39183470	KCNK5	rs10456100	39183470	1.00	0.0714
rs6478241	chr9:119252629	ASTN2	rs6478241	119252629	1.00	0.7441
rs12260159	chr10:100702737	HPSE2	rs7073636	100665866	0.78	0.05476
rs17857135	chr17:78262161	RNF213	rs17857135	78262161	1.00	0.1802
rs2506142	chr10:33468124	NRP1	rs2506144	33468456	0.93	0.9197
rs1268083	chr6:126049040	HEY2	rs1343116	126069702	0.66	0.4185
rs6791480	chr3:30480559	TGFBR2	rs4075748	30478985	0.99	0.6563
rs10895275	chr11:102083608	YAP1	rs8504	102103600	0.97	0.6107
rs12845494	chrX:40764757	MED14	rs10127045	40745226	0.80	0.5121
rs10155855	chr7:111328397	DOCK4	rs17158733	111332403	0.53	0.05003
rs1572668	chr1:73899742	LRRIQ3	rs4113050	73910055	0.98	0.4174
rs11031122	chr11:30547438	MPPED2	rs11031122	30547438	1.00	0.6469

Table 7.5: Fisher's exact test P-values for all tested SNPs mapping on loci previously implicated in migraine²⁷². MO: migraine without aura.

7.6 Analysis of loci previously implicated in smoking dependence

The relationship between smoking and CH is not clear; tobacco use could be an environmental trigger for CH in genetically predisposed subjects, or, conversely, specific genetic risk factors involved in smoking behaviors could also predispose individuals to CH. Therefore, in order to investigate the latter hypothesis, we inspected different genes encoding for nicotinic acetylcholine receptor (nAChR) subunits, which represent confirmed associated loci to tobacco addiction and smoking-related traits. In particular we focused our analysis on the *CHRNA5-CHRNA3-CHRNA4* cluster, the *CHRNA6-CHRNA3* cluster and *CHRNA4*. We observed that the allele frequency for each variant tested in these genes did not significantly differ between CH patients and control smokers (including the functional SNP rs16969968). Given the availability of smoking measures (FTND score and CPD) for CH patients and control smokers included in our study, we also performed a linear regression analysis to test for association of the variants with FTND score and CPD, adding age, sex and CH status as covariates. This analysis did not reveal an effect of SNPs tested in nAChR genes on both smoking measures.

7.7 Gene based analysis

In order to increase power to detect variants directly involved in the disorder, we restricted our analysis only to rare (MAF < 0.05) protein altering variants (PAV) located on several candidate genes for CH. The comprehensive collection of candidate genes was made according to Gene Ontology (GO) biological process annotations (<http://geneontology.org/page/download-annotations>). We selected those genes related to cellular processes with a plausible role in CH, including circadian rhythm, pain perception and response, neuropeptide signalling, vasodilation and vasoconstriction, ion channels, nicotinic acetylcholine receptors, alcohol metabolism, TNF signalling. The list of selected genes and GO terms is shown in the appendix (Table s1 and Table s2). In total 2568 rare protein altering variants located in 745 candidate genes have been used to carry out the gene based analysis by SNP-set Kernel Association Test (SKAT)²⁶⁴. Using this approach all the rare variants within a candidate gene are considered jointly and the analysis provide a gene-level P value that indicates the enrichment level of rare variants associations in a gene. The gene based association analysis results with a nominal P-value < 0.01 are listed in table 7.6.

	SKAT P-value	Single SNPs P-value ^a	R A	RAF case/control	RAF 1000G_all (1000G_EUR; 1000G_TSI) ^b	RAF in ExAC_all (ExAC_NFE) ^c	Function	PolyPhen-2 (Prediction) ^d	CADD score _e
Gene MME	2.55x10 ⁻⁵								
rs61762319		0.42	G	0.030/0.021	0.0072(0.023; 0.019)	0.0164(0.0226)	Missense p.M8V	0.524(P)	15.63
rs147564881		2.03x10 ⁻⁵	C	0.035/0	0.001(0.002; 0.009)	0.0022(0.0033)	Missense p.G225A	1 (D)	21
rs61758194		1	A	0/0.0014	0.0002(0; 0)	0.0021(0.0035)	Missense p.V345I	0.001(B)	11.65
Gene NPY1R	1.18x10 ⁻³								
rs5578		3.80x10 ⁻³	C	0.040/0.0084	0.003(0.007; 0.019)	0.0047(0.0067)	Missense p.K374T	0.421(B)	12.96
rs78156188		1	A	0/0.0028	0.0004(0.002; 0)	0.0006(0.001)	Missense p.A111V	0.023(B)	3.073
Gene BDKRB1	3.30x10 ⁻³								
rs143823168		1	C	0/0.0028	0.0018(0.003; 0)	0.0024(0.0036)	Missense p.L191V	0.999(D)	9.214
rs45528332		9.23x10 ⁻³	A	0.030/0.0056	0.0036(0.004; 0.005)	0.0062(0.0052)	Missense p.G241R	0.926(P)	9.661
Gene SLC5A3	4.94x10 ⁻³								
rs35707420		0.014	A	0.025/0.0042	0.0026(0.006; 0.009)	0.0062(0.0087)	Missense V370M	1(D)	18.46
rs199948762		0.39	G	0.0051/0.0014	.	0.000099(0.0001)	Missense N557K	0.001(B)	8.533
Gene CCL26	7.02x10 ⁻³								
rs41463245		0.022	A	0.020/0.0028	0.0036(0.016; 0.023)	0.0086(0.0131)	Nonsense W44X	.	23.1
Gene GRM1	9.45x10 ⁻³								
rs41305288		0.017	A	0.035/0.0098	0.01(0.017; 0.023)	0.0172(0.0185)	Missense p.P729T	1(D)	19.24
rs362936		1	A	0.0051/0.0097	0.004(0.017; 0.009)	0.0212(0.031)	Missense p.G884E	0.998(D)	13.22
rs138759146		1	C	0/0.0014	.	0.0001(0.0002)	Missense p.M909L	0.017(B)	1.328
rs2941		0.14	A	0.0051/0.022	0.0092(0.025; 0.019)	0.0132(0.0182)	Missense p.V929I	0.111(B)	18.3
rs79336287		0.071	A	0.015/0.0023	0.005(0.004; 0)	0.0017(0.0013)	Missense p.P1069L	0(B)	11.39

Table 7.6: results of SKAT gene-based tests in CH

Abbreviations: RA = rare allele; RAF =rare allele frequency; ^a single SNP Fisher's exact test P-value; ^b rare allele frequency in 1000 Genomes all populations (1000G_all) in european populations (1000G_EUR) and in Tuscans from Italy (1000G_TSI); ^c rare allele frequency in Exome Aggregation Consortium (ExAC) Non-Finnish European (NFE) populations; ^d PolyPhen-2 HumDiv score; B=benign, P=possibly damaging, D=probably damaging, ^e CADD v1.3, PHRED-like (-10*log₁₀(rank/total)) scaled C-score

The most significant result was detected for the *MME* gene (P value of 2.5×10^{-5}), encoding for Membrane Metallo Endopeptidase, also called neprilysin. This association result remains statistically significant also after the Bonferroni correction for multiple testing (threshold: $p < 6.7 \times 10^{-5}$). Individually, all *MME* rare variants included in the gene based analysis had good genotyping cluster properties and genotyping rate $> 99.9\%$.

The missense variant rs14756488 (p.G225A) is the most significant (p-value= 2.03×10^{-5}) in the gene based analysis. It causes a substitution of amino acid glycine with alanine at position 225 (Gly225Ala). This variant was found in 7 out of 99 CH patients and in none of the 359 control smokers.

The rs14756488 genotypes are represented in Figure 7.5, grouped in two different Geneplots based on different batches of Illumina Infinium® PsychArray microarrays (**A**: v1.0 and **B**: v1.1) used for SNPs genotyping. The red cluster is empty in both Geneplots indicating the absence of homozygous individuals for rs14756488 risk allele. Instead, in the purple cluster we observed 7 dots in graph B indicating the presence of heterozygous individuals for rs14756488, which are all CH patients. These genotyping results were confirmed by Sanger sequencing (paragraph 7.8).

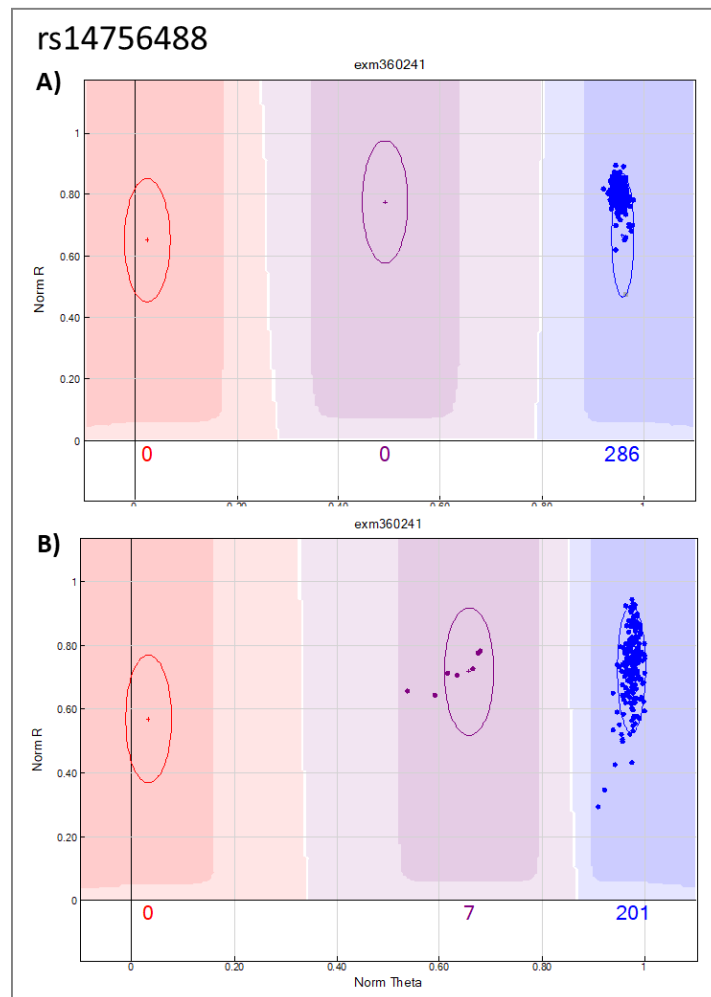


Figure 7.5: Plots for rs14756488 genotype in CH and controls sample genotyped by PsychArray-24 v1.0.(A) and by PsychArray-24 v1.1 (B). Genotype are called for each sample (dots) by their signal intensity (Norm-R; y-axis) and Allele Frequency (Norm Theta; x-axis) relative canonical cluster position for a given SNP marker. The colours indicate the genotype: red= CC; purple= GC and blue= GG.

Analysis of rs14756488 frequency in the public databases “1000 Genome Project” (<http://www.1000genomes.org/>) and Exome Aggregation Consortium (ExAC) (<http://exac.broadinstitute.org/>) showed that this missense variant is very rare in the general population: MAF = 0.1% in all 1000 Genome Project phase 3 individuals and 0.2% in 60706 individuals of ExAC. We used two online bioinformatic tools to predict the deleteriousness of variant rs14756488 in the human proteins: PolyPhen-2 and CADD²⁷⁰. This variant is predicted to be damaging by PolyPhen-2 (PolyPhen score=1), and the phred-CADD score is 21 indicating that the variant is predicted to be among the 1% most deleterious SNVs present in the human genome (Table 7.6).

The clinical details of individuals with CH carrying rs14756488 are reported in Table 7.7. These subjects did not present significant differences in clinical signs that allow to distinguish them to the rest of subjects with CH.

ID	Sex	Age	Age of CH onset (years)	Number of CH episodes/year	Number of CH Attacks/day	Relatives with headache	Smoking Parents	Smoking initiation age (years)	Fagerstrom Test	CPD
56	F	64	40	chronic CH	4	No	Yes	15	4	12
61	M	48	43	1	3	No	Yes	14	5	30
71	M	67	35	1	3	No	Yes	15	4	20
80	F	38	6	chronic CH	4	No	Yes	16	5	20
81	M	33	20	1	3	No	Yes	17	4	5
92	M	81	46	1	1	Yes (CH)	Yes	NA	NA	0
G002	M	68	50	1	2	Yes (CH)	Yes	13	0	20

Table 7.7: Clinical features of CH patients with the p.G225A MME variant

The other suggestive results ($p < 0.01$) from SKAT analysis have been identified in genes encoding for Neuropeptide Y receptor type 1 (*NPY1R*), B1 bradykinin receptor (*BDKRB1*), Sodium/myo-inositol cotransporter (*SLC5A3*) C-C motif chemokine 26 (*CCL26*) and Metabotropic glutamate receptor 1 (*GRM1*) (Table 7.6).

7.8 MME mutation screening

In order to test the presence of other rare protein altering variants in *MME* gene, we performed a mutation screening of the entire *MME* coding region in all 99 CH patients by Sanger sequencing.

This mutation screening allowed to confirm the two rare variants identified by gene-based analysis and to detect a rare synonymous SNP (rs200455903) in one subject with CH (Table 7.8). However, no additional rare protein altering variants were identified in our CH patients sample.

PsychArray SNP	rsID	Rare allele	Freq in case/control	MAF in 1000G_all (1000G_EUR)	MAF in ExAC_all (ExAC_NFE)	Function
exm360204	rs61762319	G	0.03/0.021	0.0072(0.023)	0.016(0.0226)	Missense p.M8V
exm360241	rs147564881	C	0.035/0	0.001(0.002)	0.002(0.0033)	Missense p.G225A
	rs200455903	C	0,0049		0.00003297 (0.00001499)	synonymous

Table 7.8: Rare variants identified in *MME* mutation screening, the first two variants were previously detected by Illumina Infinium® PsychArray microarrays and confirmed by mutation screening. In red is indicated a new rare synonymous variant detected by mutation screening.

DISCUSSION

CHAPTER 8

8.1 Role of $\alpha 7$ nAChR in nicotine dependence

The World Health Organization (WHO) has defined cigarette smoking as “the single most preventable cause of death in the world today”². Tobacco dependence is caused by nicotine, a substance found in high concentration in cigarette smoke. Nicotine produces physical and mood-altering effects in the brain that are temporarily pleasing. At the same time, stopping tobacco use causes withdrawal symptoms, including irritability and anxiety. Yet, despite the widespread awareness of the harms of smoking, millions continue to smoke around the world partly due to the difficulty it takes to quit smoking. It has been shown that approximately 80% of smokers who attempt to quit on their own relapse within the first month of abstinence and only about 3-5% remain abstinent for 6 months²⁷³. Pharmacological treatment and behavioural counselling have been shown to increase the rate of successful smoking cessation. According to the latest estimate from the U.S. Preventive Services Task Force (USPSTF), behavioural interventions resulted in 7%-13% smoking cessation rates, versus cessation rates in controls of 5%-11%. Nicotine replacement therapy (NRT), bupropion, and varenicline all increased smoking cessation rates versus control therapy; varenicline showed the greatest rates of cessation (28%), followed by bupropion SR (19%) and NRT (17%) at 6 to 12 months¹⁶⁷. Combination of both medication and behavioural counselling has been shown to be more effective than either intervention alone²⁷⁴. Tobacco addiction (like other drug addictions) involves the interplay of pharmacology, genetics, and social and environmental factors. Heritability estimates for different nicotine addiction traits (such as the level of dependence, the number of cigarettes smoked per day and smoking persistence) are in the range of 50% to 60%^{46,47}.

Recently, several large genetic studies have started to shed some light on genetic susceptibility to nicotine dependence.

The *CHRNA5-CHRNA3-CHRNB4* gene cluster on chromosome 15 encoding for nicotinic receptor (nAChR) subunits harbours the strongest and most replicated genetic risk factor for

several smoking behaviours^{61,98}. In addition, genome-wide association studies (GWAS) of smoking phenotypes and nicotine dependence reported associations for other genes encoding nAChR subunits, including *CHRNA3-CHRNA6*⁵ gene cluster and the *CHRNA4* gene²⁴³.

Preclinical studies demonstrated that the activation of heteropentameric $\beta 2$ subunit-containing nicotinic receptors ($\beta 2^*$ nAChRs) have a role in promoting nicotine addiction phenotypes^{3,275,276}. Moreover, recent functional studies have suggested that $\alpha 7$ nAChRs, encoded by *CHRNA7* gene, may be involved in addiction mechanisms^{161,162}, possibly by modulating the activity of $\beta 2^*$ nAChRs in the VTA¹⁶³. GWAS studies for nicotine addiction have not identified a significant association in *CHRNA7*, but this lack of association could be due to the complex genetic architecture of this genomic region, which is among the most unstable regions of the human genome. The presence of a chimeric gene, *CHRFAM7A*, deriving from the fusion between a duplication of *CHRNA7* exons 5–10 and *FAM7A* exons A–E, and the very high C+G content of *CHRNA7* promoter region, hampers genetic analysis of this region by standard genotyping chips or next generation sequencing. In particular, no SNP probes are present in the *CHRNA7* promoter in the most commonly used genotyping arrays (including Illumina 1M array or Affymetrix 6.0) (Figura5.1). Likewise, the $\Delta 2$ bp *CHRFAM7A* variant (rs67158670) is not represented in commercial SNPs arrays and SNPs located in the duplicated portion of *CHRNA7* and *CHRFAM7A* are not reliable.

The *CHRFAM7A* function is still unknown, however *in vitro* studies have suggested that it encodes for a truncated form of the $\alpha 7$ subunit, called dup $\alpha 7$, which could act as a dominant negative regulator of *CHRNA7* function, as it assembles with $\alpha 7$ subunits and causes a decrease of acetylcholine-stimulated current^{140,141}.

The aim of this study was to examine the hypothesis that genetic variation affecting $\alpha 7$ nAChR function may influence smoking behaviors and the effectiveness of varenicline in smoking cessation. We performed a comprehensive analysis of the *CHRNA7* and *CHRFAM7A* loci, considering sequence and copy number variants in these two genes, in a cohort of 408 treatment-seeking smokers, which included a subgroup of 142 individuals who were treated with varenicline.

Sequence analysis of the *CHRNA7* promoter region in the entire cohort of smokers led to the identification of an association of rs28531779 with smoking dependence (FNTD and CPD). To our knowledge, this is the first study reporting a significant association of a *CHRNA7*

promoter variant with smoking quantity and nicotine dependence. Interestingly, a previous study¹⁵⁰ reported that, in luciferase assay, the minor allele of rs28531779 (C) may reduce *CHRNA7* promoter activity. We attempted to confirm this result using the luciferase assay, and we observed the same trend reported by Leonard et al.¹⁵⁰, but without reaching the threshold of statistical significance. It should be noted that the main disadvantage of luciferase assay is the analysis of variant effects outside their normal environment; thus, we cannot exclude that the associated variant could have a stronger effect when the DNA is in its normal cellular context and/or it could be influenced by other variants in the genome. Analysis of *CHRNA7* expression in cells of subjects carrying the rs28531779 minor allele could help to better understand the role of this variant on *CHRNA7* expression. Therefore, we are currently recruiting blood samples from smokers to test *CHRNA7* expression in monocytes and macrophages, as *CHRNA7* has been shown to be specifically expressed in these blood cell types^{277,278}.

Interestingly, the same rs28531779 promoter variant has been previously associated to the schizophrenia endophenotype P50 inhibitory deficit¹⁵⁰, and to schizophrenia¹⁵¹. Therefore, these data suggest that rs28531779, possibly by decreasing the expression of $\alpha 7$ nAChR, could be involved in susceptibility to both nicotine dependence and schizophrenia. This hypothesis is also supported by post-mortem studies showing reduced levels of $\alpha 7$ nAChR in the brain of individuals with schizophrenia^{279,280}, and *in vivo* studies in rodents which report that reductions in $\alpha 7$ nAChR function promote nicotine use¹⁶¹. Moreover, the high prevalence of tobacco consumption in schizophrenic subjects is in line with the presence of a shared genetic background between these two disorders. There are increasing evidences for cross-disorder effects of genetic variation: first, genomic studies have showed that the same CNVs may influence risk for different neuropsychiatric disorders, such as schizophrenia, ASD, intellectual disability (ID), developmental delay and ADHD²⁸¹; second, analysis of GWAS data has demonstrated the existence of substantial sharing of genetic risk factors represented by common SNPs across five major neuropsychiatric disorders (schizophrenia, bipolar disorder, major depressive disorder, autism spectrum disorders and attention-deficit/hyperactivity disorder)²⁸².

A second interesting finding of our study is the observation that *CHRFAM7A* copy number, seems to influence the success of smoking cessation in subjects treated with varenicline. In particular, *CHRFAM7A* copy number positively correlates with smoking cessation success,

with higher abstinence rates in subjects carrying two or three copies in comparison to subjects with 0-1 copies. The effect of *CHRFAM7A* copy number on smoking abstinence was not detected in the remaining sample of 266 individuals who were not treated with varenicline, according to the hypothesis that *CHRFAM7A* copy number influences smoking cessation by interacting with varenicline treatment. Testing for interaction between the varenicline treatment and *CHRFAM7A* copy number provided a p value of 0.04.

Even if the biological basis for this effect is presently unknown, some evidence in reconstituted systems suggests that incorporation of dup $\alpha 7$ in $\alpha 7$ receptors modestly increases the sensitivity of $\alpha 7$ receptors to varenicline.²⁸³ Our study thus supports the hypothesis of an involvement of $\alpha 7$ nAChRs activation in the varenicline mode of action for smoking cessation treatment.

The product of *CHRFAM7A*, $\alpha 7$ dup has been hypothesized to be a negative regulator of $\alpha 7$ receptor function¹⁴⁰, and a link between $\alpha 7$ receptor and varenicline also comes from the association of *CHRNA7/CHRFAM7A* variants to schizophrenia^{142,151} and the effects of varenicline treatment in schizophrenic subjects^{165,166}. More specifically, *CHRFAM7A* copy number and 2bp deletion polymorphisms have been associated to schizophrenia. Moreover, alterations in the *CHRFAM7A/CHRNA7* expression ratios have been detected in schizophrenia and bipolar disorder, due mainly to overexpression of *CHRFAM7A*¹⁴⁹. Interestingly, varenicline treatment in schizophrenic subjects leads to cognitive improvements and anti-smoking effect^{165,166}, suggesting that $\alpha 7$ nAChRs may mediate the action of varenicline as a treatment for smoking cessation and schizophrenia.

By contrast, in our study we found no evidence for an effect on smoking phenotypes of the *CHRFAM7A* $\Delta 2$ bp polymorphism, previously shown to be associated to schizophrenia and the P50 sensory gating deficit. This could be explained by the small sample size of our study, thus lacking an adequate power to detect a significant association for this variant; alternatively the *CHRFAM7A* $\Delta 2$ bp may specifically influence psychiatric phenotypes.

The major limitation of this study is the relatively small sample size that does not ensure sufficient power to draw definitive conclusions on the association results obtained, as none of our significant values would survive multiple testing correction. Replication of *CHRNA7* and *CHRFAM7A* genetic analysis in larger and independent cohorts is therefore required to confirm our initial results.

In conclusion, this study is the first one to report a significant association of *CHRNA7* promoter variants with smoking quantity and nicotine dependence, suggesting that variation in *CHRNA7* expression could have a critical role in tobacco addiction mechanisms. Furthermore, our work provides the first evidence that *CHRFAM7A* copy number variation could affect the response to varenicline treatment.

It has been estimated that 50% of the risk for a failed attempt at smoking cessation can be attributed to genetic factors^{48,49}. Therefore, the identification of genetic factors that could improve the effectiveness of pharmacologic approaches to smoking cessation may represent a very important finding. Altogether, these results point to a critical role for the *CHRFAM7A/CHRNA7* locus in tobacco addiction mechanisms.

8.2 Genetic analysis of cluster headache

Cluster Headache (CH) is a rare primary headache characterized by recurrent unilateral short-lasting attacks of excruciating orbitotemporal pain, often appearing with a clockwise regularity. Despite its clear clinical presentation CH biology is poorly understood. Because of the typical rhythmicity of attacks the involvement of the biological clock has been proposed. Evidence for activation of the trigeminovascular (CGRP) and cranial parasympathetic (VIP) nervous systems, which are involved in controlling cranial vascular reactivity, has also been reported¹⁹⁷. Smoking is the most consistent lifetime habit reported in CH patients²⁴⁰, but the link between CH and cigarette consumption is not clear. Tobacco use could be an environmental trigger for CH in genetically predisposed subjects, or specific genetic risk factors for CH may also predispose individuals to tobacco smoking.

Family and twin studies indicate that complex genetic factors play an important, but still unknown, role in CH¹⁸⁸. Molecular genetic investigations have been in part hampered by the complex nature of the disorder and its low prevalence. Most studies investigated the involvement of variants in candidate genes thought to be involved in CH pathophysiology. Association studies suggested a role for the hypocretin system in CH susceptibility^{218,239}. No associations or conflicting results were found for variants in *CACNA1A*²³⁰, *NOS*²²⁹, *MTHFR*²³⁵, *PER3*²²⁶, *SERPINA*²³⁶, and *ADH4*^{221,223}.

In contrast to candidate gene studies, genome-wide association studies (GWAS), take a hypothesis-free approach to identifying genetic variants for disease. Over recent years, GWAS provided novel suggestion into the biological and genetic factors involved in many complex traits, including migraine²⁷².

In general, GWAS focus on common SNPs (MAF > 5% in the general population) with modest effects on disease risk or quantitative trait variation, therefore large samples are needed.

The advent of whole-exome next-generation sequencing allowed to highlight the role of rare coding variants in the aetiology of many complex diseases. Thus, more recently, “exome genotyping arrays” were introduced as a cost effective alternative to exome sequencing. These arrays were created to genotype rare coding variants identified by exome sequencing of thousands of individuals²⁸⁴.

Therefore, to identify genetic variants involved in CH, we decided to use this kind of array, specifically the Infinium PsychArray (Illumina)²⁵⁷ that allows testing genome-wide common variants as well as low frequency protein-coding variants in exons, with a particular focus on

genes implicated in neuropsychiatric disorders: the combination of these two characteristics results in a gain in power, given the unknown genetic architecture of CH. Genotype data were used to perform a single marker genome-wide association analysis using common SNP and a gene-based association analysis considering only rare exonic variants in candidate genes with a possible role in CH.

The GWAS provided an interesting suggestive association of CH with a common polymorphism in the *ADCYAP1R1* encoding for pituitary adenylate cyclase activating peptide (PACAP) receptor gene 1 (PAC1). Moreover, from the gene-based analysis, we identified an interesting association with a rare coding variant in the *MME* gene. Both *ADCYAP1R1* and *MME* are genes known to be involved in pain mechanisms.

PACAP is a member of the vasoactive intestinal peptide-like peptide family, it is expressed in the trigeminal ganglia, the pituitary gland, cerebral cortex, the trigeminal nucleus caudalis²⁸⁵. PACAP binds to and activates 3 different receptors: the PAC1 receptor, activated only by PACAP, and the VPAC1 and VPAC2 receptors, activated by PACAP and the vasoactive intestinal polypeptide (VIP)²⁸⁶. Studies performed on animal models demonstrated that PACAP and its receptors are present in the spinal dorsal horn and dorsal root ganglia and suggested a critical role of PACAP receptors signalling system in the regulation of pain transmission²⁸⁷. More specifically, administration of PACAP to rodents sensitized neurons to pain²⁸⁷, while PACAP antagonists reduced pain sensitivity²⁸⁸. Furthermore, mice deficient in PAC1 receptors displayed a decreased chronic responses to chemical, thermal and mechanical stimuli and did not show neuropathic pain after carrageenan-induced inflammation or nerve transection^{289,290}. PACAP has been recently reported to induce migraine-like attacks likely acting in the trigeminovascular system²⁸⁶, in contrast, the infusion of VIP does not cause migraine attacks^{291,292}. Thus, the PAC1 receptor seems to be the likely pathophysiological target of PACAP in migraine. Moreover, a recent study measured the plasma PACAP levels during different phases of CH, revealing that PACAP plasma level were higher during ictal phase compare to inter-bout periods²⁹³. Finally, recent evidence suggested that PACAP/PAC1 signalling is important for circadian rhythms²⁹⁴ and, interestingly, CH attacks show a circadian regularity.

Considering these findings, the PAC1 receptor could be the target for new drug development to treat migraine and CH. There is large interest in evaluating if antibodies against the PACAP peptide and PAC1 receptor have an effect in preventing migraine attacks²⁸⁵.

From our gene-based analysis we also identified a significant association in the *MME* gene. *MME* encodes for a zinc-dependent metallopeptidases, also named neprilysin or neutral endopeptidase (NEP). Neprilysin hydrolyzes different peptide hormones including glucagon, enkephalins, substance P, neurotensin, atrial and brain natriuretic peptides, oxytocin, and bradykinin²⁹⁵. These peptides are implied in pain modulation in the central nervous system, in regulation of trigeminal nociceptive inputs and, moreover, in stress and circadian rhythms. Interestingly, alteration in all these mechanisms are thought to have a role in the clinical features of CH²⁹⁶⁻²⁹⁸. NEP knockout mice showed enhanced pain behaviour and neurogenic inflammation after injury of sciatic nerve²⁹⁹.

The associated *MME* missense variant from our gene-based analysis (p.G225A) was not identified in control subjects without CH, but it is reported in public control databases with low frequency (MAF=0.02%). Therefore, even if the frequency of primary headache in public databases is not known, this data could reflect the incomplete penetrance and/or the interplay with other genetic and/or environmental factors. Moreover, recent studies reported that rare loss-of-function and missense variants in *MME* predispose individuals to late-onset axonal neuropathies, the Charcot–Marie–Tooth disease type 2 (CMT2)^{300,301} and to a rare autosomal recessive form of CMT2³⁰². Patients with this neuropathy have not been reported to suffer from migraine or CH, but subjects carrying *MME* variants were reported to manifest neuropathic pain³⁰⁰. Considering the different peptides hydrolysed by neprilysin and their wide expression pattern, it is possible that pathogenic mutations in *MME* genes could have a role in the etiology of different neurological traits. Further studies are warranted in order to explore the molecular mechanisms predisposing to different phenotypes. We can speculate that severe, very rare deleterious variants contribute to axonal neuropathies, while, the more frequent p.G225A missense mutation could have a slighter damaging effect, leading to an increased risk for CH susceptibility by interaction with other genetic or environmental factors.

Very recently, a Swedish study attempted to replicate the most significant association results emerged from our study (rs1006417 in intergenic region, rs12668955 in *ADCYAP1R1*, rs147564881 in *MME*) in a cohort of 542 CH patients and 581 controls, but no significant result was detected at any of the tested variants³⁰³.

The contrasting results coming from our study and the Swedish replication study might have several reasons. For example, the control samples employed by the two studies have

different characteristics: in our study we genotyped 360 individuals matched for age and smoking status with the case group, while in the Swedish study used DNA from anonymous donors as controls. Furthermore, the gender ratio is significantly different among our sample and the Swedish sample: our CH cohort has a higher percentage of males (84%) in comparison with the Swedish cohort (68,3%).

We should also consider that there could be a different genetic background between the Italian and Swedish population; in fact, the associated variant have different MAF in the two populations. Lastly, the replication study only tested the three single top variants without testing additional SNPs in the same loci. Therefore, the lack of replication could also be due to the potential diversity of linkage-disequilibrium structure across populations. Furthermore, the lack of the specific rare missense mutation rs147564881 in *MME* in the Swedish cohort does not exclude that other rare functional variants in the same gene might contribute to CH risk.

The principal limitation of this study is the small sample size that does not provide enough power to detect genome-wide significant associations. Moreover, the suggestive association detected in the *ADCYAP1R1* gene is supported only by a single intronic variant (rs12668955). To exclude the presence of genotyping errors that might have affected this result, we have carefully double checked the genotyping data in our case-control sample. Only 11 common variants in *ADCYAP1R1*, spanning about 59 Kb, are present on the Psychiatric array (Illumina)²⁵⁷, and no other variants in LD with rs12668955 is present. Therefore, more comprehensive analysis of this gene is warranted in order to fine map the association signal and better understand the role of *ADCYAP1R1* in CH susceptibility.

To address these issues, we are currently recruiting an additional larger independent sample of CH subjects to confirm our preliminary association results. In particular, we are planning to test additional SNPs in *ADCYAP1R1* to obtain an adequate higher coverage of this genetic region and to extend the *MME* mutation screening in this new larger CH cohort.

Moreover, given the established importance of CNVs in the clinical manifestation of many complex disorders, we would like to explore the role of structural variants in CH susceptibility. To date, no CNVs studies have been performed in CH subjects, except a very small analysis in 10 CH subjects using comparative genomic hybridization (array-CGH)²²¹, leaving this field completely unexplored. Therefore, we will exploit the SNPs genotyping data to perform a CNV analysis on CH sample.

In spite of these limitations, our study provides the first evidence that genetic variation in genes related to pain processing might have a role in CH susceptibility, and it acts as pilot study to provide preliminary insights into the genetic architecture of CH. A better understanding of the molecular pathways involved in the disease, could lead to better treatments and/or prevention.

BIBLIOGRAPHY

1. Shaik SS, Doshi D, Bandari SR, Madupu PR, Kulkarni S. Tobacco Use Cessation and Prevention - A Review. *J Clin Diagn Res.* 2016;10(5):ZE13-17.
2. WHO. WHO global report on mortality attributable to tobacco. Geneva: World Health Organization. 2012.
3. Changeux JP. Nicotine addiction and nicotinic receptors: lessons from genetically modified mice. *Nat Rev Neurosci.* 2010;11(6):389-401.
4. Di Chiara G. Role of dopamine in the behavioural actions of nicotine related to addiction. *Eur J Pharmacol.* 2000;393(1-3):295-314.
5. Greenbaum L, Lerer B. Differential contribution of genetic variation in multiple brain nicotinic cholinergic receptors to nicotine dependence: recent progress and emerging open questions. *Mol Psychiatry.* 2009;14(10):912-945.
6. Stolerman IP, Shoaib M. The neurobiology of tobacco addiction. *Trends Pharmacol Sci.* 1991;12(12):467-473.
7. Corrigan WA. Nicotine self-administration in animals as a dependence model. *Nicotine Tob Res.* 1999;1(1):11-20.
8. Dani JA, Harris RA. Nicotine addiction and comorbidity with alcohol abuse and mental illness. *Nat Neurosci.* 2005;8(11):1465-1470.
9. Baldwin PR, Alanis R, Salas R. The Role of the Habenula in Nicotine Addiction. *J Addict Res Ther.* 2011;S1(2).
10. Corringer PJ, Le Novère N, Changeux JP. Nicotinic receptors at the amino acid level. *Annu Rev Pharmacol Toxicol.* 2000;40:431-458.
11. Albuquerque EX, Pereira EF, Alkondon M, Rogers SW. Mammalian nicotinic acetylcholine receptors: from structure to function. *Physiol Rev.* 2009;89(1):73-120.
12. Nashmi R, Lester HA. CNS localization of neuronal nicotinic receptors. *J Mol Neurosci.* 2006;30(1-2):181-184.
13. Laviolette SR, van der Kooy D. The neurobiology of nicotine addiction: bridging the gap from molecules to behaviour. *Nat Rev Neurosci.* 2004;5(1):55-65.
14. Kalamida D, Poulas K, Avramopoulou V, et al. Muscle and neuronal nicotinic acetylcholine receptors. Structure, function and pathogenicity. *FEBS J.* 2007;274(15):3799-3845.
15. Hogg RC, Raggenbass M, Bertrand D. Nicotinic acetylcholine receptors: from structure to brain function. *Rev Physiol Biochem Pharmacol.* 2003;147:1-46.
16. Buisson B, Bertrand D. Nicotine addiction: the possible role of functional upregulation. *Trends Pharmacol Sci.* 2002;23(3):130-136.
17. Gray R, Rajan AS, Radcliffe KA, Yakehiro M, Dani JA. Hippocampal synaptic transmission enhanced by low concentrations of nicotine. *Nature.* 1996;383(6602):713-716.
18. Dani JA, Bertrand D. Nicotinic acetylcholine receptors and nicotinic cholinergic mechanisms of the central nervous system. *Annu Rev Pharmacol Toxicol.* 2007;47:699-729.
19. Albuquerque EX, Alkondon M, Pereira EF, et al. Properties of neuronal nicotinic acetylcholine receptors: pharmacological characterization and modulation of synaptic function. *J Pharmacol Exp Ther.* 1997;280(3):1117-1136.
20. Wonnacott S. Presynaptic nicotinic ACh receptors. *Trends Neurosci.* 1997;20(2):92-98.
21. Sher E, Chen Y, Sharples TJ, et al. Physiological roles of neuronal nicotinic receptor subtypes: new insights on the nicotinic modulation of neurotransmitter release, synaptic transmission and plasticity. *Curr Top Med Chem.* 2004;4(3):283-297.
22. Vijayaraghavan S, Pugh PC, Zhang ZW, Rathouz MM, Berg DK. Nicotinic receptors that bind alpha-bungarotoxin on neurons raise intracellular free Ca²⁺. *Neuron.* 1992;8(2):353-362.
23. Rathouz MM, Berg DK. Synaptic-type acetylcholine receptors raise intracellular calcium levels in neurons by two mechanisms. *J Neurosci.* 1994;14(11 Pt 2):6935-6945.

24. Vernino S, Rogers M, Radcliffe KA, Dani JA. Quantitative measurement of calcium flux through muscle and neuronal nicotinic acetylcholine receptors. *J Neurosci.* 1994;14(9):5514-5524.
25. McGehee DS, Heath MJ, Gelber S, Devay P, Role LW. Nicotine enhancement of fast excitatory synaptic transmission in CNS by presynaptic receptors. *Science.* 1995;269(5231):1692-1696.
26. Coggan JS, Paysan J, Conroy WG, Berg DK. Direct recording of nicotinic responses in presynaptic nerve terminals. *J Neurosci.* 1997;17(15):5798-5806.
27. Radcliffe KA, Dani JA. Nicotinic stimulation produces multiple forms of increased glutamatergic synaptic transmission. *J Neurosci.* 1998;18(18):7075-7083.
28. Fisher JL, Dani JA. Nicotinic receptors on hippocampal cultures can increase synaptic glutamate currents while decreasing the NMDA-receptor component. *Neuropharmacology.* 2000;39(13):2756-2769.
29. Hu M, Liu QS, Chang KT, Berg DK. Nicotinic regulation of CREB activation in hippocampal neurons by glutamatergic and nonglutamatergic pathways. *Mol Cell Neurosci.* 2002;21(4):616-625.
30. Ji D, Lape R, Dani JA. Timing and location of nicotinic activity enhances or depresses hippocampal synaptic plasticity. *Neuron.* 2001;31(1):131-141.
31. Ge S, Dani JA. Nicotinic acetylcholine receptors at glutamate synapses facilitate long-term depression or potentiation. *J Neurosci.* 2005;25(26):6084-6091.
32. Lena C, Changeux JP, Mulle C. Evidence for "preterminal" nicotinic receptors on GABAergic axons in the rat interpeduncular nucleus. *J Neurosci.* 1993;13(6):2680-2688.
33. Zarei MM, Radcliffe KA, Chen D, Patrick JW, Dani JA. Distributions of nicotinic acetylcholine receptor alpha7 and beta2 subunits on cultured hippocampal neurons. *Neuroscience.* 1999;88(3):755-764.
34. Gotti C, Clementi F, Fornari A, et al. Structural and functional diversity of native brain neuronal nicotinic receptors. *Biochem Pharmacol.* 2009;78(7):703-711.
35. Gotti C, Clementi F. Neuronal nicotinic receptors: from structure to pathology. *Prog Neurobiol.* 2004;74(6):363-396.
36. Gotti C, Riganti L, Vailati S, Clementi F. Brain neuronal nicotinic receptors as new targets for drug discovery. *Curr Pharm Des.* 2006;12(4):407-428.
37. Govind AP, Vezina P, Green WN. Nicotine-induced upregulation of nicotinic receptors: underlying mechanisms and relevance to nicotine addiction. *Biochem Pharmacol.* 2009;78(7):756-765.
38. Salas R, Orr-Urtreger A, Broide RS, Beaudet A, Paylor R, De Biasi M. The nicotinic acetylcholine receptor subunit alpha 5 mediates short-term effects of nicotine in vivo. *Mol Pharmacol.* 2003;63(5):1059-1066.
39. Kedmi M, Beaudet AL, Orr-Urtreger A. Mice lacking neuronal nicotinic acetylcholine receptor beta4-subunit and mice lacking both alpha5- and beta4-subunits are highly resistant to nicotine-induced seizures. *Physiol Genomics.* 2004;17(2):221-229.
40. Mao D, Perry DC, Yasuda RP, Wolfe BB, Kellar KJ. The alpha4beta2alpha5 nicotinic cholinergic receptor in rat brain is resistant to up-regulation by nicotine in vivo. *J Neurochem.* 2008;104(2):446-456.
41. Nguyen HN, Rasmussen BA, Perry DC. Binding and functional activity of nicotinic cholinergic receptors in selected rat brain regions are increased following long-term but not short-term nicotine treatment. *J Neurochem.* 2004;90(1):40-49.
42. Seguela P, Wadiche J, Dineley-Miller K, Dani JA, Patrick JW. Molecular cloning, functional properties, and distribution of rat brain alpha 7: a nicotinic cation channel highly permeable to calcium. *J Neurosci.* 1993;13(2):596-604.
43. Levy RB, Aoki C. Alpha7 nicotinic acetylcholine receptors occur at postsynaptic densities of AMPA receptor-positive and -negative excitatory synapses in rat sensory cortex. *J Neurosci.* 2002;22(12):5001-5015.

44. Li S, Li Z, Pei L, Le AD, Liu F. The alpha7nACh-NMDA receptor complex is involved in cue-induced reinstatement of nicotine seeking. *J Exp Med*. 2012;209(12):2141-2147.
45. Batra V, Patkar AA, Berrettini WH, Weinstein SP, Leone FT. The genetic determinants of smoking. *Chest*. 2003;123(5):1730-1739.
46. Sullivan PF, Kendler KS. The genetic epidemiology of smoking. *Nicotine Tob Res*. 1999;1 Suppl 2:S51-57; discussion S69-70.
47. Broms U, Silventoinen K, Madden PA, Heath AC, Kaprio J. Genetic architecture of smoking behavior: a study of Finnish adult twins. *Twin Res Hum Genet*. 2006;9(1):64-72.
48. Xian H, Scherrer JF, Madden PA, et al. The heritability of failed smoking cessation and nicotine withdrawal in twins who smoked and attempted to quit. *Nicotine Tob Res*. 2003;5(2):245-254.
49. Lessov CN, Martin NG, Statham DJ, et al. Defining nicotine dependence for genetic research: evidence from Australian twins. *Psychol Med*. 2004;34(5):865-879.
50. Yang J, Li MD. Converging findings from linkage and association analyses on susceptibility genes for smoking and other addictions. *Mol Psychiatry*. 2016;21(8):992-1008.
51. Fagerstrom KO. Measuring degree of physical dependence to tobacco smoking with reference to individualization of treatment. *Addict Behav*. 1978;3(3-4):235-241.
52. Rustin TA. Assessing nicotine dependence. *Am Fam Physician*. 2000;62(3):579-584, 591-572.
53. Ott J, Wang J, Leal SM. Genetic linkage analysis in the age of whole-genome sequencing. *Nat Rev Genet*. 2015;16(5):275-284.
54. Gelernter J. Genetics of complex traits in psychiatry. *Biol Psychiatry*. 2015;77(1):36-42.
55. Li MD. Identifying susceptibility loci for nicotine dependence: 2008 update based on recent genome-wide linkage analyses. *Hum Genet*. 2008;123(2):119-131.
56. Hardin J, He Y, Javitz HS, et al. Nicotine withdrawal sensitivity, linkage to chr6q26, and association of OPRM1 SNPs in the SMOKing in FAMilies (SMOFAM) sample. *Cancer Epidemiol Biomarkers Prev*. 2009;18(12):3399-3406.
57. Swan GE, Hops H, Wilhelmsen KC, et al. A genome-wide screen for nicotine dependence susceptibility loci. *Am J Med Genet B Neuropsychiatr Genet*. 2006;141B(4):354-360.
58. Han S, Gelernter J, Luo X, Yang BZ. Meta-analysis of 15 genome-wide linkage scans of smoking behavior. *Biol Psychiatry*. 2010;67(1):12-19.
59. Risch N, Merikangas K. The future of genetic studies of complex human diseases. *Science*. 1996;273(5281):1516-1517.
60. Loukola A, Hallfors J, Korhonen T, Kaprio J. Genetics and smoking. *Curr Addict Rep*. 2014;1(1):75-82.
61. Saccone SF, Hinrichs AL, Saccone NL, et al. Cholinergic nicotinic receptor genes implicated in a nicotine dependence association study targeting 348 candidate genes with 3713 SNPs. *Hum Mol Genet*. 2007;16(1):36-49.
62. Gelernter J, Yu Y, Weiss R, et al. Haplotype spanning TTC12 and ANKK1, flanked by the DRD2 and NCAM1 loci, is strongly associated to nicotine dependence in two distinct American populations. *Hum Mol Genet*. 2006;15(24):3498-3507.
63. Ducci F, Kaakinen M, Pouta A, et al. TTC12-ANKK1-DRD2 and CHRNA5-CHRNA3-CHRNA4 influence different pathways leading to smoking behavior from adolescence to mid-adulthood. *Biol Psychiatry*. 2011;69(7):650-660.
64. Ma Y, Yuan W, Jiang X, Cui WY, Li MD. Updated findings of the association and functional studies of DRD2/ANKK1 variants with addictions. *Mol Neurobiol*. 2015;51(1):281-299.
65. Ella E, Sato N, Nishizawa D, et al. Association between dopamine beta hydroxylase rs5320 polymorphism and smoking behaviour in elderly Japanese. *J Hum Genet*. 2012;57(6):385-390.
66. Leventhal AM, Lee W, Bergen AW, et al. Nicotine dependence as a moderator of genetic influences on smoking cessation treatment outcome. *Drug Alcohol Depend*. 2014;138:109-117.

67. Hirvonen K, Korhonen T, Salomaa V, Mannisto S, Kaprio J. Association of the DBH Polymorphism rs3025343 With Smoking Cessation in a Large Population-Based Sample. *Nicotine Tob Res.* 2017;19(9):1112-1115.
68. Yu Y, Panhuysen C, Kranzler HR, et al. Intronic variants in the dopa decarboxylase (DDC) gene are associated with smoking behavior in European-Americans and African-Americans. *Hum Mol Genet.* 2006;15(14):2192-2199.
69. Ma JZ, Beuten J, Payne TJ, Dupont RT, Elston RC, Li MD. Haplotype analysis indicates an association between the DOPA decarboxylase (DDC) gene and nicotine dependence. *Hum Mol Genet.* 2005;14(12):1691-1698.
70. Berrettini WH, Wileyto EP, Epstein L, et al. Catechol-O-methyltransferase (COMT) gene variants predict response to bupropion therapy for tobacco dependence. *Biol Psychiatry.* 2007;61(1):111-118.
71. Munafo MR, Freathy RM, Ring SM, St Pourcain B, Smith GD. Association of COMT Val(108/158)Met genotype and cigarette smoking in pregnant women. *Nicotine Tob Res.* 2011;13(2):55-63.
72. Tobacco, Genetics C. Genome-wide meta-analyses identify multiple loci associated with smoking behavior. *Nat Genet.* 2010;42(5):441-447.
73. Stapleton JA, Sutherland G, O'Gara C. Association between dopamine transporter genotypes and smoking cessation: a meta-analysis. *Addict Biol.* 2007;12(2):221-226.
74. Duck CH, Gyoon SW. Meta-analysis update of association between dopamine transporter SLC6A3 gene polymorphism and smoking cessation. *J Health Psychol.* 2016:1359105316648479.
75. Verhagen M, Kleinjan M, Engels RC. A systematic review of the A118G (Asn40Asp) variant of OPRM1 in relation to smoking initiation, nicotine dependence and smoking cessation. *Pharmacogenomics.* 2012;13(8):917-933.
76. Beuten J, Ma JZ, Payne TJ, et al. Single- and multilocus allelic variants within the GABA(B) receptor subunit 2 (GABAB2) gene are significantly associated with nicotine dependence. *Am J Hum Genet.* 2005;76(5):859-864.
77. Li MD, Mangold JE, Seneviratne C, et al. Association and interaction analyses of GABBR1 and GABBR2 with nicotine dependence in European- and African-American populations. *PLoS One.* 2009;4(9):e7055.
78. Beuten J, Ma JZ, Payne TJ, et al. Association of specific haplotypes of neurotrophic tyrosine kinase receptor 2 gene (NTRK2) with vulnerability to nicotine dependence in African-Americans and European-Americans. *Biol Psychiatry.* 2007;61(1):48-55.
79. Li MD, Sun D, Lou XY, Beuten J, Payne TJ, Ma JZ. Linkage and association studies in African- and Caucasian-American populations demonstrate that SHC3 is a novel susceptibility locus for nicotine dependence. *Mol Psychiatry.* 2007;12(5):462-473.
80. Lou XY, Ma JZ, Sun D, Payne TJ, Li MD. Fine mapping of a linkage region on chromosome 17p13 reveals that GABARAP and DLG4 are associated with vulnerability to nicotine dependence in European-Americans. *Hum Mol Genet.* 2007;16(2):142-153.
81. Agrawal A, Pergadia ML, Saccone SF, et al. Gamma-aminobutyric acid receptor genes and nicotine dependence: evidence for association from a case-control study. *Addiction.* 2008;103(6):1027-1038.
82. Agrawal A, Pergadia ML, Balasubramanian S, et al. Further evidence for an association between the gamma-aminobutyric acid receptor A, subunit 4 genes on chromosome 4 and Fagerstrom Test for Nicotine Dependence. *Addiction.* 2009;104(3):471-477.
83. Iordanidou M, Tavridou A, Petridis I, et al. Association of polymorphisms of the serotonergic system with smoking initiation in Caucasians. *Drug Alcohol Depend.* 2010;108(1-2):70-76.
84. Kremer I, Bachner-Melman R, Reshef A, et al. Association of the serotonin transporter gene with smoking behavior. *Am J Psychiatry.* 2005;162(5):924-930.

85. Daw J, Boardman JD, Peterson R, et al. The interactive effect of neighborhood peer cigarette use and 5HTTLPR genotype on individual cigarette use. *Addict Behav.* 2014;39(12):1804-1810.
86. Bidwell LC, Garrett ME, McClernon FJ, et al. A preliminary analysis of interactions between genotype, retrospective ADHD symptoms, and initial reactions to smoking in a sample of young adults. *Nicotine Tob Res.* 2012;14(2):229-233.
87. Yang Z, Seneviratne C, Wang S, et al. Serotonin transporter and receptor genes significantly impact nicotine dependence through genetic interactions in both European American and African American smokers. *Drug Alcohol Depend.* 2013;129(3):217-225.
88. Ma JZ, Payne TJ, Nussbaum J, Li MD. Significant association of glutamate receptor, ionotropic N-methyl-D-aspartate 3A (GRIN3A), with nicotine dependence in European- and African-American smokers. *Hum Genet.* 2010;127(5):503-512.
89. Grucza RA, Johnson EO, Krueger RF, et al. Incorporating age at onset of smoking into genetic models for nicotine dependence: evidence for interaction with multiple genes. *Addict Biol.* 2010;15(3):346-357.
90. Vink JM, Smit AB, de Geus EJ, et al. Genome-wide association study of smoking initiation and current smoking. *Am J Hum Genet.* 2009;84(3):367-379.
91. Nussbaum J, Xu Q, Payne TJ, et al. Significant association of the neurexin-1 gene (NRXN1) with nicotine dependence in European- and African-American smokers. *Hum Mol Genet.* 2008;17(11):1569-1577.
92. Sato N, Kageyama S, Chen R, et al. Association between neurexin 1 (NRXN1) polymorphisms and the smoking behavior of elderly Japanese. *Psychiatr Genet.* 2010;20(3):135-136.
93. Docampo E, Ribases M, Gratacos M, et al. Association of neurexin 3 polymorphisms with smoking behavior. *Genes Brain Behav.* 2012;11(6):704-711.
94. Portugal GS, Gould TJ. Genetic variability in nicotinic acetylcholine receptors and nicotine addiction: converging evidence from human and animal research. *Behav Brain Res.* 2008;193(1):1-16.
95. Weiss RB, Baker TB, Cannon DS, et al. A candidate gene approach identifies the CHRNA5-A3-B4 region as a risk factor for age-dependent nicotine addiction. *PLoS Genet.* 2008;4(7):e1000125.
96. Wessel J, McDonald SM, Hinds DA, et al. Resequencing of nicotinic acetylcholine receptor genes and association of common and rare variants with the Fagerstrom test for nicotine dependence. *Neuropsychopharmacology.* 2010;35(12):2392-2402.
97. Thorgeirsson TE, Gudbjartsson DF, Surakka I, et al. Sequence variants at CHRN3-CHRNA6 and CYP2A6 affect smoking behavior. *Nat Genet.* 2010;42(5):448-453.
98. Bierut LJ. Genetic vulnerability and susceptibility to substance dependence. *Neuron.* 2011;69(4):618-627.
99. Lou XY, Ma JZ, Payne TJ, Beuten J, Crew KM, Li MD. Gene-based analysis suggests association of the nicotinic acetylcholine receptor beta1 subunit (CHRN1) and M1 muscarinic acetylcholine receptor (CHRM1) with vulnerability for nicotine dependence. *Hum Genet.* 2006;120(3):381-389.
100. Ehringer MA, Clegg HV, Collins AC, et al. Association of the neuronal nicotinic receptor beta2 subunit gene (CHRN2) with subjective responses to alcohol and nicotine. *Am J Med Genet B Neuropsychiatr Genet.* 2007;144B(5):596-604.
101. Wang S, A DvdV, Xu Q, et al. Significant associations of CHRNA2 and CHRNA6 with nicotine dependence in European American and African American populations. *Hum Genet.* 2014;133(5):575-586.
102. Bergen AW, Javitz HS, Krasnow R, et al. Nicotinic acetylcholine receptor variation and response to smoking cessation therapies. *Pharmacogenet Genomics.* 2013;23(2):94-103.
103. King DP, Paciga S, Pickering E, et al. Smoking cessation pharmacogenetics: analysis of varenicline and bupropion in placebo-controlled clinical trials. *Neuropsychopharmacology.* 2012;37(3):641-650.

104. Chen LS, Baker TB, Piper ME, et al. Interplay of genetic risk factors (CHRNA5-CHRNA3-CHRNA4) and cessation treatments in smoking cessation success. *Am J Psychiatry*. 2012;169(7):735-742.
105. Chen LS, Baker TB, Jorenby D, et al. Genetic variation (CHRNA5), medication (combination nicotine replacement therapy vs. varenicline), and smoking cessation. *Drug Alcohol Depend*. 2015;154:278-282.
106. Chen LS, Baker TB, Grucza R, et al. Dissection of the phenotypic and genotypic associations with nicotinic dependence. *Nicotine Tob Res*. 2012;14(4):425-433.
107. Carter B, Long T, Cinciripini P. A meta-analytic review of the CYP2A6 genotype and smoking behavior. *Nicotine Tob Res*. 2004;6(2):221-227.
108. Chen LS, Bloom AJ, Baker TB, et al. Pharmacotherapy effects on smoking cessation vary with nicotine metabolism gene (CYP2A6). *Addiction*. 2014;109(1):128-137.
109. Johnson GC, Esposito L, Barratt BJ, et al. Haplotype tagging for the identification of common disease genes. *Nat Genet*. 2001;29(2):233-237.
110. Carlson CS, Eberle MA, Rieder MJ, Smith JD, Kruglyak L, Nickerson DA. Additional SNPs and linkage-disequilibrium analyses are necessary for whole-genome association studies in humans. *Nat Genet*. 2003;33(4):518-521.
111. Goldstein DB, Ahmadi KR, Weale ME, Wood NW. Genome scans and candidate gene approaches in the study of common diseases and variable drug responses. *Trends Genet*. 2003;19(11):615-622.
112. Roses AD. Apolipoprotein E alleles as risk factors in Alzheimer's disease. *Annu Rev Med*. 1996;47:387-400.
113. Fijnheer R, Horbach DA, Donders RC, et al. Factor V Leiden, antiphospholipid antibodies and thrombosis in systemic lupus erythematosus. *Thromb Haemost*. 1996;76(4):514-517.
114. Manolio TA, Collins FS, Cox NJ, et al. Finding the missing heritability of complex diseases. *Nature*. 2009;461(7265):747-753.
115. Bierut LJ, Madden PA, Breslau N, et al. Novel genes identified in a high-density genome wide association study for nicotine dependence. *Hum Mol Genet*. 2007;16(1):24-35.
116. Berrettini W, Yuan X, Tozzi F, et al. Alpha-5/alpha-3 nicotinic receptor subunit alleles increase risk for heavy smoking. *Mol Psychiatry*. 2008;13(4):368-373.
117. Thorgeirsson TE, Geller F, Sulem P, et al. A variant associated with nicotine dependence, lung cancer and peripheral arterial disease. *Nature*. 2008;452(7187):638-642.
118. Liu JZ, Tozzi F, Waterworth DM, et al. Meta-analysis and imputation refines the association of 15q25 with smoking quantity. *Nat Genet*. 2010;42(5):436-440.
119. Wang JC, Cruchaga C, Saccone NL, et al. Risk for nicotine dependence and lung cancer is conferred by mRNA expression levels and amino acid change in CHRNA5. *Hum Mol Genet*. 2009;18(16):3125-3135.
120. Wang JC, Grucza R, Cruchaga C, et al. Genetic variation in the CHRNA5 gene affects mRNA levels and is associated with risk for alcohol dependence. *Mol Psychiatry*. 2009;14(5):501-510.
121. Wang JC, Kapoor M, Goate AM. The genetics of substance dependence. *Annu Rev Genomics Hum Genet*. 2012;13:241-261.
122. Rice JP, Hartz SM, Agrawal A, et al. CHRNA3 is more strongly associated with Fagerstrom test for cigarette dependence-based nicotine dependence than cigarettes per day: phenotype definition changes genome-wide association studies results. *Addiction*. 2012;107(11):2019-2028.
123. Loukola A, Buchwald J, Gupta R, et al. A Genome-Wide Association Study of a Biomarker of Nicotine Metabolism. *PLoS Genet*. 2015;11(9):e1005498.
124. Johnstone E, Benowitz N, Cargill A, et al. Determinants of the rate of nicotine metabolism and effects on smoking behavior. *Clin Pharmacol Ther*. 2006;80(4):319-330.
125. Gibson G. Rare and common variants: twenty arguments. *Nat Rev Genet*. 2012;13(2):135-145.

126. Olfson E, Saccone NL, Johnson EO, et al. Rare, low frequency and common coding variants in CHRNA5 and their contribution to nicotine dependence in European and African Americans. *Mol Psychiatry*. 2016;21(5):601-607.
127. Xie P, Kranzler HR, Krauthammer M, et al. Rare nonsynonymous variants in alpha-4 nicotinic acetylcholine receptor gene protect against nicotine dependence. *Biol Psychiatry*. 2011;70(6):528-536.
128. Haller G, Druley T, Vallania FL, et al. Rare missense variants in CHRN4 are associated with reduced risk of nicotine dependence. *Hum Mol Genet*. 2012;21(3):647-655.
129. Slimak MA, Ables JL, Frahm S, et al. Habenular expression of rare missense variants of the beta4 nicotinic receptor subunit alters nicotine consumption. *Front Hum Neurosci*. 2014;8:12.
130. Yang J, Wang S, Yang Z, et al. The contribution of rare and common variants in 30 genes to risk nicotine dependence. *Mol Psychiatry*. 2015;20(11):1467-1478.
131. Gillentine MA, Schaaf CP. The human clinical phenotypes of altered CHRNA7 copy number. *Biochem Pharmacol*. 2015;97(4):352-362.
132. Lowther C, Costain G, Stavropoulos DJ, et al. Delineating the 15q13.3 microdeletion phenotype: a case series and comprehensive review of the literature. *Genet Med*. 2015;17(2):149-157.
133. Shinawi M, Schaaf CP, Bhatt SS, et al. A small recurrent deletion within 15q13.3 is associated with a range of neurodevelopmental phenotypes. *Nat Genet*. 2009;41(12):1269-1271.
134. Mikhail FM, Lose EJ, Robin NH, et al. Clinically relevant single gene or intragenic deletions encompassing critical neurodevelopmental genes in patients with developmental delay, mental retardation, and/or autism spectrum disorders. *Am J Med Genet A*. 2011;155A(10):2386-2396.
135. Hoppman-Chaney N, Wain K, Seger PR, Superneau DW, Hodge JC. Identification of single gene deletions at 15q13.3: further evidence that CHRNA7 causes the 15q13.3 microdeletion syndrome phenotype. *Clin Genet*. 2013;83(4):345-351.
136. Masurel-Paulet A, Andrieux J, Callier P, et al. Delineation of 15q13.3 microdeletions. *Clin Genet*. 2010;78(2):149-161.
137. Helbig I, Mefford HC, Sharp AJ, et al. 15q13.3 microdeletions increase risk of idiopathic generalized epilepsy. *Nat Genet*. 2009;41(2):160-162.
138. Gault J, Robinson M, Berger R, et al. Genomic organization and partial duplication of the human alpha7 neuronal nicotinic acetylcholine receptor gene (CHRNA7). *Genomics*. 1998;52(2):173-185.
139. Sinkus ML, Graw S, Freedman R, Ross RG, Lester HA, Leonard S. The human CHRNA7 and CHRFA7A genes: A review of the genetics, regulation, and function. *Neuropharmacology*. 2015;96(Pt B):274-288.
140. Araud T, Graw S, Berger R, et al. The chimeric gene CHRFA7A, a partial duplication of the CHRNA7 gene, is a dominant negative regulator of alpha7*nAChR function. *Biochem Pharmacol*. 2011;82(8):904-914.
141. de Lucas-Cerrillo AM, Maldifassi MC, Arnalich F, et al. Function of partially duplicated human alpha77 nicotinic receptor subunit CHRFA7A gene: potential implications for the cholinergic anti-inflammatory response. *J Biol Chem*. 2011;286(1):594-606.
142. Sinkus ML, Lee MJ, Gault J, et al. A 2-base pair deletion polymorphism in the partial duplication of the alpha7 nicotinic acetylcholine gene (CHRFA7A) on chromosome 15q14 is associated with schizophrenia. *Brain Res*. 2009;1291:1-11.
143. Flomen RH, Shaikh M, Walshe M, et al. Association between the 2-bp deletion polymorphism in the duplicated version of the alpha7 nicotinic receptor gene and P50 sensory gating. *Eur J Hum Genet*. 2013;21(1):76-81.
144. Gjini K, Burroughs S, Boutros NN. Relevance of attention in auditory sensory gating paradigms in schizophrenia A pilot study. *J Psychophysiol*. 2011;25(2):60-66.

145. Freedman R, Adler LE, Waldo MC, Pachtman E, Franks RD. Neurophysiological evidence for a defect in inhibitory pathways in schizophrenia: comparison of medicated and drug-free patients. *Biol Psychiatry*. 1983;18(5):537-551.
146. Raux G, Bonnet-Brilhault F, Louchart S, et al. The -2 bp deletion in exon 6 of the 'alpha 7-like' nicotinic receptor subunit gene is a risk factor for the P50 sensory gating deficit. *Mol Psychiatry*. 2002;7(9):1006-1011.
147. Rozycka A, Dorszewska J, Steinborn B, et al. Association study of the 2-bp deletion polymorphism in exon 6 of the CHRFAM7A gene with idiopathic generalized epilepsy. *DNA Cell Biol*. 2013;32(11):640-647.
148. Flomen RH, Collier DA, Osborne S, et al. Association study of CHRFAM7A copy number and 2 bp deletion polymorphisms with schizophrenia and bipolar affective disorder. *Am J Med Genet B Neuropsychiatr Genet*. 2006;141B(6):571-575.
149. Kunii Y, Zhang W, Xu Q, et al. CHRNA7 and CHRFAM7A mRNAs: co-localized and their expression levels altered in the postmortem dorsolateral prefrontal cortex in major psychiatric disorders. *Am J Psychiatry*. 2015;172(11):1122-1130.
150. Leonard S, Gault J, Hopkins J, et al. Association of promoter variants in the alpha7 nicotinic acetylcholine receptor subunit gene with an inhibitory deficit found in schizophrenia. *Arch Gen Psychiatry*. 2002;59(12):1085-1096.
151. Bertelsen B, Oranje B, Melchior L, et al. Association Study of CHRNA7 Promoter Variants with Sensory and Sensorimotor Gating in Schizophrenia Patients and Healthy Controls: A Danish Case-Control Study. *Neuromolecular Med*. 2015;17(4):423-430.
152. Stephens SH, Logel J, Barton A, et al. Association of the 5'-upstream regulatory region of the alpha7 nicotinic acetylcholine receptor subunit gene (CHRNA7) with schizophrenia. *Schizophr Res*. 2009;109(1-3):102-112.
153. Freedman R, Hall M, Adler LE, Leonard S. Evidence in postmortem brain tissue for decreased numbers of hippocampal nicotinic receptors in schizophrenia. *Biol Psychiatry*. 1995;38(1):22-33.
154. Guillozet-Bongaarts AL, Hyde TM, Dalley RA, et al. Altered gene expression in the dorsolateral prefrontal cortex of individuals with schizophrenia. *Mol Psychiatry*. 2014;19(4):478-485.
155. Marutle A, Zhang X, Court J, et al. Laminar distribution of nicotinic receptor subtypes in cortical regions in schizophrenia. *J Chem Neuroanat*. 2001;22(1-2):115-126.
156. Court J, Spurden D, Lloyd S, et al. Neuronal nicotinic receptors in dementia with Lewy bodies and schizophrenia: alpha-bungarotoxin and nicotine binding in the thalamus. *J Neurochem*. 1999;73(4):1590-1597.
157. Mexal S, Berger R, Logel J, Ross RG, Freedman R, Leonard S. Differential regulation of alpha7 nicotinic receptor gene (CHRNA7) expression in schizophrenic smokers. *J Mol Neurosci*. 2010;40(1-2):185-195.
158. de Leon J, Diaz FJ. A meta-analysis of worldwide studies demonstrates an association between schizophrenia and tobacco smoking behaviors. *Schizophr Res*. 2005;76(2-3):135-157.
159. De Luca V, Wong AH, Muller DJ, Wong GW, Tyndale RF, Kennedy JL. Evidence of association between smoking and alpha7 nicotinic receptor subunit gene in schizophrenia patients. *Neuropsychopharmacology*. 2004;29(8):1522-1526.
160. Zammit S, Spurlock G, Williams H, et al. Genotype effects of CHRNA7, CNR1 and COMT in schizophrenia: interactions with tobacco and cannabis use. *Br J Psychiatry*. 2007;191:402-407.
161. Brunzell DH, McIntosh JM. Alpha7 nicotinic acetylcholine receptors modulate motivation to self-administer nicotine: implications for smoking and schizophrenia. *Neuropsychopharmacology*. 2012;37(5):1134-1143.
162. Harenza JL, Muldoon PP, De Biasi M, Damaj MI, Miles MF. Genetic variation within the Chrna7 gene modulates nicotine reward-like phenotypes in mice. *Genes Brain Behav*. 2014;13(2):213-225.

163. Brunzell DH, McIntosh JM, Papke RL. Diverse strategies targeting alpha7 homomeric and alpha6beta2* heteromeric nicotinic acetylcholine receptors for smoking cessation. *Ann N Y Acad Sci.* 2014;1327:27-45.
164. Mihalak KB, Carroll FI, Luetje CW. Varenicline is a partial agonist at alpha4beta2 and a full agonist at alpha7 neuronal nicotinic receptors. *Mol Pharmacol.* 2006;70(3):801-805.
165. Smith RC, Lindenmayer JP, Davis JM, et al. Cognitive and antismoking effects of varenicline in patients with schizophrenia or schizoaffective disorder. *Schizophr Res.* 2009;110(1-3):149-155.
166. Hong LE, Thaker GK, McMahon RP, et al. Effects of moderate-dose treatment with varenicline on neurobiological and cognitive biomarkers in smokers and nonsmokers with schizophrenia or schizoaffective disorder. *Arch Gen Psychiatry.* 2011;68(12):1195-1206.
167. Siu AL, Force USPST. Behavioral and Pharmacotherapy Interventions for Tobacco Smoking Cessation in Adults, Including Pregnant Women: U.S. Preventive Services Task Force Recommendation Statement. *Ann Intern Med.* 2015;163(8):622-634.
168. Parrott S, Godfrey C, Raw M, West R, McNeill A. Guidance for commissioners on the cost effectiveness of smoking cessation interventions. Health Educational Authority. *Thorax.* 1998;53 Suppl 5 Pt 2:S1-38.
169. West R. The clinical significance of "small" effects of smoking cessation treatments. *Addiction.* 2007;102(4):506-509.
170. Michie S, Hyder N, Walia A, West R. Development of a taxonomy of behaviour change techniques used in individual behavioural support for smoking cessation. *Addict Behav.* 2011;36(4):315-319.
171. Rabius V, Pike KJ, Hunter J, Wiatrek D, McAlister AL. Effects of frequency and duration in telephone counselling for smoking cessation. *Tob Control.* 2007;16 Suppl 1:i71-74.
172. Clinical Practice Guideline Treating Tobacco U, Dependence Update Panel L, Staff. A clinical practice guideline for treating tobacco use and dependence: 2008 update. A U.S. Public Health Service report. *Am J Prev Med.* 2008;35(2):158-176.
173. Patnode CD, Henderson JT, Thompson JH, Senger CA, Fortmann SP, Whitlock EP. Behavioral Counseling and Pharmacotherapy Interventions for Tobacco Cessation in Adults, Including Pregnant Women: A Review of Reviews for the U.S. Preventive Services Task Force. *Ann Intern Med.* 2015;163(8):608-621.
174. Casella G, Caponnetto P, Polosa R. Therapeutic advances in the treatment of nicotine addiction: present and future. *Ther Adv Chronic Dis.* 2010;1(3):95-106.
175. Foulds J, Burke M, Steinberg M, Williams JM, Ziedonis DM. Advances in pharmacotherapy for tobacco dependence. *Expert Opin Emerg Drugs.* 2004;9(1):39-53.
176. Benowitz NL. Nicotine replacement therapy. What has been accomplished--can we do better? *Drugs.* 1993;45(2):157-170.
177. Benowitz NL, Porchet H, Sheiner L, Jacob P, 3rd. Nicotine absorption and cardiovascular effects with smokeless tobacco use: comparison with cigarettes and nicotine gum. *Clin Pharmacol Ther.* 1988;44(1):23-28.
178. Stead LF, Perera R, Bullen C, et al. Nicotine replacement therapy for smoking cessation. *Cochrane Database Syst Rev.* 2012;11:CD000146.
179. Cryan JF, Bruijnzeel AW, Skjei KL, Markou A. Bupropion enhances brain reward function and reverses the affective and somatic aspects of nicotine withdrawal in the rat. *Psychopharmacology (Berl).* 2003;168(3):347-358.
180. Slemmer JE, Martin BR, Damaj MI. Bupropion is a nicotinic antagonist. *J Pharmacol Exp Ther.* 2000;295(1):321-327.
181. John R, Hughes JKS. Shape of the relapse curve and long-term abstinence among untreated smokers. *Society for the Study of Addiction.* 99:29-38.
182. Haddad A, Davis AM. Tobacco Smoking Cessation in Adults and Pregnant Women: Behavioral and Pharmacotherapy Interventions. *JAMA.* 2016;315(18):2011-2012.

183. Rollema H, Chambers LK, Coe JW, et al. Pharmacological profile of the alpha4beta2 nicotinic acetylcholine receptor partial agonist varenicline, an effective smoking cessation aid. *Neuropharmacology*. 2007;52(3):985-994.
184. Coe JW, Brooks PR, Vetelino MG, et al. Varenicline: an alpha4beta2 nicotinic receptor partial agonist for smoking cessation. *J Med Chem*. 2005;48(10):3474-3477.
185. Gonzales D, Rennard SI, Nides M, et al. Varenicline, an alpha4beta2 nicotinic acetylcholine receptor partial agonist, vs sustained-release bupropion and placebo for smoking cessation: a randomized controlled trial. *JAMA*. 2006;296(1):47-55.
186. Jorenby D.E. HJT, Rigotti N.A., Azoulay S., Watsky E.J., Williams K.E., et al. Efficacy of varenicline, an $\alpha 4\beta 2$ nicotinic acetylcholine receptor partial agonist, vs placebo or sustained-release bupropion for smoking cessation: a randomized controlled trial. *JAMA*. 2006;296:56–63.
187. Administration USFaD. FDA Approves Novel Medication for Smoking Cessation. 2006.
188. Russell MB. Epidemiology and genetics of cluster headache. *Lancet Neurol*. 2004;3(5):279-283.
189. Headache Classification Committee of the International Headache S. The International Classification of Headache Disorders, 3rd edition (beta version). *Cephalalgia*. 2013;33(9):629-808.
190. Bahra A, May A, Goadsby PJ. Cluster headache: a prospective clinical study with diagnostic implications. *Neurology*. 2002;58(3):354-361.
191. Goadsby PJ, Cittadini E, Burns B, Cohen AS. Trigeminal autonomic cephalalgias: diagnostic and therapeutic developments. *Curr Opin Neurol*. 2008;21(3):323-330.
192. Torelli P, Manzoni GC. Behavior during cluster headache. *Curr Pain Headache Rep*. 2005;9(2):113-119.
193. Ekblom K. Nitroglycerin as a provocative agent in cluster headache. *Arch Neurol*. 1968;19(5):487-493.
194. Dodick DW, Rozen TD, Goadsby PJ, Silberstein SD. Cluster headache. *Cephalalgia*. 2000;20(9):787-803.
195. Costa F AF, Ramusino MC, Nappi G. The Neuropharmacology of Cluster Headache and other Trigeminal Autonomic Cephalalgias. *Current Neuropharmacology*. 2015;13:304-323.
196. Goadsby PJ, Edvinsson L. Human in vivo evidence for trigeminovascular activation in cluster headache. Neuropeptide changes and effects of acute attacks therapies. *Brain*. 1994;117 (Pt 3):427-434.
197. Sjostrand C. Genetic aspects of cluster headache. *Expert Rev Neurother*. 2009;9(3):359-368.
198. Tfelt-Hansen P, Le H. Calcitonin gene-related peptide in blood: is it increased in the external jugular vein during migraine and cluster headache? A review. *J Headache Pain*. 2009;10(3):137-143.
199. Buture A, Gooriah R, Nimeri R, Ahmed F. Current Understanding on Pain Mechanism in Migraine and Cluster Headache. *Anesth Pain Med*. 2016;6(3):e35190.
200. Hayes DJ, Northoff G. Common brain activations for painful and non-painful aversive stimuli. *BMC Neurosci*. 2012;13:60.
201. Olesen J, Thomsen LL, Iversen H. Nitric oxide is a key molecule in migraine and other vascular headaches. *Trends Pharmacol Sci*. 1994;15(5):149-153.
202. D'Amico D, Leone M, Ferraris A, et al. Role of nitric oxide in cluster headache. *Ital J Neurol Sci*. 1999;20(2 Suppl):S25-27.
203. Luo ZD, Cizkova D. The role of nitric oxide in nociception. *Curr Rev Pain*. 2000;4(6):459-466.
204. Meller ST, Gebhart GF. Nitric oxide (NO) and nociceptive processing in the spinal cord. *Pain*. 1993;52(2):127-136.
205. Tassorelli C, Greco R, Wang D, Sandrini M, Sandrini G, Nappi G. Nitroglycerin induces hyperalgesia in rats--a time-course study. *Eur J Pharmacol*. 2003;464(2-3):159-162.

206. Strosznajder J, Chalimoniuk M, Samochocki M. Activation of serotonergic 5-HT_{1A} receptor reduces Ca²⁺- and glutamatergic receptor-evoked arachidonic acid and No/cGMP release in adult hippocampus. *Neurochem Int.* 1996;28(4):439-444.
207. Strecker T, Dux M, Messlinger K. Nitric oxide releases calcitonin-gene-related peptide from rat dura mater encephali promoting increases in meningeal blood flow. *J Vasc Res.* 2002;39(6):489-496.
208. Schwenger N, Dux M, de Col R, Carr R, Messlinger K. Interaction of calcitonin gene-related peptide, nitric oxide and histamine release in neurogenic blood flow and afferent activation in the rat cranial dura mater. *Cephalalgia.* 2007;27(6):481-491.
209. Brzezinski A. Melatonin in humans. *N Engl J Med.* 1997;336(3):186-195.
210. May A, Bahra A, Buchel C, Frackowiak RS, Goadsby PJ. Hypothalamic activation in cluster headache attacks. *Lancet.* 1998;352(9124):275-278.
211. Morelli N, Pesaresi I, Cafforio G, et al. Functional magnetic resonance imaging in episodic cluster headache. *J Headache Pain.* 2009;10(1):11-14.
212. Holland P, Goadsby PJ. The hypothalamic orexinergic system: pain and primary headaches. *Headache.* 2007;47(6):951-962.
213. Russell MB, Andersson PG, Thomsen LL. Familial occurrence of cluster headache. *J Neurol Neurosurg Psychiatry.* 1995;58(3):341-343.
214. Rainero I, Rubino E, Paemeleire K, et al. Genes and primary headaches: discovering new potential therapeutic targets. *J Headache Pain.* 2013;14:61.
215. Aridon P, D'Andrea G, Rigamonti A, Leone M, Casari G, Bussone G. Elusive amines and cluster headache: mutational analysis of trace amine receptor cluster on chromosome 6q23. *Neurol Sci.* 2004;25 Suppl 3:S279-280.
216. D'Andrea G TS, Leon A, Fortin D, Perini F, Granella F, Bussone G. Elevated levels of circulating trace amines in primary headaches. *Neurology.* 2004;62(10):1701-1705.
217. Baumber L, Sjostrand C, Leone M, et al. A genome-wide scan and HCRTR2 candidate gene analysis in a European cluster headache cohort. *Neurology.* 2006;66(12):1888-1893.
218. Rainero I, Gallone S, Valfre W, et al. A polymorphism of the hypocretin receptor 2 gene is associated with cluster headache. *Neurology.* 2004;63(7):1286-1288.
219. Sutcliffe JG, de Lecea L. The hypocretins: excitatory neuromodulatory peptides for multiple homeostatic systems, including sleep and feeding. *J Neurosci Res.* 2000;62(2):161-168.
220. Schurks M, Kurth T, Geissler I, Tessmann G, Diener HC, Roskopf D. Cluster headache is associated with the G1246A polymorphism in the hypocretin receptor 2 gene. *Neurology.* 2006;66(12):1917-1919.
221. Zarrilli F, Tomaiuolo R, Ceglia C, et al. Molecular analysis of cluster headache. *Clin J Pain.* 2015;31(1):52-57.
222. Weller CM, Wilbrink LA, Houwing-Duistermaat JJ, et al. Cluster headache and the hypocretin receptor 2 reconsidered: a genetic association study and meta-analysis. *Cephalalgia.* 2015;35(9):741-747.
223. Fourier C, Ran C, Steinberg A, Sjostrand C, Waldenlind E, Carmine Belin A. Screening of Two ADH4 Variations in a Swedish Cluster Headache Case-Control Material. *Headache.* 2016.
224. Cevoli S, Mochi M, Pierangeli G, et al. Investigation of the T3111C CLOCK gene polymorphism in cluster headache. *J Neurol.* 2008;255(2):299-300.
225. Zhang EE, Kay SA. Clocks not winding down: unravelling circadian networks. *Nat Rev Mol Cell Biol.* 2010;11(11):764-776.
226. Ofte HK, Tronvik E, Alstadhaug KB. Lack of association between cluster headache and PER3 clock gene polymorphism. *J Headache Pain.* 2015;17:18.
227. Gupta S, Nahas SJ, Peterlin BL. Chemical mediators of migraine: preclinical and clinical observations. *Headache.* 2011;51(6):1029-1045.
228. Sharma JN, Al-Omran A, Parvathy SS. Role of nitric oxide in inflammatory diseases. *Inflammopharmacology.* 2007;15(6):252-259.

229. Sjostrand C, Modin H, Masterman T, Ekblom K, Waldenlind E, Hillert J. Analysis of nitric oxide synthase genes in cluster headache. *Cephalalgia*. 2002;22(9):758-764.
230. Sjostrand C, Giedratys V, Ekblom K, Waldenlind E, Hillert J. CACNA1A gene polymorphisms in cluster headache. *Cephalalgia*. 2001;21(10):953-958.
231. Ophoff RA, Terwindt GM, Vergouwe MN, et al. Familial hemiplegic migraine and episodic ataxia type-2 are caused by mutations in the Ca²⁺ channel gene CACNL1A4. *Cell*. 1996;87(3):543-552.
232. Tietjen GE. Migraine as a systemic vasculopathy. *Cephalalgia*. 2009;29(9):987-996.
233. Rubino E, Ferrero M, Rainero I, Binello E, Vaula G, Pinessi L. Association of the C677T polymorphism in the MTHFR gene with migraine: a meta-analysis. *Cephalalgia*. 2009;29(8):818-825.
234. Schurks M, Rist PM, Kurth T. MTHFR 677C>T and ACE D/I polymorphisms in migraine: a systematic review and meta-analysis. *Headache*. 2010;50(4):588-599.
235. Schurks M, Neumann FA, Kessler C, et al. MTHFR 677C>T polymorphism and cluster headache. *Headache*. 2011;51(2):201-207.
236. Summ O, Gregor N, Marziniak M, Gralow I, Husstedt IW, Evers S. Cluster headache and Alpha 1-antitrypsin deficiency. *Cephalalgia*. 2010;30(1):113-117.
237. Rainero I, Rivoiro C, Rubino E, et al. Prevalence of HFE (hemochromatosis) gene mutations in patients with cluster headache. *Headache*. 2005;45(9):1219-1223.
238. Hagen K, Stovner LJ, Asberg A, Thorstensen K, Bjerve KS, Hveem K. High headache prevalence among women with hemochromatosis: the Nord-Trondelag health study. *Ann Neurol*. 2002;51(6):786-789.
239. Schurks M. Genetics of cluster headache. *Curr Pain Headache Rep*. 2010;14(2):132-139.
240. Schurks M, Diener HC. Cluster headache and lifestyle habits. *Curr Pain Headache Rep*. 2008;12(2):115-121.
241. Rozen TD. Cluster headache as the result of secondhand cigarette smoke exposure during childhood. *Headache*. 2010;50(1):130-132.
242. Thorgeirsson TE, Steinberg S, Reginsson GW, et al. A rare missense mutation in CHRNA4 associates with smoking behavior and its consequences. *Mol Psychiatry*. 2016;21(5):594-600.
243. Hancock DB, Reginsson GW, Gaddis NC, et al. Genome-wide meta-analysis reveals common splice site acceptor variant in CHRNA4 associated with nicotine dependence. *Transl Psychiatry*. 2015;5:e651.
244. Bekkelund SI, Ofte HK, Alstadhaug KB. Patient satisfaction with conventional, complementary, and alternative treatment for cluster headache in a Norwegian cohort. *Scand J Prim Health Care*. 2014;32(3):111-116.
245. Schurks M, Kurth T, Stude P, et al. G protein beta3 polymorphism and triptan response in cluster headache. *Clin Pharmacol Ther*. 2007;82(4):396-401.
246. Helyes Z, Pinter E, Nemeth J, et al. Anti-inflammatory effect of synthetic somatostatin analogues in the rat. *Br J Pharmacol*. 2001;134(7):1571-1579.
247. Matharu MS, Levy MJ, Meeran K, Goadsby PJ. Subcutaneous octreotide in cluster headache: randomized placebo-controlled double-blind crossover study. *Ann Neurol*. 2004;56(4):488-494.
248. Kittrelle JP, Grouse DS, Seybold ME. Cluster headache. Local anesthetic abortive agents. *Arch Neurol*. 1985;42(5):496-498.
249. Robbins L. Intranasal lidocaine for cluster headache. *Headache*. 1995;35(2):83-84.
250. Fogan L. Treatment of cluster headache. A double-blind comparison of oxygen v air inhalation. *Arch Neurol*. 1985;42(4):362-363.
251. Andersson PG, Jespersen LT. Dihydroergotamine nasal spray in the treatment of attacks of cluster headache. A double-blind trial versus placebo. *Cephalalgia*. 1986;6(1):51-54.
252. Blau JN, Engel HO. Individualizing treatment with verapamil for cluster headache patients. *Headache*. 2004;44(10):1013-1018.

253. Ito Y, Mitsufuji T, Asano Y, et al. Naratriptan in the Prophylactic Treatment of Cluster Headache. *Intern Med.* 2017;56(19):2579-2582.
254. Eekers PJ, Koehler PJ. Naratriptan prophylactic treatment in cluster headache. *Cephalalgia.* 2001;21(1):75-76.
255. Lord C, Rutter M, Le Couteur A. Autism Diagnostic Interview-Revised: a revised version of a diagnostic interview for caregivers of individuals with possible pervasive developmental disorders. *J Autism Dev Disord.* 1994;24(5):659-685.
256. Lord C, Risi S, Lambrecht L, et al. The autism diagnostic observation schedule-generic: a standard measure of social and communication deficits associated with the spectrum of autism. *J Autism Dev Disord.* 2000;30(3):205-223.
257. Kit IP-. Psychiatric predisposition microarray. <http://www.willuminacom/products/psycharrayhtml>. 2016.
258. Peiffer DA, Le JM, Steemers FJ, et al. High-resolution genomic profiling of chromosomal aberrations using Infinium whole-genome genotyping. *Genome Res.* 2006;16(9):1136-1148.
259. Wang K, Li M, Hadley D, et al. PennCNV: an integrated hidden Markov model designed for high-resolution copy number variation detection in whole-genome SNP genotyping data. *Genome Res.* 2007;17(11):1665-1674.
260. Colella S, Yau C, Taylor JM, et al. QuantiSNP: an Objective Bayes Hidden-Markov Model to detect and accurately map copy number variation using SNP genotyping data. *Nucleic Acids Res.* 2007;35(6):2013-2025.
261. Livak KJ, Schmittgen TD. Analysis of relative gene expression data using real-time quantitative PCR and the 2⁻(Delta Delta C(T)) Method. *Methods.* 2001;25(4):402-408.
262. Korbie DJ, Mattick JS. Touchdown PCR for increased specificity and sensitivity in PCR amplification. *Nat Protoc.* 2008;3(9):1452-1456.
263. Chang CC, Chow CC, Tellier LC, Vattikuti S, Purcell SM, Lee JJ. Second-generation PLINK: rising to the challenge of larger and richer datasets. *Gigascience.* 2015;4:7.
264. Ionita-Laza I LS, Makarov V, Buxbaum JD, Lin X. Sequence kernel association tests for the combined effect of rare and common variants. *Am J Hum Genet.* 2013;92:841-853.
265. Guo Y, He J, Zhao S, et al. Illumina human exome genotyping array clustering and quality control. *Nat Protoc.* 2014;9(11):2643-2662.
266. Purcell S, Neale B, Todd-Brown K, et al. PLINK: a tool set for whole-genome association and population-based linkage analyses. *Am J Hum Genet.* 2007;81(3):559-575.
267. Buchmann R HS. Creating Structure Plots - Genesis Manual 0.1. <http://www.bioinf.wits.ac.za/software/genesis>. 2016.
268. Pruim RJ, Welch RP, Sanna S, et al. LocusZoom: regional visualization of genome-wide association scan results. *Bioinformatics.* 2010;26(18):2336-2337.
269. Adzhubei I, Jordan DM, Sunyaev SR. Predicting functional effect of human missense mutations using PolyPhen-2. *Curr Protoc Hum Genet.* 2013;Chapter 7:Unit7 20.
270. Kircher M, Witten DM, Jain P, O'Roak BJ, Cooper GM, Shendure J. A general framework for estimating the relative pathogenicity of human genetic variants. *Nat Genet.* 2014;46(3):310-315.
271. Schizophrenia Working Group of the Psychiatric Genomics C. Biological insights from 108 schizophrenia-associated genetic loci. *Nature.* 2014;511(7510):421-427.
272. Gormley P, Anttila V, Winsvold BS, et al. Meta-analysis of 375,000 individuals identifies 38 susceptibility loci for migraine. *Nat Genet.* 2016;48(8):856-866.
273. Hughes JR KJ, Naud S. Shape of the relapse curve and long-term abstinence among untreated smokers. *Addiction.* 2004;99:29-38.
274. Rigotti NA. Strategies to help a smoker who is struggling to quit. *JAMA.* 2012;308(15):1573-1580.
275. Picciotto MR, Kenny PJ. Molecular mechanisms underlying behaviors related to nicotine addiction. *Cold Spring Harb Perspect Med.* 2013;3(1):a012112.

276. Gotti C, Guiducci S, Tedesco V, et al. Nicotinic acetylcholine receptors in the mesolimbic pathway: primary role of ventral tegmental area alpha6beta2* receptors in mediating systemic nicotine effects on dopamine release, locomotion, and reinforcement. *J Neurosci*. 2010;30(15):5311-5325.
277. Olofsson PS, Katz DA, Rosas-Ballina M, et al. alpha7 nicotinic acetylcholine receptor (alpha7nAChR) expression in bone marrow-derived non-T cells is required for the inflammatory reflex. *Mol Med*. 2012;18:539-543.
278. Cedillo JL, Arnalich F, Martin-Sanchez C, et al. Usefulness of alpha7 nicotinic receptor messenger RNA levels in peripheral blood mononuclear cells as a marker for cholinergic antiinflammatory pathway activity in septic patients: results of a pilot study. *J Infect Dis*. 2015;211(1):146-155.
279. Martin-Ruiz CM, Haroutunian VH, Long P, et al. Dementia rating and nicotinic receptor expression in the prefrontal cortex in schizophrenia. *Biol Psychiatry*. 2003;54(11):1222-1233.
280. Young JW, Geyer MA. Evaluating the role of the alpha-7 nicotinic acetylcholine receptor in the pathophysiology and treatment of schizophrenia. *Biochem Pharmacol*. 2013;86(8):1122-1132.
281. Kirov G, Rees E, Walters JT, et al. The penetrance of copy number variations for schizophrenia and developmental delay. *Biol Psychiatry*. 2014;75(5):378-385.
282. Cross-Disorder Group of the Psychiatric Genomics C, Lee SH, Ripke S, et al. Genetic relationship between five psychiatric disorders estimated from genome-wide SNPs. *Nat Genet*. 2013;45(9):984-994.
283. Wang Y, Xiao C, Indersmitten T, Freedman R, Leonard S, Lester HA. The duplicated alpha7 subunits assemble and form functional nicotinic receptors with the full-length alpha7. *J Biol Chem*. 2014;289(38):26451-26463.
284. Nievergelt CM, Wineinger NE, Libiger O, et al. Chip-based direct genotyping of coding variants in genome wide association studies: utility, issues and prospects. *Gene*. 2014;540(1):104-109.
285. Vollesen ALH, Ashina M. PACAP38: Emerging Drug Target in Migraine and Cluster Headache. *Headache*. 2017;57 Suppl 2:56-63.
286. Sundrum T, Walker CS. Pituitary adenylate cyclase-activating polypeptide receptors in the trigeminovascular system: implications for migraine. *Br J Pharmacol*. 2017.
287. Yokai M, Kurihara T, Miyata A. Spinal astrocytic activation contributes to both induction and maintenance of pituitary adenylate cyclase-activating polypeptide type 1 receptor-induced long-lasting mechanical allodynia in mice. *Mol Pain*. 2016;12.
288. Akerman S, Goadsby PJ. Neuronal PAC1 receptors mediate delayed activation and sensitization of trigeminocervical neurons: Relevance to migraine. *Sci Transl Med*. 2015;7(308):308ra157.
289. Jongasma H, Pettersson LM, Zhang Y, et al. Markedly reduced chronic nociceptive response in mice lacking the PAC1 receptor. *Neuroreport*. 2001;12(10):2215-2219.
290. Mabuchi T, Shintani N, Matsumura S, et al. Pituitary adenylate cyclase-activating polypeptide is required for the development of spinal sensitization and induction of neuropathic pain. *J Neurosci*. 2004;24(33):7283-7291.
291. Edvinsson L, Uddman R. Neurobiology in primary headaches. *Brain Res Brain Res Rev*. 2005;48(3):438-456.
292. Hansen JM, Sitarz J, Birk S, et al. Vasoactive intestinal polypeptide evokes only a minimal headache in healthy volunteers. *Cephalalgia*. 2006;26(8):992-1003.
293. Tuka B, Szabo N, Toth E, et al. Release of PACAP-38 in episodic cluster headache patients - an exploratory study. *J Headache Pain*. 2016;17(1):69.
294. Racz B, Horvath G, Faluhelyi N, et al. Effects of PACAP on the circadian changes of signaling pathways in chicken pinealocytes. *J Mol Neurosci*. 2008;36(1-3):220-226.
295. Bayes-Genis A, Barallat J, Richards AM. A Test in Context: Nephilysin: Function, Inhibition, and Biomarker. *J Am Coll Cardiol*. 2016;68(6):639-653.

296. Barloese MC. A Review of Cardiovascular Autonomic Control in Cluster Headache. *Headache*. 2016;56(2):225-239.
297. Barloese M, Lund N, Petersen A, Rasmussen M, Jennum P, Jensen R. Sleep and chronobiology in cluster headache. *Cephalalgia*. 2015;35(11):969-978.
298. Goadsby PJ. Pathophysiology of cluster headache: a trigeminal autonomic cephalgia. *Lancet Neurol*. 2002;1(4):251-257.
299. Kramer HH, He L, Lu B, Birklein F, Sommer C. Increased pain and neurogenic inflammation in mice deficient of neutral endopeptidase. *Neurobiol Dis*. 2009;35(2):177-183.
300. Auer-Grumbach M, Toegel S, Schabhuttl M, et al. Rare Variants in MME, Encoding Metalloprotease Neprilysin, Are Linked to Late-Onset Autosomal-Dominant Axonal Polyneuropathies. *Am J Hum Genet*. 2016;99(3):607-623.
301. Depondt C, Donatello S, Rai M, et al. MME mutation in dominant spinocerebellar ataxia with neuropathy (SCA43). *Neurol Genet*. 2016;2(5):e94.
302. Higuchi Y, Hashiguchi A, Yuan J, et al. Mutations in MME cause an autosomal-recessive Charcot-Marie-Tooth disease type 2. *Ann Neurol*. 2016;79(4):659-672.
303. Ran C, Fourier C, Michalska JM, et al. Screening of genetic variants in ADCYAP1R1, MME and 14q21 in a Swedish cluster headache cohort. *J Headache Pain*. 2017;18(1):88.

APPENDIX

Table S1: list of selected candidate genes used in CH gene-based analysis

GENE	N of rare PAV/gene	SKAT P-value	GO term
MME	3	2.55E-05	GO:0019233
NPY1R	2	1.18E-03	GO:0004983 GO:0007218 GO:0008015 GO:0008217 GO:0019233 GO:0045907
BDKRB1	2	3.30E-03	GO:0019233
SLC5A3	2	4.94E-03	GO:0006814
CCL26	1	7.02E-03	GO:0071356
GRM1	5	9.45E-03	GO:0019233 GO:0051930
KCNJ16	6	1.11E-02	GO:0006813
OPN4	2	1.47E-02	GO:0042752
KCND3	3	1.52E-02	GO:0006813
NPR3	2	1.64E-02	GO:0008217
SERPINE1	1	1.67E-02	GO:0007623
SCN11A	6	1.83E-02	GO:0001518 GO:0006814 GO:0051930
HRH1	4	2.13E-02	GO:0019229 GO:0045907
COL4A3	11	2.19E-02	GO:0008015
HCRTR2	3	2.41E-02	GO:0007218 GO:0008188 GO:0045187
KDM5A	5	2.61E-02	GO:0032922
HOXB2	2	2.66E-02	GO:0008015
SORCS1	6	3.13E-02	GO:0007218 GO:0008188
ATP7B	11	3.19E-02	GO:0007623
RAI1	5	3.49E-02	GO:0032922
APOE	2	3.49E-02	GO:0042311
TNFRSF11B	2	3.49E-02	GO:0005031 GO:0033209
SLC38A8	6	3.50E-02	GO:0006814
RBM4B	1	3.62E-02	GO:0007623 GO:0032922 GO:0043153
EDA2R	2	3.91E-02	GO:0005031 GO:0033209
STXBP5	2	3.92E-02	GO:0005892
GSTP1	2	3.94E-02	GO:0010804
DBH	9	4.43E-02	GO:0045907 GO:0048265
SLC24A4	7	4.53E-02	GO:0005262 GO:0006813
GIT2	2	5.25E-02	GO:0048266
ANKRD1	2	5.41E-02	GO:0071356
TRPM2	15	5.51E-02	GO:0005262
SLC24A2	1	5.65E-02	GO:0005262 GO:0006813
ASS1	3	5.68E-02	GO:0071356
CASP8	3	5.68E-02	GO:0005164 GO:0010803
HMOX1	3	5.68E-02	GO:0008217 GO:0045909
MEOX2	3	5.68E-02	GO:0008015
CACNG4	1	5.69E-02	GO:0005262 GO:0005891
CACNG6	1	5.69E-02	GO:0005891
CNR1	1	5.69E-02	GO:0019233
COMMD9	1	5.69E-02	GO:0006814
CXCL16	1	5.69E-02	GO:0034612
FAM19A4	1	5.69E-02	GO:0051930
GJA4	1	5.69E-02	GO:0048265
IL18BP	1	5.69E-02	GO:0071356
MAP3K14	1	5.69E-02	GO:0033209
MAPK9	1	5.69E-02	GO:0042752 GO:0071356
NR1D2	1	5.69E-02	GO:0042752
NXPH2	1	5.69E-02	GO:0007218
P2RX1	1	5.69E-02	GO:0008217 GO:0042310
PRKAA2	1	5.69E-02	GO:0042752
PRKCG	1	5.69E-02	GO:0042752 GO:0048265
SLC9A1	1	5.69E-02	GO:0051930
TAC3	1	5.69E-02	GO:0007218
TRADD	1	5.69E-02	GO:0005164 GO:0010803 GO:0033209
ZC3H12A	1	5.69E-02	GO:0071356
ADH1C	1	5.70E-02	GO:0004022 GO:0004024
CCL25	1	5.70E-02	GO:0071356
PTGER3	1	5.75E-02	GO:0045907 GO:0046010
RXFP4	5	5.96E-02	GO:0007218

AVPR2	3	6.07E-02	GO:0045907
MTNR1B	3	6.17E-02	GO:0007623 GO:0045909 GO:0046010
OPN3	3	6.42E-02	GO:0042752
NMUR1	2	7.26E-02	GO:0007218 GO:0008188
SLC6A4	2	7.26E-02	GO:0007623 GO:0042310
KCNA5	3	7.29E-02	GO:0006813 GO:0019229
CCL23	1	7.89E-02	GO:0071356
RELN	17	8.27E-02	GO:0048265
NFIL3	2	8.49E-02	GO:0007623
SLC38A7	2	8.50E-02	GO:0006814
ECE1	4	8.58E-02	GO:0003100 GO:0019229 GO:0042312
NPPA	2	8.77E-02	GO:0005184 GO:0007218
ALOX12	4	9.18E-02	GO:0045909
FBXL21	4	9.20E-02	GO:0043153
GRIN3A	11	9.31E-02	GO:0005262
KCNK7	1	9.32E-02	GO:0005267 GO:0006813
PSMB6	1	9.32E-02	GO:0033209
ADM	1	9.35E-02	GO:0008015
ARNTL2	6	9.44E-02	GO:0007623 GO:0009649 GO:0042753
PROKR1	1	9.62E-02	GO:0004983 GO:0007218 GO:0007623
TRPV3	8	9.91E-02	GO:0005262
QRFP	3	9.99E-02	GO:0005184 GO:0007218
NPFFR2	6	1.01E-01	GO:0007218 GO:0008188
CD34	2	1.03E-01	GO:0008217
NPSR1	5	1.04E-01	GO:0007218 GO:0008188
SETX	12	1.04E-01	GO:0007623
TNFRSF1B	1	1.10E-01	GO:0005031 GO:0033209
TIMELESS	11	1.10E-01	GO:0007623 GO:0042752
A2M	6	1.11E-01	GO:0043120
PSME4	2	1.12E-01	GO:0033209
CHGA	5	1.12E-01	GO:0008217 GO:0045908
BAG4	3	1.16E-01	GO:0033209 GO:0071356
ALDH3B2	9	1.20E-01	GO:0006066
HMGCR	2	1.21E-01	GO:0045908
MC1R	10	1.21E-01	GO:0019233
KCNK18	3	1.25E-01	GO:0005267 GO:0006813
ALDH3B1	4	1.26E-01	GO:0006066
OTULIN	2	1.27E-01	GO:0010803
AGT	7	1.30E-01	GO:0008217 GO:0019229 GO:0042311 GO:0042312
ADCY6	4	1.30E-01	GO:0042312
SIK1	3	1.33E-01	GO:0043153
HTR1B	1	1.34E-01	GO:0042310
PKD2	5	1.36E-01	GO:0005267
AFF3	4	1.37E-01	GO:0034612
F5	10	1.42E-01	GO:0008015
CHRNA4	2	1.42E-01	GO:0004889 GO:0005892 GO:0019233
ACVRL1	2	1.42E-01	GO:0008015 GO:0008217
CACNA1D	2	1.42E-01	GO:0005891
DRD1	2	1.42E-01	GO:0019229 GO:0042311 GO:0042321
HTR3E	2	1.42E-01	GO:0004889 GO:0005892
KCNMB1	2	1.42E-01	GO:0006813
NLGN1	2	1.42E-01	GO:0010841
PAX4	2	1.42E-01	GO:0007623
TRAF3	2	1.42E-01	GO:0005164 GO:0033209
QRFPR	5	1.46E-01	GO:0004983 GO:0007218
NPPB	2	1.49E-01	GO:0008217 GO:0042312
KCNJ11	1	1.54E-01	GO:0071356
UBE3A	1	1.54E-01	GO:0042752
CCDC109B	4	1.56E-01	GO:0005262
NPFFR1	5	1.66E-01	GO:0007218 GO:0008188
MC4R	1	1.66E-01	GO:0042923
TNF	1	1.66E-01	GO:0005164 GO:0010803 GO:0033209
POSTN	3	1.68E-01	GO:0071356
KCNK5	3	1.74E-01	GO:0005267 GO:0006813
CRHR2	3	1.79E-01	GO:0019233
HTR3C	3	1.80E-01	GO:0004889 GO:0005892
MBP	3	1.83E-01	GO:0034612
AHR	7	1.84E-01	GO:0032922
CACNA1E	5	1.86E-01	GO:0005262 GO:0005891
MYH6	6	1.89E-01	GO:0008217

TRIM32	3	1.89E-01	GO:0034612
TNFRSF10D	2	1.95E-01	GO:0005031 GO:0033209
ASIC4	1	1.96E-01	GO:0005272
METTL3	1	1.96E-01	GO:0007623
NXPH3	2	1.96E-01	GO:0007218
SLC5A6	2	1.96E-01	GO:0006814
ID1	2	1.98E-01	GO:0007623
SSTR4	2	1.99E-01	GO:0042923
SSTR5	5	2.00E-01	GO:0042923
KEL	4	2.03E-01	GO:0042310
P2RX4	3	2.05E-01	GO:0008217 GO:0019233
GAS6	2	2.05E-01	GO:0010804
CACNA2D1	2	2.06E-01	GO:0005891
PSMD13	2	2.06E-01	GO:0033209
KCNK4	2	2.13E-01	GO:0005267 GO:0006813
APOB	36	2.19E-01	GO:0071356
TRPM3	7	2.20E-01	GO:0005262
SLC10A5	5	2.24E-01	GO:0006814
SMTNL1	3	2.24E-01	GO:0045907 GO:0045908
TRHDE	3	2.24E-01	GO:0008217
F2RL1	2	2.26E-01	GO:0045909 GO:0010804
RELA	2	2.28E-01	GO:0071356
KCNMB3	1	2.30E-01	GO:0006813
CHD7	7	2.30E-01	GO:0008015
GUCY1B3	1	2.34E-01	GO:0008015
KCNJ6	1	2.38E-01	GO:0006813
NTSR2	3	2.41E-01	GO:0007218
GUCY1A3	3	2.43E-01	GO:0008015 GO:0008217
DHRS9	3	2.47E-01	GO:0004022
AGTR1	3	2.48E-01	GO:0019229 GO:0042312
MC2R	3	2.52E-01	GO:0007218
NOS3	8	2.54E-01	GO:0003100 GO:0008217 GO:0045909
OCSTAMP	2	2.54E-01	GO:0071356
NOS1	9	2.54E-01	GO:0045906 GO:0051930
NISCH	6	2.54E-01	GO:0008217
SLC17A2	3	2.56E-01	GO:0006814
HCRTR1	3	2.59E-01	GO:0007218 GO:0008188 GO:0045187
BRS3	1	2.59E-01	GO:0008217
RAD51L3-RFFL	4	2.61E-01	GO:0010804
MTHFR	5	2.62E-01	GO:0008015
SLC5A11	3	2.62E-01	GO:0006814
LGR4	5	2.63E-01	GO:0032922
KCNK6	3	2.64E-01	GO:0005267 GO:0006813
SELE	3	2.64E-01	GO:0034612
RET	2	2.71E-01	GO:0048265
MRGPRX2	3	2.71E-01	GO:0019233 GO:0042923
HS3ST2	1	2.71E-01	GO:0007623
MCHR1	5	2.73E-01	GO:0007218 GO:0008188
SSTR3	5	2.73E-01	GO:0042923
IKKB	3	2.77E-01	GO:0010803 GO:0033209 GO:0071356
PTPRM	3	2.77E-01	GO:0045909
ADRB2	1	2.82E-01	GO:0045909 GO:0051930
SLC12A8	7	2.85E-01	GO:0006813
GPR1	2	2.87E-01	GO:0007218 GO:0042923
KCNK10	2	2.87E-01	GO:0005267
NEDD4L	2	2.87E-01	GO:0006814
PSME1	2	2.87E-01	GO:0033209
HTR3A	3	2.88E-01	GO:0004889 GO:0005892
CACNA2D4	10	2.90E-01	GO:0005891
NPY4R	3	2.90E-01	GO:0007218 GO:0008015
GRIN2A	4	2.91E-01	GO:0005262 GO:0019233 GO:0051930
KCNIP3	1	2.91E-01	GO:0005267
COL1A1	5	2.92E-01	GO:0071356
CD40LG	1	2.92E-01	GO:0005164 GO:0033209
EDAR	1	2.92E-01	GO:0033209
KCNMA1	1	2.92E-01	GO:0006813
NPY	1	2.92E-01	GO:0005184 GO:0007218 GO:0008015 GO:0008217
CACNA1B	4	2.94E-01	GO:0005262 GO:0005891 GO:0008217 GO:0071356
MMP24	2	2.98E-01	GO:0050965
GBA	2	2.99E-01	GO:0071356

SLC4A4	8	2.99E-01	GO:0006814
KCNU1	7	3.01E-01	GO:0005267
CCL14	2	3.05E-01	GO:0071356
NTRK1	8	3.06E-01	GO:0007623 GO:0050965 GO:0050966
MGLL	3	3.06E-01	GO:0051930
SLC9B2	3	3.06E-01	GO:0006814
GHRHR	1	3.08E-01	GO:0046010
HYAL3	2	3.10E-01	GO:0071356
SLC9C2	4	3.10E-01	GO:0006814
HTR3B	4	3.16E-01	GO:0004889 GO:0005892
LRP5	4	3.16E-01	GO:0008217
SLC5A4	10	3.18E-01	GO:0006814
KCNH4	4	3.18E-01	GO:0006813
NPR1	4	3.20E-01	GO:0008217 GO:0042312
HTR2A	2	3.22E-01	GO:0045907 GO:0050965 GO:0050966
IL12B	3	3.25E-01	GO:0019233
RORC	3	3.25E-01	GO:0032922
FAM134B	4	3.27E-01	GO:0019233
KCNH1	2	3.28E-01	GO:0006813
KCNJ8	1	3.29E-01	GO:0006813 GO:0042311
KCNS1	1	3.29E-01	GO:0006813
NOCT	1	3.29E-01	GO:0007623 GO:0032922 GO:0042752
NPBWR1	1	3.29E-01	GO:0007218 GO:0008188 GO:0042923
PTGS2	1	3.29E-01	GO:0008217 GO:0019233 GO:0045907 GO:0034612
PYY	1	3.29E-01	GO:0005184 GO:0007218
SREBF1	1	3.29E-01	GO:0007623
CACNA1H	12	3.29E-01	GO:0005891
ADAM9	4	3.29E-01	GO:0034612
TRPC6	1	3.30E-01	GO:0005262
TNFRSF21	4	3.31E-01	GO:0005031 GO:0033209 GO:0071356
KNG1	4	3.32E-01	GO:0042311
NOL3	4	3.32E-01	GO:0010804
TRAP1	15	3.32E-01	GO:0005164
CCAR2	3	3.33E-01	GO:0042752
HTR1A	2	3.35E-01	GO:0042310
ACSM3	5	3.39E-01	GO:0008217
SLC9C1	5	3.41E-01	GO:0006814
PER3	7	3.44E-01	GO:0032922 GO:0045187
PIRT	3	3.44E-01	GO:0048266
BRCA1	10	3.47E-01	GO:0071356
DENND5B	2	3.47E-01	GO:0005262
FYN	2	3.50E-01	GO:0050966
PKD2L1	13	3.53E-01	GO:0005262 GO:0005272
TRAF4	2	3.53E-01	GO:0005164
LSM14B	2	3.55E-01	GO:0033209
TPH1	2	3.55E-01	GO:0007623
PRKCQ	2	3.56E-01	GO:0019229
CCL17	1	3.57E-01	GO:0071356
SORT1	2	3.57E-01	GO:0007218
GRIN3B	5	3.59E-01	GO:0005262
NTS	1	3.61E-01	GO:0005184
EPHB1	1	3.62E-01	GO:0050965 GO:0045909
HYAL2	1	3.62E-01	GO:0071356
KCNQ2	1	3.62E-01	GO:0005267 GO:0006813
LTB4R	1	3.62E-01	GO:0007218
PAWR	1	3.62E-01	GO:0050965 GO:0050966
PROX1	1	3.62E-01	GO:0007623 GO:0042752
PSMF1	1	3.62E-01	GO:0033209
TMEM37	1	3.62E-01	GO:0005262
TNFRSF18	1	3.62E-01	GO:0005031 GO:0033209
ZNF675	1	3.62E-01	GO:0010804
GPD1	5	3.62E-01	GO:0071356
KMT2A	8	3.64E-01	GO:0032922
CPS1	7	3.67E-01	GO:0045909
ADIPOQ	4	3.67E-01	GO:0007623 GO:0010804 GO:0034612
CARD14	11	3.67E-01	GO:0033209
TRPV5	5	3.69E-01	GO:0005262
CACNA2D2	2	3.71E-01	GO:0005891 GO:0060024
HTR7	2	3.72E-01	GO:0007623 GO:0008015 GO:0042310
TRPM4	11	3.72E-01	GO:0005262

MYOF	16	3.76E-01	GO:0008015
SLC22A5	4	3.79E-01	GO:0006814
NONO	1	3.81E-01	GO:0007623 GO:0042752
VCAM1	2	3.82E-01	GO:0071356
SLC17A4	3	3.82E-01	GO:0006814
CARTPT	3	3.82E-01	GO:0007218 GO:0032922
CYSLTR2	8	3.85E-01	GO:0007218
KCNA4	2	3.86E-01	GO:0006813
NPBWR2	4	3.86E-01	GO:0007218 GO:0008188 GO:0042923
KCNQ3	3	3.87E-01	GO:0005267 GO:0006813
AQP1	4	3.88E-01	GO:0005267 GO:0006813
CHRNE	3	3.88E-01	GO:0004889 GO:0005892
PSMB9	3	3.89E-01	GO:0033209
ADAM10	3	3.91E-01	GO:0034612
SCN2A	5	3.93E-01	GO:0001518
NFKB1	6	3.95E-01	GO:0071356
TRPM8	5	3.95E-01	GO:0005262
SLC24A1	2	3.97E-01	GO:0005262
KCNK16	5	4.00E-01	GO:0005267 GO:0006813
CHRND	6	4.04E-01	GO:0004889 GO:0005892
ADAMTS12	7	4.07E-01	GO:0071356
NUB1	2	4.08E-01	GO:0034612
TOP2A	5	4.09E-01	GO:0042752
PSMD6	2	4.09E-01	GO:0033209
SLC24A3	5	4.10E-01	GO:0005262 GO:0006813
RPE65	2	4.11E-01	GO:0007623
LOXHD1	16	4.14E-01	GO:0005262
SCN1A	6	4.16E-01	GO:0001518 GO:0006814
CACNB2	3	4.16E-01	GO:0005262 GO:0005891
KLF9	2	4.20E-01	GO:0007623
CHRNA10	3	4.20E-01	GO:0004889 GO:0005262 GO:0005892
PLVAP	2	4.24E-01	GO:0033209
TRPA1	3	4.31E-01	GO:0005262 GO:0019233 GO:0048265 GO:0050966 GO:0050968
SCN4B	1	4.32E-01	GO:0001518 GO:0006814
TNFRSF17	1	4.32E-01	GO:0033209
ENTPD2	3	4.34E-01	GO:0071356
AVPR1A	2	4.35E-01	GO:0008015 GO:0045907
KCNJ3	1	4.40E-01	GO:0006813
DAB2IP	3	4.41E-01	GO:0071356
GLRA1	4	4.41E-01	GO:0007218
EPHX2	3	4.49E-01	GO:0008217
OPRM1	5	4.49E-01	GO:0007218 GO:0019233 GO:0051930
DCSTAMP	5	4.52E-01	GO:0071356
CNR2	2	4.53E-01	GO:0019233
HTR3D	1	4.56E-01	GO:0004889 GO:0005892
PSMD9	1	4.56E-01	GO:0033209
ROCK2	1	4.56E-01	GO:0042752
ADH4	1	4.57E-01	GO:0004022 GO:0004024 GO:0006066
ALB	1	4.57E-01	GO:0046010
ATOH7	1	4.57E-01	GO:0007623 GO:0009649
CACNG2	1	4.57E-01	GO:0005262 GO:0005891
CALCRL	1	4.57E-01	GO:0004948
CCL11	1	4.57E-01	GO:0071356
CD58	1	4.57E-01	GO:0071356
CPT1A	1	4.57E-01	GO:0007623
DRD2	1	4.57E-01	GO:0032922 GO:0042321
EZH2	1	4.57E-01	GO:0042752
GPR84	1	4.57E-01	GO:0007218
KCNAB3	1	4.57E-01	GO:0006813
KLF10	1	4.57E-01	GO:0007623 GO:0042752
LEP	1	4.57E-01	GO:0007623 GO:0008217 GO:0045906
PDE4D	1	4.57E-01	GO:0005891
PPARD	1	4.57E-01	GO:0045909
PSMB2	1	4.57E-01	GO:0033209
RBCK1	1	4.57E-01	GO:0010803
SLC17A8	1	4.57E-01	GO:0006814
TNFSF14	1	4.57E-01	GO:0005164 GO:0033209
TPH2	1	4.57E-01	GO:0007623
CCL24	1	4.58E-01	GO:0071356
SYK	1	4.61E-01	GO:0010803

CASQ2	2	4.61E-01	GO:0005891
CHRNA2	2	4.61E-01	GO:0004889 GO:0005892
ENDOG	2	4.61E-01	GO:0034612
POMK	2	4.63E-01	GO:0019233
CHRNA6	2	4.63E-01	GO:0004889 GO:0005892
MCOLN1	2	4.63E-01	GO:0005262
SLC10A1	2	4.63E-01	GO:0006814
MKKS	3	4.63E-01	GO:0042311
KCNN4	2	4.63E-01	GO:0005267 GO:0006813
MYBBP1A	25	4.65E-01	GO:0032922
KCNK13	4	4.66E-01	GO:0005267
AHCY	3	4.68E-01	GO:0042745
NFE2L2	2	4.71E-01	GO:0071356
CALCA	4	4.71E-01	GO:0007218 GO:0048265 GO:0050965 GO:0071356
ZACN	4	4.76E-01	GO:0004889 GO:0005892
MTNR1A	6	4.77E-01	GO:0007623
ADRA1A	6	4.77E-01	GO:0045907
NTSR1	10	4.77E-01	GO:0007218 GO:0050965 GO:0051930
TRAPPC10	4	4.80E-01	GO:0006814
LTB	1	4.81E-01	GO:0005164 GO:0033209
NLGN3	1	4.81E-01	GO:0060024
TNFRSF13B	6	4.82E-01	GO:0033209
ALOXE3	5	4.82E-01	GO:0019233
TNFRSF14	1	4.83E-01	GO:0005031 GO:0033209
GAL	2	4.85E-01	GO:0005184 GO:0007218
CHUK	2	4.86E-01	GO:0010803 GO:0071356
PROKR2	4	4.90E-01	GO:0004983 GO:0007218 GO:0007623
SIRT1	3	4.92E-01	GO:0032922 GO:0071356
EPB41	2	4.92E-01	GO:0008015
MAGEL2	7	4.95E-01	GO:0042752
TRPM1	9	4.95E-01	GO:0005262
YTHDC2	4	4.96E-01	GO:0034612
HDAC4	5	4.99E-01	GO:0071356
SCN8A	4	5.00E-01	GO:0001518 GO:0006814
ADH7	5	5.02E-01	GO:0004022 GO:0004024
NPS	4	5.03E-01	GO:0007218 GO:0010841
SCNN1G	3	5.04E-01	GO:0005272 GO:0006814
CACNA1C	5	5.05E-01	GO:0005891
KCNA10	7	5.07E-01	GO:0006813
EP300	7	5.08E-01	GO:0007623 GO:0034612
STK39	2	5.09E-01	GO:0008217
CX3CL1	3	5.12E-01	GO:0045906 GO:0071356
CYB5R3	3	5.12E-01	GO:0008015
TAX1BP1	4	5.13E-01	GO:0010803
EPO	3	5.13E-01	GO:0008015
FXRD4	1	5.17E-01	GO:0005267
SLC9A3	5	5.21E-01	GO:0007623
TRPV1	9	5.22E-01	GO:0005262
TNFRSF10C	3	5.23E-01	GO:0005031 GO:0033209
SLC38A4	2	5.31E-01	GO:0006814
PSMB11	7	5.34E-01	GO:0033209
SLC5A10	2	5.37E-01	GO:0006814
DENND5A	4	5.39E-01	GO:0005262
FAS	2	5.41E-01	GO:0007623 GO:0005031 GO:0033209
NOS2	3	5.44E-01	GO:0007623 GO:0045909
CCL8	3	5.45E-01	GO:0071356
PRKCDBP	2	5.52E-01	GO:0032922
TRIM37	3	5.53E-01	GO:0005164
TRDN	3	5.55E-01	GO:0005891
SLC38A10	7	5.55E-01	GO:0006814
MADD	9	5.60E-01	GO:0010803
IL6	2	5.61E-01	GO:0045188 GO:0071356
GALR2	4	5.63E-01	GO:0007218 GO:0042923
PKD1L3	9	5.69E-01	GO:0005262
NDUFA9	2	5.71E-01	GO:0006814
CALCR	3	5.71E-01	GO:0004948
HTR1D	3	5.71E-01	GO:0042310
TRPM7	3	5.71E-01	GO:0005262
TSC1	3	5.73E-01	GO:0006813
KCNK17	3	5.74E-01	GO:0005267 GO:0006813

KAT2B	7	5.76E-01	GO:0045909
CACNA1F	2	5.76E-01	GO:0005891
ATP1A4	11	5.77E-01	GO:0006813 GO:0006814
COL1A2	4	5.78E-01	GO:0008217
BBS2	1	5.80E-01	GO:0042311
SLC6A15	4	5.81E-01	GO:0006814
BMPR2	1	5.83E-01	GO:0045906
PSMB8	3	5.86E-01	GO:0033209
TMEM38B	5	5.96E-01	GO:0005267
PPARA	3	5.96E-01	GO:0032922 GO:0042752
NCOA2	1	5.96E-01	GO:0032922
PTGDR2	1	5.97E-01	GO:0007218 GO:0042923
PTEN	1	5.98E-01	GO:0060024
SLC13A2	2	5.98E-01	GO:0006814
BTRC	1	5.99E-01	GO:0042752 GO:0042753
PDE4B	1	5.99E-01	GO:0005891
PSMB3	1	5.99E-01	GO:0033209
TRPC1	1	5.99E-01	GO:0005262
LTB4R2	3	5.99E-01	GO:0007218
OPRL1	3	5.99E-01	GO:0007218 GO:0019233 GO:0042923
ACPP	1	5.99E-01	GO:0051930
ADORA1	1	5.99E-01	GO:0045908 GO:0050965 GO:0051930
ADORA2A	2	5.99E-01	GO:0008015
ADRA1D	1	5.99E-01	GO:0045907
ADRA2B	1	5.99E-01	GO:0019229
AGTRAP	1	5.99E-01	GO:0008217
ALDH2	2	5.99E-01	GO:0006066
ALOX5	1	5.99E-01	GO:0019233 GO:0045907
BDKRB2	1	5.99E-01	GO:0008015 GO:0019229 GO:0042310 GO:0042311
BIRC2	1	5.99E-01	GO:0010803 GO:0033209
CACFD1	1	5.99E-01	GO:0005262
CCL4	1	5.99E-01	GO:0071356
CD38	1	5.99E-01	GO:0045907
CD40	2	5.99E-01	GO:0005031 GO:0033209
CHI3L1	1	5.99E-01	GO:0034612 GO:0071356
COMT	1	5.99E-01	GO:0048265 GO:0051930
CRCP	1	5.99E-01	GO:0007218
CRHBP	1	5.99E-01	GO:0071356
CSNK1D	1	5.99E-01	GO:0032922 GO:0042752
CXCL12	1	5.99E-01	GO:0008015
DBP	1	5.99E-01	GO:0007623
DRD3	1	5.99E-01	GO:0032922 GO:0045187
DRD4	1	5.99E-01	GO:0007623 GO:0042752
EDA	1	5.99E-01	GO:0005164 GO:0033209
EDN3	1	5.99E-01	GO:0003100 GO:0008015 GO:0019229 GO:0042310
ENOX2	1	5.99E-01	GO:0007624
FASLG	1	5.99E-01	GO:0005164
FGA	1	5.99E-01	GO:0045907
FLI1	1	5.99E-01	GO:0008015
GJA1	1	5.99E-01	GO:0045907 GO:0045909
GLRA2	1	5.99E-01	GO:0007218
GLRB	1	5.99E-01	GO:0007218
GNB3	1	5.99E-01	GO:0008217
GPER1	1	5.99E-01	GO:0045909 GO:0071356
GSS	1	5.99E-01	GO:0034612
HDAC2	1	5.99E-01	GO:0032922
HEBP1	1	5.99E-01	GO:0007623
HIPK1	1	5.99E-01	GO:0010803
HOXB8	1	5.99E-01	GO:0019233
IAPP	1	5.99E-01	GO:0019233
IMMP2L	1	5.99E-01	GO:0008015
INPP5K	1	5.99E-01	GO:0071356
KCNC1	1	5.99E-01	GO:0006813
KCNK15	1	5.99E-01	GO:0005267
KCNK3	1	5.99E-01	GO:0005267 GO:0006813
KCNQ4	1	5.99E-01	GO:0005267 GO:0006813
MAPK3	1	5.99E-01	GO:0019233
MTA1	1	5.99E-01	GO:0032922 GO:0043153
NDN	1	5.99E-01	GO:0019233
NEU1	1	5.99E-01	

NGFR	1	5.99E-01	GO:0019233 GO:0032922 GO:0005031 GO:0033209
NMU	1	5.99E-01	GO:0007218
NPFF	1	5.99E-01	GO:0005184
NPY5R	1	5.99E-01	GO:0004983 GO:0007218
NR1H3	1	5.99E-01	GO:0042752
NTRK2	1	5.99E-01	GO:0007623 GO:0071356
OXTR	1	5.99E-01	GO:0045907
PDE2A	1	5.99E-01	GO:0005262
PELI3	1	5.99E-01	GO:0010804
PIAS4	1	5.99E-01	GO:0010804
POMC	1	5.99E-01	GO:0005184 GO:0007218
PPY	1	5.99E-01	GO:0005184 GO:0007218
PSMC5	1	5.99E-01	GO:0033209
PSMD3	1	5.99E-01	GO:0033209
PSMD8	1	5.99E-01	GO:0033209
RBM14	1	5.99E-01	GO:0043153
RPS6KB1	1	5.99E-01	GO:0034612
RXFP3	1	5.99E-01	GO:0007218
SCN1B	1	5.99E-01	GO:0001518
SERPING1	1	5.99E-01	GO:0008015
SHC1	1	5.99E-01	GO:0045907
SLC10A4	1	5.99E-01	GO:0006814
SLC23A2	1	5.99E-01	GO:0006814
SLC4A11	1	5.99E-01	GO:0005272 GO:0006814
SLC5A7	1	5.99E-01	GO:0006814
SPX	1	5.99E-01	GO:0005184
TBX20	1	5.99E-01	GO:0008015
THBS1	1	5.99E-01	GO:0048266
TMEM100	1	5.99E-01	GO:0051930
TNFRSF6B	1	5.99E-01	GO:0005031 GO:0033209
TOP1	1	5.99E-01	GO:0007623 GO:0032922
TRAIIP	1	5.99E-01	GO:0010804
TRPC7	1	5.99E-01	GO:0005262
VPS4B	1	5.99E-01	GO:0006813
YBX3	1	5.99E-01	GO:0071356
PANX1	1	5.99E-01	GO:0005262
SCN3A	7	6.00E-01	GO:0001518
CXCL8	1	6.00E-01	GO:0071356
KCNK1	4	6.01E-01	GO:0005267 GO:0005272 GO:0006814
GALP	1	6.02E-01	GO:0007218
PSMB7	1	6.02E-01	GO:0033209
NPVF	2	6.04E-01	GO:0007218
TENM1	4	6.07E-01	GO:0007218
P2RX7	11	6.08E-01	GO:0019233
CDKN1B	2	6.09E-01	GO:0006813
HCN4	2	6.10E-01	GO:0008015
MCOLN2	2	6.10E-01	GO:0005262
MCOLN3	2	6.10E-01	GO:0005262
NMS	2	6.10E-01	GO:0007218
PRLH	2	6.10E-01	GO:0005184
PSMD1	2	6.10E-01	GO:0033209
SLC12A2	2	6.10E-01	GO:0006813 GO:0006814
TH	2	6.10E-01	GO:0042745
THRAP3	2	6.10E-01	GO:0007623 GO:0042753
GHRH	1	6.14E-01	GO:0046005
INSR	3	6.18E-01	GO:0034612
AVPR1B	1	6.21E-01	GO:0045907
DLL1	1	6.21E-01	GO:0008217
PSMB10	1	6.21E-01	GO:0033209
PTPN2	1	6.21E-01	GO:0010804
TNFSF18	1	6.21E-01	GO:0032813 GO:0033209
PTGS1	4	6.22E-01	GO:0008217 GO:0019233 GO:0045907
KCNJ13	1	6.23E-01	GO:0006813
PROK1	1	6.23E-01	GO:0007623
SLC38A11	1	6.23E-01	GO:0006814
JAK2	4	6.23E-01	GO:0033209 GO:0034612
NMUR2	4	6.24E-01	GO:0007218 GO:0048265
PDYN	1	6.35E-01	GO:0005184 GO:0007218
LPA	15	6.37E-01	GO:0008015
LNPEP	5	6.37E-01	GO:0008217

TNFRSF19	4	6.37E-01	GO:0005031 GO:0033209
TNFSF9	2	6.37E-01	GO:0005164 GO:0032813
PML	8	6.39E-01	GO:0032922 GO:0042752 GO:0043153
ERAP1	4	6.40E-01	GO:0008217 GO:0043120
CACTIN	1	6.45E-01	GO:0071356
NOX1	3	6.45E-01	GO:0008217
SLC38A2	4	6.47E-01	GO:0006814
ERBB2IP	4	6.48E-01	GO:0071356
ECEL1	4	6.48E-01	GO:0007218
TRAF1	2	6.49E-01	GO:0005164 GO:0010803
CCL15	4	6.50E-01	GO:0071356
RNF31	5	6.50E-01	GO:0010803
PER2	5	6.50E-01	GO:0007623 GO:0019229 GO:0032922
P2RY2	3	6.51E-01	GO:0019233 GO:0042312
SLC10A6	3	6.51E-01	GO:0006814
TNFRSF8	4	6.51E-01	GO:0005031 GO:0033209
SLC10A7	4	6.52E-01	GO:0006814
SGK1	1	6.53E-01	GO:0006814 GO:0008217
DDC	4	6.53E-01	GO:0007623
PSMD5	3	6.58E-01	GO:0033209
HTR2B	4	6.58E-01	GO:0042310
TRPV2	4	6.59E-01	GO:0005262
ZFH3	27	6.60E-01	GO:0032922
P2RX2	4	6.63E-01	GO:0048266
SCN7A	8	6.71E-01	GO:0001518 GO:0006814
MECP2	3	6.72E-01	GO:0019233
NRIP1	5	6.73E-01	GO:0007623 GO:0032922
ADAM17	7	6.76E-01	GO:0033209
ADH6	3	6.76E-01	GO:0004022 GO:0004024
CHRNA9	3	6.76E-01	GO:0004889 GO:0005262 GO:0005892
GPR149	3	6.76E-01	GO:0007218 GO:0042923
TNFRSF10B	3	6.76E-01	GO:0005031 GO:0033209
SCNN1B	3	6.77E-01	GO:0006814
PTK2B	5	6.78E-01	GO:0033209
CIART	3	6.79E-01	GO:0032922
PER1	8	6.84E-01	GO:0007623 GO:0009649 GO:0032922 GO:0042752 GO:0043153
ADCY1	4	6.84E-01	GO:0007623 GO:0042752
GLRA4	6	6.86E-01	GO:0007218
SORCS3	2	6.87E-01	GO:0007218 GO:0008188
PKD2L2	5	6.94E-01	GO:0005262
CHRNA9	5	6.94E-01	GO:0004889 GO:0005892
SCN4A	12	6.94E-01	GO:0001518 GO:0006813 GO:0006814
CACNA1G	8	6.96E-01	GO:0005891
SLC5A9	7	6.96E-01	GO:0006814
NRG1	9	6.97E-01	GO:0008217
PRKDC	14	6.97E-01	GO:0042752
SLC38A6	2	6.98E-01	GO:0006814
UBD	2	7.00E-01	GO:0034612
ACE2	3	7.03E-01	GO:0019229 GO:0042312
DLG2	5	7.04E-01	GO:0019233
CACNA1S	11	7.05E-01	GO:0005891
PKD1L2	52	7.12E-01	GO:0005262
ABCC8	4	7.18E-01	GO:0005267 GO:0006813
NCOR1	5	7.21E-01	GO:0007623
SLC10A2	9	7.31E-01	GO:0006814
SLC34A3	10	7.31E-01	GO:0006814
CHRNA1	3	7.34E-01	GO:0004889 GO:0005892
SLC17A3	3	7.34E-01	GO:0006814
CASP3	3	7.34E-01	GO:0034612
CPE	3	7.34E-01	GO:0007218
CHRNA3	2	7.39E-01	GO:0004889 GO:0005892
ACE	10	7.41E-01	GO:0008217
SORCS2	7	7.45E-01	GO:0007218 GO:0008188
F7	3	7.50E-01	GO:0007623
GJA5	2	7.58E-01	GO:0006813 GO:0045907 GO:0045909
SPHK1	4	7.58E-01	GO:0010803
NPB	2	7.59E-01	GO:0007218
PENK	2	7.59E-01	GO:0005184 GO:0007218
TNFRSF4	2	7.59E-01	GO:0005031 GO:0033209
ANO1	2	7.59E-01	GO:0050965

ATP1A2	2	7.59E-01	GO:0006813 GO:0006814 GO:0008217 GO:0019229
BIRC3	2	7.59E-01	GO:0010803 GO:0033209
CACNG1	2	7.59E-01	GO:0005891
CAV1	2	7.59E-01	GO:0042310 GO:0045907
CRTC1	2	7.59E-01	GO:0043153
EDN1	2	7.59E-01	GO:0003100 GO:0019229 GO:0019233 GO:0042310 GO:0051930 GO:0071356
ESR2	2	7.59E-01	GO:0045909
GPR83	2	7.59E-01	GO:0004983 GO:0007218
HNF1B	2	7.59E-01	GO:0032922
TNFSF10	2	7.59E-01	GO:0005164
TRH	2	7.59E-01	GO:0005184
ID3	2	7.61E-01	GO:0007623
ADH1B	4	7.61E-01	GO:0004024
ASIC2	2	7.61E-01	GO:0019229
TMEM38A	2	7.61E-01	GO:0005267
TRAF2	2	7.61E-01	GO:0005164 GO:0010803 GO:0033209
THBS4	7	7.61E-01	GO:0048266
ITGA2	5	7.65E-01	GO:0050966
SCNN1D	10	7.66E-01	GO:0006814
CYBA	1	7.67E-01	GO:0071356
KCNJ1	1	7.67E-01	GO:0006813
PTAFR	1	7.67E-01	GO:0045907 GO:0045909
PYDC2	1	7.67E-01	GO:0010804
AIM2	3	7.70E-01	GO:0033209
ERAP2	6	7.72E-01	GO:0008217
TBC1D8	5	7.72E-01	GO:0008015
USP2	4	7.72E-01	GO:0032922
ICAM1	7	7.72E-01	GO:0045907 GO:0071356
SLC5A12	2	7.78E-01	GO:0006814
HYAL1	6	7.79E-01	GO:0071356
LTBR	1	7.80E-01	GO:0005031 GO:0033209
PKD1L1	23	7.84E-01	GO:0005262
ELN	10	7.91E-01	GO:0008015
CACNA2D3	4	7.92E-01	GO:0005262 GO:0005891
GALR3	2	7.92E-01	GO:0007218
CIB1_GDPGP1	6	7.97E-01	GO:0071356
ADAMTS7	2	7.97E-01	GO:0071356
RYR2	7	8.07E-01	GO:0005262
LVRN	8	8.07E-01	GO:0008217
CACNB1	2	8.11E-01	GO:0005891
PSEN1	1	8.15E-01	GO:0005262
TNFAIP3	5	8.15E-01	GO:0010803
CHRNA1	3	8.43E-01	GO:0004889
CORIN	3	8.43E-01	GO:0008217
FGFR1	3	8.43E-01	GO:0051930
LXN	7	8.43E-01	GO:0050965
KCNJ10	3	8.46E-01	GO:0006813
NALCN	1	8.52E-01	GO:0005272
C3AR1	1	8.53E-01	GO:0008015 GO:0008217
PLA2G6	5	8.55E-01	GO:0045909
CACNA1I	6	8.65E-01	GO:0005891
KCNB2	1	8.69E-01	GO:0006813
KCNJ15	1	8.69E-01	GO:0006813
CRP	1	8.71E-01	GO:0045908
HBB	1	8.71E-01	GO:0008217
GHRL	3	8.71E-01	GO:0042322 GO:0046010
GPR139	3	8.74E-01	GO:0007218 GO:0008188
SLC13A3	3	8.74E-01	GO:0006814
TRPC4AP	3	8.74E-01	GO:0005262
TNFRSF13C	1	8.77E-01	GO:0033209
TRPV6	3	8.85E-01	GO:0005262
TRPV4	2	8.86E-01	GO:0005262
GCGR	2	8.87E-01	GO:0008217
CATSPER3	5	8.91E-01	GO:0006814
SLC23A1	4	8.91E-01	GO:0006814
SLC12A3	6	8.93E-01	GO:0006814
SCN9A	19	8.94E-01	GO:0001518 GO:0006814 GO:0019233 GO:0048266
RELT	6	8.99E-01	GO:0005031 GO:0033209
ITGA1	4	9.06E-01	GO:0042311
RENBP	4	9.08E-01	GO:0008217

RIPK1	3	9.09E-01	GO:0010803 GO:0033209 GO:0034612 GO:0071356
SLC6A2	4	9.16E-01	GO:0048265
PKDREJ	15	9.20E-01	GO:0005262
ADCYAP1R1	2	9.24E-01	GO:0042923
SLC5A2	4	9.27E-01	GO:0006814
EDARADD	1	9.29E-01	GO:0033209
NPNT	6	9.30E-01	GO:0071356
CHRN3	1	9.30E-01	GO:0004889 GO:0005892
CXCL10	1	9.30E-01	GO:0008015
KCNS2	1	9.30E-01	GO:0006813
PPARGC1A	5	9.31E-01	GO:0007623 GO:0032922 GO:0042752 GO:0071356
HIF1A	5	9.32E-01	GO:0045906
UTS2	2	9.38E-01	GO:0008217 GO:0010841 GO:0045909 GO:0046005
TRPM6	7	9.39E-01	GO:0005262
TXNDC17	2	9.39E-01	GO:0033209
SCN10A	12	9.41E-01	GO:0001518 GO:0019233
ATP1A1	1	9.42E-01	GO:0008217
LIPC	4	9.44E-01	GO:0007623
CACNA1A	5	9.46E-01	GO:0005262 GO:0005891 GO:0071356 GO:0060024
TNFRSF10A	4	9.47E-01	GO:0005031
ATP4B	3	9.52E-01	GO:0006813 GO:0006814
RYR1	23	9.52E-01	GO:0005262
GALR1	4	9.52E-01	GO:0007218 GO:0042923
CHRN4	6	9.54E-01	GO:0004889 GO:0005892
SLC12A1	4	9.55E-01	GO:0006813 GO:0006814
KCNH3	2	9.62E-01	GO:0006813
FGB	4	9.63E-01	GO:0045907
AANAT	1	9.64E-01	GO:0007623
PHLPP1	4	9.68E-01	GO:0009649
PKD1	9	9.72E-01	GO:0005262
SLC5A8	5	9.75E-01	GO:0006814
SLC17A6	2	9.76E-01	GO:0006814
SCN5A	11	9.77E-01	GO:0001518 GO:0006814
MCHR2	1	9.81E-01	GO:0007218
SLC5A1	6	9.83E-01	GO:0006814
TNFRSF9	2	9.86E-01	GO:0005031 GO:0033209
TRPM5	8	9.90E-01	GO:0005267
CCL22	3	9.97E-01	GO:0071356
ABCC9	2	1.00E+00	GO:0005267 GO:0006813
ADAMTS13	3	1.00E+00	GO:0034612
AGTR2	2	1.00E+00	GO:0008217 GO:0045909
ASIC3	3	1.00E+00	GO:0005272 GO:0050965 GO:0050966 GO:0050968
BRE	2	1.00E+00	GO:0005164
CD27	2	1.00E+00	GO:0005031 GO:0033209
CHRNA5	2	1.00E+00	GO:0004889 GO:0005892
CLOCK	3	1.00E+00	GO:0007623 GO:0009649
EDNRB	3	1.00E+00	GO:0008217 GO:0019233 GO:0042310 GO:0042311 GO:0048265 GO:0051930
FGG	3	1.00E+00	GO:0045907
HOXD1	2	1.00E+00	GO:0019233
PSME2	2	1.00E+00	GO:0033209
PTGER4	2	1.00E+00	GO:0042322 GO:0046010
RELB	2	1.00E+00	GO:0032922
TNFRSF11A	3	1.00E+00	GO:0060086 GO:0005031 GO:0033209 GO:0034612
TNFRSF1A	3	1.00E+00	GO:0005031 GO:0010803 GO:0033209 GO:0005164
TNFSF15	3	1.00E+00	GO:0005164 GO:0033209
AOA0G2JLG4	0	#N/D	GO:0005272
ACTA2	0	#N/D	GO:0008217
ADCYAP1	0	#N/D	GO:0005184 GO:0007218 GO:0019233 GO:0045909
ADH1A	0	#N/D	GO:0004022 GO:0004024 GO:0006066
ADH5	0	#N/D	GO:0004022
ADK	0	#N/D	GO:0032922
ADRA1B	0	#N/D	GO:0045907
ADRA2A	0	#N/D	GO:0019229 GO:0045909
ADRA2C	0	#N/D	GO:0045907 GO:0051930
AGRP	0	#N/D	GO:0005184 GO:0007218 GO:0007623
AKT1	0	#N/D	GO:0045907
APLN	0	#N/D	GO:0045906 GO:0045909
APOA1	0	#N/D	GO:0010804
ARHGEF2	0	#N/D	GO:0071356
ARNTL	0	#N/D	GO:0007623 GO:0032922 GO:0042753

ARRB2	0	#N/D	GO:0050965
ASIC1	0	#N/D	GO:0006814
ATF4	0	#N/D	GO:0032922
ATF5	0	#N/D	GO:0007623
ATG5	0	#N/D	GO:0042311
AVP	0	#N/D	GO:0005184 GO:0042310 GO:0045907
BHLHE40	0	#N/D	GO:0032922 GO:0043153
BHLHE41	0	#N/D	GO:0032922
CACNB3	0	#N/D	GO:0005262 GO:0005891
CACNB4	0	#N/D	GO:0005262 GO:0005891
CACNG3	0	#N/D	GO:0005891
CACNG7	0	#N/D	GO:0005891
CACNG8	0	#N/D	GO:0005891
CALCB	0	#N/D	GO:0005184
CCK	0	#N/D	GO:0005184 GO:0051930
CCL1	0	#N/D	GO:0071356
CCL13	0	#N/D	GO:0071356
CCL16	0	#N/D	GO:0071356
CCL18	0	#N/D	GO:0071356
CCL19	0	#N/D	GO:0071356
CCL2	0	#N/D	GO:0071356
CCL20	0	#N/D	GO:0071356
CCL21	0	#N/D	GO:0071356
CCL3	0	#N/D	GO:0051930 GO:0071356
CCL3L1	0	#N/D	GO:0071356
CCL4L1	0	#N/D	GO:0071356
CCL5	0	#N/D	GO:0071356
CCL7	0	#N/D	GO:0071356
CD14	0	#N/D	GO:0034612
CD70	0	#N/D	GO:0005164 GO:0033209
CDIP1	0	#N/D	GO:0033209
CDK2	0	#N/D	GO:0006813
CDK4	0	#N/D	GO:0007623
CDK5	0	#N/D	GO:0019233
CHP1	0	#N/D	GO:0006813
CHRNA7	0	#N/D	GO:0004889 GO:0005892
CHRNB2	0	#N/D	GO:0004889 GO:0005892 GO:0019233 GO:0042320 GO:0045188
CLCA3P	0	#N/D	GO:0005262
CLDN4	0	#N/D	GO:0007623
CLIP3	0	#N/D	GO:0010803
COMMD3	0	#N/D	GO:0006814
COMMD7	0	#N/D	GO:0033209
CORT	0	#N/D	GO:0005184
CREB1	0	#N/D	GO:0007623 GO:0042752
CREM	0	#N/D	GO:0032922 GO:0042752
CRH	0	#N/D	GO:0005184 GO:0010841 GO:0046005 GO:0048265
CRX	0	#N/D	GO:0007623
CRY1	0	#N/D	GO:0032922 GO:0042752 GO:0043153
CRY2	0	#N/D	GO:0007623 GO:0032922 GO:0042752 GO:0043153
CSNK1E	0	#N/D	GO:0032922 GO:0042752
CUL5	0	#N/D	GO:0005262
CYLD	0	#N/D	GO:0010803
CYP11B1	0	#N/D	GO:0008217
CYP4F2	0	#N/D	GO:0008217
CYSLTR1	0	#N/D	GO:0007218
DAXX	0	#N/D	GO:0071356
DHRS4	0	#N/D	GO:0006066
DLL4	0	#N/D	GO:0008015
DYRK1A	0	#N/D	GO:0007623
E2F4	0	#N/D	GO:0008015
EDN2	0	#N/D	GO:0003100 GO:0019229 GO:0042310
EDNRA	0	#N/D	GO:0008217 GO:0019233 GO:0042310
EGR2	0	#N/D	GO:0007622
EGR3	0	#N/D	GO:0007623
F2R	0	#N/D	GO:0045907 GO:0051930
FADD	0	#N/D	GO:0005164 GO:0032813
FBXL3	0	#N/D	GO:0042752 GO:0043153
FBXW11	0	#N/D	GO:0042753
FOXO3	0	#N/D	GO:0033209
GATA3	0	#N/D	GO:0071356

GCH1	0	#N/D	GO:0008217 GO:0042311 GO:0071356 GO:0034612
GFPT1	0	#N/D	GO:0032922
GIP	0	#N/D	GO:0019233
GLRA3	0	#N/D	GO:0007218
GNA11	0	#N/D	GO:0009649
GNAQ	0	#N/D	GO:0009649
GPM6A	0	#N/D	GO:0005262
GPR143	0	#N/D	GO:0007218
GPX1	0	#N/D	GO:0042311
GRIN1	0	#N/D	GO:0005262 GO:0019233
GRIN2D	0	#N/D	GO:0051930
GRP	0	#N/D	GO:0005184 GO:0007218
GSK3B	0	#N/D	GO:0007623
HOY8X5	0	#N/D	GO:0007623
HAS2	0	#N/D	GO:0071356
HCN1	0	#N/D	GO:0005267 GO:0006813
HCRT	0	#N/D	GO:0005184 GO:0007218
HDAC1	0	#N/D	GO:0032922
HDAC3	0	#N/D	GO:0007623
HNRNPD	0	#N/D	GO:0042752
HNRNPR	0	#N/D	GO:0007623
HNRNPU	0	#N/D	GO:0032922
HRH2	0	#N/D	GO:0045907
ID2	0	#N/D	GO:0032922 GO:0042752 GO:0043153
ID4	0	#N/D	GO:0007623
IGBP1	0	#N/D	GO:0034612
IKBKG	0	#N/D	GO:0010803
IL10	0	#N/D	GO:0051930
INS	0	#N/D	GO:0045908 GO:0045909
IRG1	0	#N/D	GO:0071356
JUN	0	#N/D	GO:0007623
JUND	0	#N/D	GO:0007623
KAT2A	0	#N/D	GO:0071356
KCNA1	0	#N/D	GO:0005267 GO:0006813 GO:0050966
KCNA2	0	#N/D	GO:0005267 GO:0006813 GO:0019233 GO:0045188
KCNA3	0	#N/D	GO:0006813
KCNA6	0	#N/D	GO:0006813
KCNAB1	0	#N/D	GO:0006813
KCND2	0	#N/D	GO:0019233
KCNF1	0	#N/D	GO:0005267 GO:0006813
KCNG1	0	#N/D	GO:0005267 GO:0006813
KCNG2	0	#N/D	GO:0006813
KCNIP1	0	#N/D	GO:0005267
KCNIP2	0	#N/D	GO:0006813
KCNIP4	0	#N/D	GO:0005267
KCNJ12	0	#N/D	GO:0006813
KCNJ2	0	#N/D	GO:0006813
KCNJ4	0	#N/D	GO:0006813
KCNJ5	0	#N/D	GO:0006813
KCNK4	0	#N/D	GO:0005267 GO:0006813 GO:0019233
KCNK9	0	#N/D	GO:0005267 GO:0006813
KCNMB2	0	#N/D	GO:0006813 GO:0019229
KCNMB4	0	#N/D	GO:0006813 GO:0019229
KCNN1	0	#N/D	GO:0006813
KCNN2	0	#N/D	GO:0006813
KCNS3	0	#N/D	GO:0006813
KCNV1	0	#N/D	GO:0006813
KISS1R	0	#N/D	GO:0007218 GO:0008188 GO:0042923
KLF2	0	#N/D	GO:0071356
KRT18	0	#N/D	GO:0033209
KRT8	0	#N/D	GO:0033209
LTA	0	#N/D	GO:0005164 GO:0033209
MAGED1	0	#N/D	GO:0032922 GO:0042752
MAP2K7	0	#N/D	GO:0034612
MAP4K3	0	#N/D	GO:0034612
MAPK1	0	#N/D	GO:0019233
MAPK10	0	#N/D	GO:0042752
MAPK8	0	#N/D	GO:0042752
MC3R	0	#N/D	GO:0008217 GO:0032922 GO:0042923
MCU	0	#N/D	GO:0005262

MFSD4B	0	#N/D	GO:0006814
NAMPT	0	#N/D	GO:0007623 GO:0032922
NFE2	0	#N/D	GO:0008015
NIPSNAP1	0	#N/D	GO:0019233
NKX2-1	0	#N/D	GO:0042753
NKX3-1	0	#N/D	GO:0071356
NLGN2	0	#N/D	GO:0019233
NLRP2P	0	#N/D	GO:0010804
NMB	0	#N/D	GO:0007218
NPAS2	0	#N/D	GO:0007623 GO:0032922
NPPC	0	#N/D	GO:0045909
NPR2	0	#N/D	GO:0008217
NPW	0	#N/D	GO:0007218
NPY2R	0	#N/D	GO:0004983 GO:0007218 GO:0046005 GO:0051930
NPY6R	0	#N/D	GO:0004983 GO:0007218 GO:0008015
NR1D1	0	#N/D	GO:0007623 GO:0032922 GO:0042752 GO:0060086
NR2F6	0	#N/D	GO:0043153 GO:0050965
NSF	0	#N/D	GO:0006813
NTRK3	0	#N/D	GO:0007623
NXPH4	0	#N/D	GO:0007218
OGT	0	#N/D	GO:0032922
OLR1	0	#N/D	GO:0008015
OPRD1	0	#N/D	GO:0007218 GO:0019233 GO:0042923
OPRK1	0	#N/D	GO:0007218 GO:0019233 GO:0042923 GO:0051930
OSM	0	#N/D	GO:0048266
P2RY1	0	#N/D	GO:0019233 GO:0042312
PCSK1N	0	#N/D	GO:0007218
PID1	0	#N/D	GO:0071356
PLN	0	#N/D	GO:0008015
PLOD3	0	#N/D	GO:0042311
PMCH	0	#N/D	GO:0007218
PNOC	0	#N/D	GO:0005184 GO:0007218
PPARG	0	#N/D	GO:0008217 GO:0042752
PPP1CA	0	#N/D	GO:0032922 GO:0042752 GO:0043153
PPP1CB	0	#N/D	GO:0032922 GO:0042752 GO:0043153
PPP1CC	0	#N/D	GO:0032922 GO:0042752 GO:0043153
PRKAA1	0	#N/D	GO:0042752
PRLHR	0	#N/D	GO:0004983 GO:0007218 GO:0008188
PRMT5	0	#N/D	GO:0032922
PROK2	0	#N/D	GO:0007218 GO:0007623 GO:0019233
PROL1	0	#N/D	GO:0051930
PRPF8	0	#N/D	GO:0071356
PSMA1	0	#N/D	GO:0033209
PSMA2	0	#N/D	GO:0033209
PSMA3	0	#N/D	GO:0033209
PSMA4	0	#N/D	GO:0033209
PSMA5	0	#N/D	GO:0033209
PSMA6	0	#N/D	GO:0033209
PSMA8	0	#N/D	GO:0033209
PSMB1	0	#N/D	GO:0033209
PSMB4	0	#N/D	GO:0033209
PSMB5	0	#N/D	GO:0033209
PSMC1	0	#N/D	GO:0033209
PSMC2	0	#N/D	GO:0033209
PSMC3	0	#N/D	GO:0033209
PSMC4	0	#N/D	GO:0033209
PSMC6	0	#N/D	GO:0033209
PSMD10	0	#N/D	GO:0033209
PSMD11	0	#N/D	GO:0033209
PSMD12	0	#N/D	GO:0033209
PSMD14	0	#N/D	GO:0033209
PSMD2	0	#N/D	GO:0033209
PSMD4	0	#N/D	GO:0033209
PSMD7	0	#N/D	GO:0033209
PSME3	0	#N/D	GO:0033209
PSPC1	0	#N/D	GO:0042752
PTGDS	0	#N/D	GO:0045187
PTH2	0	#N/D	GO:0007218
PYCARD	0	#N/D	GO:0010803 GO:0033209 GO:0071356
PYDC1	0	#N/D	GO:0010804 GO:0033209

PYY2	0	#N/D	GO:0005184 GO:0007218
PYY3	0	#N/D	GO:0005184 GO:0007218
RACK1	0	#N/D	GO:0010803
RAMP1	0	#N/D	GO:0004948
RAMP2	0	#N/D	GO:0008217
RAPGEF2	0	#N/D	GO:0007218
RCAN1	0	#N/D	GO:0008015
REN	0	#N/D	GO:0008217
RORA	0	#N/D	GO:0032922 GO:0042753 GO:0071356
RORB	0	#N/D	GO:0007623 GO:0042752 GO:0042753
RPS27A	0	#N/D	GO:0010803 GO:0033209
SCG5	0	#N/D	GO:0007218
SCN2B	0	#N/D	GO:0001518
SCN3B	0	#N/D	GO:0001518 GO:0006814 GO:0019233
SCPEP1	0	#N/D	GO:0045909
SFPQ	0	#N/D	GO:0042752
SFRP1	0	#N/D	GO:0071356
SHARPIN	0	#N/D	GO:0010803
SLC13A5	0	#N/D	GO:0006814
SLC22A4	0	#N/D	GO:0006814
SLC24A5	0	#N/D	GO:0005262 GO:0006813
SLC38A1	0	#N/D	GO:0006814
SLC38A3	0	#N/D	GO:0006814
SLC4A10	0	#N/D	GO:0006814
SLC4A8	0	#N/D	GO:0006814
SLC6A8	0	#N/D	GO:0006814
SMPD4	0	#N/D	GO:0071356
SOD1	0	#N/D	GO:0008217
SOD2	0	#N/D	GO:0008217
SOX14	0	#N/D	GO:0009649
SSTR1	0	#N/D	GO:0007218 GO:0042923
SSTR2	0	#N/D	GO:0007218 GO:0042923
STAT1	0	#N/D	GO:0008015 GO:0043120 GO:0033209
SYNCRIP	0	#N/D	GO:0007623
TAC1	0	#N/D	GO:0007218 GO:0008217 GO:0019233 GO:0048265
TAC4	0	#N/D	GO:0008217
TACR1	0	#N/D	GO:0019233 GO:0045907 GO:0048265
TBXA2R	0	#N/D	GO:0045907
TDGF1	0	#N/D	GO:0071356
TNFRSF12A	0	#N/D	GO:0033209
TNFRSF25	0	#N/D	GO:0005031 GO:0033209
TNFSF11	0	#N/D	GO:0005164 GO:0032813 GO:0033209
TNFSF12	0	#N/D	GO:0005164 GO:0033209
TNFSF12-	0	#N/D	GO:0005164
TNFSF13	0	#N/D	GO:0005164 GO:0033209
TNFSF13B	0	#N/D	GO:0005164 GO:0033209
TNFSF4	0	#N/D	GO:0005164 GO:0032813 GO:0033209
TNFSF8	0	#N/D	GO:0005164
TP53	0	#N/D	GO:0043153
TRAF6	0	#N/D	GO:0005164
TRPC3	0	#N/D	GO:0005262
TRPC4	0	#N/D	GO:0005262
TRPC5	0	#N/D	GO:0005262
TSPO	0	#N/D	GO:0048266
TYMS	0	#N/D	GO:0007623
UBA52	0	#N/D	GO:0010803 GO:0033209
UBB	0	#N/D	GO:0010803 GO:0033209
UBC	0	#N/D	GO:0010803 GO:0033209
UCHL1	0	#N/D	GO:0019233
UCN	0	#N/D	GO:0005184 GO:0007218
UTS2B	0	#N/D	GO:0008217 GO:0042312
UTS2R	0	#N/D	GO:0007218 GO:0008015 GO:0010841 GO:0042312 GO:0045906 GO:0010841
VGF	0	#N/D	GO:0005184
VIP	0	#N/D	GO:0005184 GO:0051930
VWA1	0	#N/D	GO:0048266
XCL1	0	#N/D	GO:0071356
XCL2	0	#N/D	GO:0008015 GO:0071356
ZFAND6	0	#N/D	GO:0071356

Table S2: GO terms annotations

Go term description	GO term
voltage-gated sodium channel complex	GO:0001518
regulation_of_systemic_arterial_blood_pressure_by_endothelin	GO:0003100
alcohol_dehydrogenase_(NAD)_activity	GO:0004022
alcohol_dehydrogenase_activity,_zinc-dependent	GO:0004024
nicotinic_acetylcholine-activated_cation-selective_channel_activity	GO:0004889
calcitonin_receptor_activity	GO:0004948
neuropeptide_Y_receptor_activity	GO:0004983
tumor_necrosis_factor_receptor_activity	GO:0005031
tumor_necrosis_factor_receptor_binding	GO:0005164
neuropeptide_hormone_activity	GO:0005184
calcium_channel_activity	GO:0005262
potassium_channel_activity	GO:0005267
sodium_channel_activity	GO:0005272
voltage-gated_calcium_channel_complex	GO:0005891
nicotinic_acetylcholine-gated_receptor-channel_complex	GO:0005892
alcohol_metabolic_process	GO:0006066
potassium_ion_transport	GO:0006813
sodium_ion_transport	GO:0006814
neuropeptide_signaling_pathway	GO:0007218
rhythmic_behavior	GO:0007622
circadian_rhythm	GO:0007623
ultradian_rhythm	GO:0007624
blood_circulation	GO:0008015
neuropeptide_receptor_activity	GO:0008188
regulation_of_blood_pressure	GO:0008217
entrainment_of_circadian_clock	GO:0009649
regulation_of_tumor_necrosis_factor-mediated_signaling_pathway	GO:0010803
negative_regulation_of_tumor_necrosis_factor-mediated_signaling_pathway	GO:0010804
positive_regulation_of_circadian_sleep/wake_cycle,_wakefulness	GO:0010841
regulation_of_vasoconstriction	GO:0019229
sensory_perception_of_pain	GO:0019233
tumor_necrosis_factor_receptor_superfamily_binding	GO:0032813
circadian_regulation_of_gene_expression	GO:0032922
tumor_necrosis_factor-mediated_signaling_pathway	GO:0033209
response_to_tumor_necrosis_factor	GO:0034612
Vasoconstriction	GO:0042310
Vasodilation	GO:0042311
regulation_of_vasodilation	GO:0042312
regulation_of_circadian_sleep/wake_cycle,_REM_sleep	GO:0042320
negative_regulation_of_circadian_sleep/wake_cycle,_sleep	GO:0042321
negative_regulation_of_circadian_sleep/wake_cycle,_REM_sleep	GO:0042322
circadian_sleep/wake_cycle	GO:0042745
regulation_of_circadian_rhythm	GO:0042752
positive_regulation_of_circadian_rhythm	GO:0042753
neuropeptide_binding	GO:0042923
tumor_necrosis_factor_binding	GO:0043120
entrainment_of_circadian_clock_by_photoperiod	GO:0043153
rhythmic_excitation	GO:0043179
regulation_of_circadian_sleep/wake_cycle,_sleep	GO:0045187
regulation_of_circadian_sleep/wake_cycle,_non-REM_sleep	GO:0045188
negative_regulation_of_vasoconstriction	GO:0045906
positive_regulation_of_vasoconstriction	GO:0045907
negative_regulation_of_vasodilation	GO:0045908
positive_regulation_of_vasodilation	GO:0045909
positive_regulation_of_circadian_sleep/wake_cycle,_REM_sleep	GO:0046005
positive_regulation_of_circadian_sleep/wake_cycle,_non-REM_sleep	GO:0046010
alcohol_catabolic_process	GO:0046164
response_to_pain	GO:0048265
behavioral_response_to_pain	GO:0048266
detection_of_temperature_stimulus_involved_in_sensory_perception_of_pain	GO:0050965
detection_of_mechanical_stimulus_involved_in_sensory_perception_of_pain	GO:0050966
detection_of_chemical_stimulus_involved_in_sensory_perception_of_pain	GO:0050968
regulation_of_sensory_perception_of_pain	GO:0051930
rhythmic_synaptic_transmission	GO:0060024
circadian_temperature_homeostasis	GO:0060086
cellular_response_to_tumor_necrosis_factor	GO:0071356

